2019

Patterns, Processes, And Scale: An Evaluation Of Ecological And Biogeochemical Functions Across An Arctic Stream Network

Samuel P. Parker
University of Vermont

PATTERNS, PROCESSESS, AND SCALE: AN EVALUATION OF ECOLOGICAL AND BIOGEOCHEMICAL FUNCTIONS ACROSS AN ARCTIC STREAM NETWORK

A Dissertation Presented

by

Samuel P. Parker

to

The Faculty of the Graduate College

of

The University of Vermont

In Partial Fulfillment of the Requirements
for the Degree of Doctor of Philosophy
Specializing in Natural Resources

January, 2019

Defense Date: September 28, 2018
Dissertation Examination Committee:

William Breck Bowden, Ph.D., Advisor
Michael B. Flinn, Ph.D., Co-Advisor
Arne Bomblies, Ph.D., Chairperson
Donna Rizzo, Ph.D.
Carol Adair, Ph.D.
Cynthia J. Forehand, Ph.D., Dean of the Graduate College

ABSTRACT

Ecosystems are highly variable in space and time. Understanding how spatial and temporal scales influence the patterns and processes occurring across watersheds presents a fundamental challenge to aquatic ecologists. The goal of this research was to elucidate the importance of spatial scale on stream structure and function within the Oksrukuyik Creek, an Arctic watershed located on the North Slope of Alaska (68°36'N, 149°12'W). The studies that comprise this dissertation address issues of scale that affect our ability to assess ecosystem function, such as: methodologies used to scale ecosystem measurements, multiple interacting scales, translation between scales, and scale-dependencies.

The first methodological study examined approaches used to evaluate chlorophyll *a* in ethanol extracts of aquatic biofilms. Quantification of chlorophyll *a* is essential to the study of aquatic ecosystems, yet differences in methodology may introduce significant errors to its determination that can lead to issues of comparability between studies. A refined analytical procedure for the determination of chlorophyll *a* was developed under common acidification concentrations at multiple common reaction times. The refined procedure was used to develop a series of predictive equations that could be used to correct and normalize previously evaluated chlorophyll *a* data. The predictive equations were validated using benthic periphyton samples from northern Alaska and northwestern Vermont, U.S.A.

The second study examined interaction and translation between scales by examining how normalization approaches affect measurements of metabolism and nutrient uptake in stream sediment biofilms. The effect of particle size and heterogeneity on rates of biofilm metabolism and nutrient uptake was evaluated in colonized and native sediments normalized using two different scaling approaches. Functional rates were normalized by projected surface area and sediment surface area scaling approaches, which account for the surface area in plan view (looking top-down) and the total surface area of all sediment particles, respectively. Findings from this study indicated that rates of biogeochemical function in heterogeneous habitats were directly related to the total sediment surface area available for biofilm colonization. The significant interactions between sediment surface area and rates of respiration and nutrient uptake suggest that information about the size and distribution of sediment particles could substantially improve our ability to predict and scale measurements of important biogeochemical functions in streams.

The final study examined how stream nutrient dynamics are influenced by the presence or absence of lakes across a variety of discharge conditions and how catchment characteristics can be used to predict stream nutrients. Concentrations of dissolved organic carbon (DOC) and other inorganic nutrients were significantly greater in streams without lakes than in streams in with lakes and DOC, total dissolved nitrogen (TDN), and soluble reactive phosphorus concentrations increased as a function of discharge. Catchment characteristic models explained between 20% and 76% of the variance of the nutrients measured. Organic nutrient models were driven by antecedent precipitation and watershed vegetation cover type while inorganic nutrients were driven by antecedent precipitation, landscape characteristics and reach vegetation cover types. The developed models contribute to existing and future understanding of the changing Arctic and lend new confidence to the prediction of nutrient dynamics in streams where lakes are present.

CITATIONS

Material from this dissertation has been accepted for publication in *Limology and Oceanography: Methods* on (11 August 2016) in the following form:

Parker, S. P., Bowden, W. B., and Flinn, M. B.. (2016). The effect of acid strength and postacidification reaction time on the determination of chlorophyll a in ethanol extracts of aquatic periphyton. Limnol. Oceanogr. Methods, 14: 839-852. doi:10.1002/lom3.10130

Material from this dissertation has been accepted for publication in *Ecosphere* on (10 January 2018) in the following form:

Parker, S. P., Bowden, W. B., Flinn, M. B., Giles, C. D., Arndt, K. A., Beneš, J. P., and Jent, D. G.. (2018). Effect of particle size and heterogeneity on sediment biofilm metabolism and nutrient uptake scaled using two approaches. Ecosphere 9(3):e02137. 10.1002/ecs2.2137.

ACKNOWLEDGEMENTS

I would like to thank my advisor, Breck Bowden, and my co-advisor, Michael Flinn, for their continued guidance, knowledge, insight, and support throughout this process. I would also like to thank the other members of the Scale, Consumer and Lotic Ecosystem Rates (SCALER) project: Christina L. Baker, Ford Ballantyne IV, Walter K. Dodds, Kaitlin J. Farrell, Tamara K. Harms, Jeremy B. Jones, Lauren E. Koenig, John S. Kominoski, William H. McDowell, Amy D. Rosemond, Matt T. Trentman, Janine Rüegg, Ken Sheehan, Chao Song, Matt Whiles, and Wilfred M. Wollheim for their direction, support, and camaraderie. I would also like to thank Ryan Sleeper, Kyle Arndt, and Joshua Beneš for the countless hours in the field and laboratory assisting with experiments. My defense committee: Carol Adair, Arne Bomblies, and Donna Rizzo also provided invaluable technical guidance and instruction throughout my graduate tenure. Gary Long has also played a critical role in this process—from initial encouragement to pursue this degree to allowing me flexibility in the office to finish—cheers to THH. I would also like to thank my family members for their encouragement to pursue my passion and take the road less traveled. Finally, I'd like to thank my bride, Courtney, for joining me on such a wild ride.

TABLE OF CONTENTS

LIST OF TABLES

LIST OF FIGURES

CHAPTER 1: COMPREHENSIVE LITERATURE REVIEW

ABSTRACT

This literature review is intended to provide relevant background information applicable to scaling, an integral component of all articles presented. Information is provided on the issues of scale and scaling in ecology, patterns and processes in stream ecosystems, and the opportunities of scale to improve our understanding of stream function. The information discussed helps to inform the field and laboratory studies and experiments that comprise this article-based dissertation.

1.0 Scale in Ecology

An ecosystem is a community of interacting organisms and their functional and structural relationships with the physical environment (Odum 1971). By definition, ecosystems are bound by some spatial extent and the processes within them operate on a broad range of temporal periods. This is why understanding scale is perhaps the most fundamental problem to all ecological studies (Wiens 1989, Levin 1992, Schneider 2001). Although scale has been an important subject of research for quite some time, it is often viewed implicitly or as a nuisance (Wiens 1989). Scale has only recently been considered explicitly in ecological studies (Hewitt et al. 2007, Sandel and Smith 2009). The following sections discuss: 1) the need for clarification on the terms scale and scaling, and 2) the prominent issues of scale relevant to all ecological studies.

1.1 Defining Scale

The terms scale and scaling are so commonly used in ecological studies that it begs the question—what is *scale*? Scale can be interpreted in many ways, but to avoid confusion it is best to identify how scale has previously been defined and how it will be used throughout this dissertation. Specifically, scale refers to some metric, which quantifies an observation (Peterson and Parker 1998). In this context, scale is no different than a unit (e.g., grams) or a transformed value (e.g., log-scale nitrate concentration). In the context of this dissertation *scale* refers to any observed value, which is indexed relative to a specific spatial and temporal dimension (Wiens 1989, Levin 1992, Peterson and Parker 1998, Schneider 2001). For example, stream discharge is an observed volume of water and is

defined relative to some temporal scale (L^3 T^{-1}). A second example is species density, which is defined as the number of individuals relative to a unit of area (# individuals L^{-2}). Spatial scales can be viewed in terms of *grain* and *extent*, where grain is the smallest dimensional unit of observation and extent is the total spatial area being studied (Wiens 1989, Levin 1992, Schneider 2001).

Scaling has two meanings in ecological research. The first meaning refers to the interpolation or extrapolation of values made at one scale to another of differing magnitude. *Scaling* is used to describe this translation between levels of organization (Peterson and Parker 1998). *Up-scaling or scaling-up* is the extrapolation of values made at small spatial and temporal scales to larger scales. Ecological observations are frequently made at small scales and applied to broader scales (Thrush et al. 1997, Schindler 1998, Schneider 2001); however, simple proportional or linear scaling of ecological data can lead to inaccurate results as will be discussed later in this review (Hewitt et al. 2007, Sandel and Smith 2009). The second meaning of scaling involves the use of mathematical power relationships, in which some variable is expressed as a function of another variable raised to an exponent. In this definition, the exponent variable is known as the *scaling factor* or *scaling exponent* (Calder 1983, Schneider 2001). Scaling exponents are often used in bioenergetics modeling to describe the relationship between body size and temperature or the energy requirements of organisms. These relationships are referred to as allometric equations (*sensu* Brown et al. 2004). It is also common to use power functions for the scaling of abiotic processes, such as hydraulic geometry curves (Leopold and Maddock 1953).

Perhaps the greatest challenge to the clear use of nomenclature in aquatic studies is the distinction between *scale* and *level*. Levels are bins or groups within a hierarchically organized system (Peterson and Parker 1998), whereas scales have defined temporal and spatial dimensions. Levels can have scale and be defined based on observations made at particular scales, but they can also be independent of spatial and temporal scales (Allen and Hoekstra 1990). Levels are often defined *a priori* and contain a pre-imposed structure, which lacks any reference to scale (Peterson and Parker 1998). Conventional levels of organization (e.g., cells, organisms, populations, communities) provide an example of categorical levels, which lack spatial and temporal scale (Allen and Hoekstra 1990). Stream and river networks are typically characterized into smaller organizational sub-units (e.g., segments, reaches, habitat patches, and microhabitats) and each hierarchical level is associated with multiple scales (Frissell et al. 1986, Minshall 1988). Therefore, it is important to recognize that there is no specific *patch-, reach-, or network-scale*, but rather a hierarchical level that contains multiple scales.

Strahler's (1954, 1957) stream order classification is an excellent example of a hierarchical organizational structure that lacks specific scale. To most, a first-order stream is considered a small-scale catchment with relatively consistent spatial scales. Depending on physiographical region, topography, and climate of the catchment, first-order streams occupy a very large range of spatial scales. The drainage area of one first-order stream may be twice that of another stream in the same watershed and the process and structure present may be completely different. Thus, it is not possible to make any direct comparison of

ecological phenomena between two equivocal levels if they are not represented in the same scale (Wiens 1989, Levin 1992, Peterson and Parker 1998).

1.2 Issues of Scale

There are several prominent issues of scale that are common to any study of terrestrial, freshwater, and marine ecosystems. First, no single appropriate scale exists to study natural phenomena within an ecosystem (Levin 1992) and phenomena are affected by processes occurring at multiple interacting spatial and temporal scales (Wiens 1989, Schneider 2001). The second issue is the result of observational bias, whereby methodological and logistical constraints fix the physical dimensions of a particular measurement to one scale (Wiens 1989, Levin 1992). These constraints may affect extrapolation or translation of natural phenomena from small to large scales. The third issue is related to the determination of whether or not an observation is scale-dependent (Hewitt et al. 2007, Sandel and Smith 2009, Chase and Knight 2013).

1.2.1 Recognizing Multiple Interacting Scales

The theoretical relationship between grain size and spatial variance helps to explain why no single appropriate scale exists to study natural phenomena (Wiens 1989, Levin 1992, Horne and Schneider 1995). For example, if a 100 m^2 field with variably distributed grass species is sampled 10 times with a one square meter quadrat, the variance of the observed number of blades of grass per square meter will be greater than the variance of ten measurements taken using 10m^2 quadrat. This process could be repeated with an infinite number of quadrat sizes, and each grain size would have its own unique variance. Changes

in observed variance with increasing plot or quadrat size was empirically demonstrated by Bormann (1953), who found that variance per unit area tended to decrease as plot size increased. In general, as the grain size of an observation increases, the spatial variance of that observation decreases. In homogenous environments, this decay follows a power relationship or a linear relationship if the variance and grain size is log-log transformed (Levin 1992). The shape of the relationship between grain size and variance depends largely on the variable being measured and its arrangement within the study extent (Wiens 1989). Changes to the extent of an ecological study also affect the variance in observed natural phenomena by changing the population measured by sampling (Turner et al. 1989). Because variance is not stationary across grain sizes and extents, it is impossible to choose one scale that is representative of all ecological processes.

The precise relationship between grain size and variance is often difficult to demonstrate because processes occurring at multiple scales can influence singular, natural phenomena (Wiens 1989, Levin 1992). This is especially important when considering the hierarchical arrangement and structure of organisms within an ecosystem (O'Neill et al. 1989). Palmer et al. (1996) found that regional processes, such as high-flow events, act more strongly on the dispersal of freshwater benthic invertebrate communities than local processes, and Bilton et al. (2001) found that the biodiversity of stream insects is most strongly influenced by localized factors. These somewhat conflicting results suggest that multiple spatial and temporal scales drive benthic invertebrate community assemblages. Large-scale processes drive the movement of benthic invertebrates, but the small-scale localized habitat also affects the biodiversity present. Therefore, it is not appropriate to

examine the distribution of invertebrates or other ecological processes without considering the scales that are acting on a particular process.

1.2.2 Observational Bias and Translation Between Scales

The second issue of scale is that we are technologically, methodologically, and logistically constrained to evaluate a limited number of scales. The act of observation or experimental evaluation of natural phenomena fixes measurements to a particular physical dimension (Wiens 1989, Levin 1992, Schneider 2001). A review by Schindler (1998) highlighted many shortcomings of using small-scale microcosm and mesocosm experiments to explain physical, chemical, and biological processes in the Experimental Lakes Area (ELA), where whole ecosystem manipulation experiments were conducted. Manipulation of small, isolated chambers tended to have much lower variability and increased repeatability, but were not comparable to the whole ecosystem studies, due to numerous experimental artifacts (Carpenter 1996). Early attempts to measure phytoplankton productivity in lakes were traditionally conducted using strings of bottles, which were filled with lake-water and suspended in the water column. These experiments were easy to conduct, but removed the disruptive effects of wind-mixing on phytoplankton growth in the upper few meters of the lake and also enhanced photosynthesis due to bottle transparency (Schindler 1998). This methodological artifact becomes a scaling issue when results measured at the bottle-scale (0.5L) are extrapolated up to the entire ecosystem.

Similarly, increasing the experimental grain size from microcosms to mesocosms also imposes methodological constraints and issues of transferability to larger scales (Frost

et al. 1988). Levine and Schindler (1992) tried to experimentally induce cyanobacteria algae blooms in mesocosms by decreasing the molar ratio of nitrogen to phosphorus. Previous whole-lake nutrient enrichment studies indicated that cyanobacteria blooms occurred when N:P ratios were between 11:1 and 33:1. When the shallow (2m) mesocosms were enriched to a ratio of 4:1 no blooms occurred because strong sediment sorption and/or periphyton growth limited the total available nutrients in the mesocosms (Schindler 1998). It was only when the mesocosms were moved to deeper lakes that the nutrient enrichment produce cyanobacteria blooms (Levine and Schindler 1992).

These examples from the ELA clearly demonstrate that the scale of observation or experimentation impose logistical and technological constraints when considering natural phenomena. Without whole-ecosystem experiments, like those conducted at the ELA, there would be no way to validate whether or not small-scale observations are transferable to larger scales. Therefore, it is critical to recognize and understand the limitations imposed by observational scale and to develop experiments that identify and remove methodological artifacts before drawing conclusions or extrapolating results to larger spatial or temporal scales.

1.2.3 Evaluating Scale Dependencies

The final issue of scale is determining whether a particular natural phenomenon is scale-dependent and how scale can be used to explain its relationship with other variables, processes, or spatial location (Hewitt et al. 2007, Sandel and Smith 2009). Because there is no ‘correct’ scale to study natural phenomena (due to technological, methodological, and

logistical constraints), resolving scale dependencies can be extremely challenging. Two distinct orders of scale-dependence exist in ecological studies: first-order and second-order scale-dependence. First-order scale-dependence is the direct relationship between some natural phenomena and its physical dimensions. For example, stream discharge generally increases as catchment area increases, thus discharge is scale-dependent on the areal extent of the basin.

Second-order scale-dependence involves the relationship between two natural phenomena that change at different scales (Sandel and Smith 2009). Second-order scale-dependence can be problematic in ecological studies because most correlative relationships hinge on assumptions of independence, normality, and homoscedasticity. If the two natural phenomena have different responses to changes in scale, then scale becomes the only independent variable. As a result, the relationship between the natural phenomena may differ dramatically depending on the scale of observation (Schneider 2001, Sandel and Smith 2009).

Whole stream metabolism (WSM), an integrated measure of a stream's ability to consume and produce organic matter (Odum 1956, Mulholland et al. 2001, Staehr et al. 2012), provides an excellent example of second-order scale-dependence (Roberts et al. 2007). Whole stream metabolism is the sum of ecosystem respiration (ER; i.e., the catabolic breakdown of complex organic molecules into carbon dioxide), and gross primary production (GPP; i.e., the anabolic synthesis of new organic molecules and oxygen from light and carbon dioxide). Roberts et al. (2007) found that GPP and ER were both suppressed immediately following storm events; however, the post-storm recovery was

quite different for the two processes. GPP recovered very slowly as algal communities re-established, but ER rates actually increased higher than they were before the storm event. Although this example involves WSM response to an episodic storm event, it clearly illustrates second-order scale-dependence. If antecedent conditions and their spatial and temporal scales are not known, then the interpretation of results could lead to false conclusions about the metabolic processes present in the stream.

In addition to the first-order areal and second-order temporal scale-dependence discussed above, natural phenomena often exhibit spatial dependencies due to their continuity in space (Isaaks and Srivastava 1989). Unlike scale-dependence, where a natural phenomenon is a function of planar or volumetric physical dimensions in space, spatial dependence explores a natural phenomenon as a function of its location in space (i.e., xyz coordinates). To this end, geostatistical analyses are used to identify spatial-dependencies of natural phenomena, make predictions, and evaluate observational uncertainty (Rossi et al. 1992, Goovaerts 1998).

1.3 Scale in Stream Ecosystems

Unlike terrestrial or marine environments, streams and rivers are hierarchically nested dendritic systems that require special considerations of scale (Lowe et al. 2006, Thorp et al. 2006, Campbell Grant et al. 2007, Peterson et al. 2013). Aquatic ecologists have long recognized the dynamic nature of streams and rivers, and that the highly variable abiotic and biotic elements within them form unique patterns across the landscape (Hynes 1970, Minshall 1988, Pringle et al. 1988, Cooper et al. 1997, Lowe et al. 2006). This

subsection discusses: 1) several conceptual frameworks used to describe the unique spatial patterns found within lotic ecosystems, and 2) the challenges associated with linking patterns, and processes.

1.3.1 Frameworks to Describe Stream Pattern

The unique spatial arrangement of streams and rivers across the landscape has given rise to numerous classification approaches and conceptual frameworks to describe patterns and processes across multiple scales (Vannote et al. 1980, Statzner and Higler 1985, Frissell et al. 1986, Minshall 1988, Pringle et al. 1988, Townsend 1989, Montgomery 1999, Poole 2002, Benda et al. 2004, Thorp et al. 2006). General and specific conceptual frameworks addressing the large and small-scale arrangement of streams are summarized below.

1.3.1.1 General Spatial Frameworks

The River Continuum Concept (RCC), arguably the most influential aquatic ecology paper of the last century, hypothesized that structural and functional gradients occur as a function of stream order throughout a river network (Vannote et al. 1980). This large-scale framework describes the spatial arrangement of a stream or river as a structural and functional continuum from the headwaters to the mouth. The continua concepts borrowed heavily from geomorphological research that pioneered our understanding of the physical behavior of stream and river systems (Leopold and Maddock 1953, Leopold and Langbein 1962), as well as the spiraling concepts developed by Webster and Patten (1979). Much like rivers tending towards a steady physical condition or dynamic/quasi-

equilibrium, Vannote et al. (1980) postulated that the biological systems present in a particular lotic body strive to a similar stable state. Moreover, the structure and function of the system arranges to best utilize the available energy and self-regulate to a mean physical state at any one point along the drainage network. Because resources are in a constant state of down-gradient flux, the authors theorized that biological communities seek strategies to minimize energy loss and thus communities are assembled to capitalize on resources that are available from upstream sources (e.g., processing inefficiencies).

The RCC gave rise to other approaches that considered longitudinal changes in stream structure and function across entire river networks such as the Process Domain Concept (Montgomery 1999), the Network Dynamics Hypothesis (Benda et al. 2004), and others (Newbold et al. 1982, Gomi et al. 2002). Thorp et al. (2006) incorporated many of large-scale frameworks into a comprehensive, heuristic model called the Riverine Ecosystem Synthesis (RES). The RES describes the arrangement of stream and rivers as longitudinally distributed hydrogeomorphic units formed by catchment geomorphology and regional climate. Additionally, several compelling critiques of the RCC focused on discontinuities common to stream and river systems (Ward and Stanford 1983, Statzner and Higler 1985, Poole 2002, Jones 2010b).

Other frameworks were developed to classify the spatial arrangement of streams at smaller scales (Frissell et al. 1986, Pringle et al. 1988, Townsend 1989, Wadeson 1994, Townsend et al. 1997a, Lake 2000, Poole 2002, Winemiller et al. 2010). Drawing from terrestrial (Forman and Godron 1981) and marine (Levin and Paine 1974, Paine and Levin 1981) ecology, the stream patch dynamics concept considered the natural heterogeneity

within lotic systems (Townsend 1989, Pringle 1990, Winemiller et al. 2010). Stream patches are spatially arranged as a "mosaic" of homogenous structural and functional units that interact throughout the riverscape (Forman and Godron 1981, Pringle et al. 1988, Wiens 2002). Stream patches can be structured into clearly defined hierarchical levels (Frissell et al. 1986) and the interaction between patches is called the Hierarchical Patch Dynamics (HPD) concept (Wu and Loucks 1995, Thoms and Parsons 2002). Patches can also be structured using biological habitat templates (Townsend and Hildrew 1994, Townsend et al. 1997a, Parker and Huryn 2011), geomorphic habitat templates (Wadeson and Rowntree 1998, Thomson et al. 2001), or using hierarchical filters (Poff 1997). The HPD is important because it recognizes the nesting of scales in stream ecosystems as well as the connection between patches. Patch function can be disturbance based (Townsend et al. 1997b, Lake 2000) or directly linked to existing stream conditions (Palmer and Poff 1997, Palmer et al. 2000, Thomson et al. 2001, Cardinale et al. 2002).

1.3.1.2 Spatial Framework of Interest

The frameworks used in this proposal to describe the spatial patterns of streams at large and fine-scales include the stream discontinuum concept, HDP, and habitat templates. Ward and Stanford (1983) developed the Serial Discontinuity Concept to describe the influence of reservoirs and other impoundments on the structure and function of streams. This was recently expanded upon by Jones (2010b) highlighting the need for lakes to be incorporated into conceptual frameworks of streams and rivers. The hierarchical classification of stream reaches into distinct levels is also an important method to describe patterns in streams (Frissell et al. 1986). Using HPD approaches microhabitats/point

measurements (1.0 – 0.1m^2) and habitat patches (100 – 1.0 m^2) can be hierarchically nested within study reaches (10,000m^2 – 100m^2) based on geomorphic characteristics and hydraulics (Wadeson 1994, Wadeson and Rowntree 1998, Thomson et al. 2001). Finally, habitat templates are critical frameworks because they allow disturbances to be incorporated into the patterns observed in streams at multiple scales (Townsend et al. 1997a, Parker and Huryn 2011).

1.3.2 Challenges Linking Scales, Patterns, and Process

Once spatial patterns have been determined in streams it is necessary to understand how hierarchical units and their associated processes link together (Lowe et al. 2006, Campbell Grant et al. 2007, Sandel and Smith 2009, Peterson et al. 2013). There are two critical challenges to linking scale, pattern, and processes in streams: 1) the unique network arrangement of streams is strongly directionally connected by the flow of water, and 2) interactions between the stream and the floodplain as well as areas of transient storage.

The strong longitudinal connectivity between any stream reach or habitat patch and downstream organizational units is a critical characteristic of lotic ecosystems (Gomi et al. 2002). Microhabitats, habitat patches, and reaches at one location are in some way linked to downstream patterns and processes (Lowe et al. 2006). Junctions in dendritic stream networks are especially unique because any point downstream of a tributary incorporates both network and two-dimensional structural and functional attributes from the upstream channels (Ver Hoef and Peterson 2010, Peterson et al. 2013). Longitudinal linkages have been described at large-scales using directional geostatistical approaches that incorporate

network shape and hydrologic distances (Ver Hoef and Peterson 2010, Peterson et al. 2013) and at small-scale using traditional geostatistical methods (Clifford et al. 2005, Legleiter 2014).

Reach and patch function is further complicated by horizontal interactions between the stream and its adjacent floodplain as well as the vertical exchanges between surface and subsurface waters (Ward 1989, Boulton et al. 1998, Schiemer et al. 2001, Wiens 2002). Inshore retention (Shcheimer et al. 2001) or transient storage zones (Fellows et al. 2001, Argerich et al. 2011) have been shown to significantly impact the function of entire stream ecosystems. Transient storage zones are areas connected to a main advective stream flow where surface water velocity is slowed down by stream features (Zarnetske et al. 2007). The transient storage occurs in the hyporheic zones below the benthic surface as well as in pool backwaters and eddies (Runkel and Bencala 1995). The hyporheic zone is particularly important to stream function (Brunke and Gonser 1997, Boulton et al. 1998, Boulton et al. 2010) and has similar temporal and spatial heterogeneity as the benthic surface of the stream (Jones et al. 1995, Jones and Holmes 1996).

1.3.3 Opportunities for Linking Scale, Patterns, and Process

The three issues presented above reinforce why scale is a fundamental challenge to all ecological studies (Wiens 1989, Levin 1992, Schneider 2001) and provide opportunities for identifying critical gaps in our understanding of aquatic ecosystems (Palmer and Poff 1997, Cooper et al. 1998, Wiens 2002, Lowe et al. 2006, Thorp et al. 2006). Pringle et al. (1988) recognized that choosing appropriate scales is situation-dependent, yet the issue of

choosing the appropriate study scale(s) and recognizing multiple interacting scales of influence still eludes aquatic ecologists. Observational and methodological bias and translation between scales is additionally problematic in stream ecosystem studies; specifically, the use of microcosms and mesocosms (Bott et al. 1978, Grimm and Fisher 1984, Naegeli and Uehlinger 1997, Fellows et al. 2001, Fellows et al. 2006) need to be evaluated for their limitations and relevance to larger-scale estimates of ecosystem process (Thrush et al. 1997, Hewitt et al. 2007). Finally, the issue of scale-dependence needs to be explored in lotic ecosystems (Cooper et al. 1997, Hewitt et al. 2007, Sandel and Smith 2009). Determining where scale and spatial dependencies exists and how those dependencies affect stream structure and function presents a critical gap in our understanding of lotic ecosystems.

1.4 Summary

A variety of methodologically and analytical techniques are presented in this dissertation to evaluate issues of scale in stream and rivers. The following chapters address issues of scale that affect our ability to assess ecosystem function, such as: methodologies used to scale ecosystem measurements, multiple interacting scales, translation between scales, and scale-dependencies.

The first study provides a robust assessment methodology used to evaluate chlorophyll a in aquatic biofilms. Quantification of chlorophyll a is essential to the study of aquatic ecosystems, yet differences in methodology may introduce significant errors to its determination in ethanol extracts. These errors can lead to issues of comparability

between studies, especially when chlorophyll a biomass is used as a scaling variable for key ecosystem functions, such as metabolism. The second study examined interacting scales and translation between scales by examining how normalization approaches effect measurements of aquatic biofilm metabolism. The final study examined how watershed level inorganic and organic nutrient dynamics are influenced by the presence and absence of lakes and how catchment characteristics can be used to predict nutrient concentrations. The findings of this study can be used to quantify dissolved organic carbon (DOC), dissolved organic nitrogen (DON), and TDN throughout a watershed.

CHAPTER 2: THE EFFECT OF ACID STRENGTH AND POSTACIDIFICATION REACTION TIME ON THE DETERMINATION OF CHLOROPHYLL *A* IN ETHANOL EXTRACTS OF AQUATIC PERIPHYTON

ABSTRACT

Quantification of chlorophyll *a* (Chl *a*) is essential to the study of aquatic ecosystems, yet differences in methodology may introduce significant errors to its determination in ethanol extracts. Insufficient acidification slows the conversion of Chl *a* to pheophytin *a* leading to an underestimate of Chl *a* concentration. Furthermore, slight differences in the postacidification reaction time can introduce greater errors in calculated Chl *a* and impede our ability to make cross-study comparisons. We used known concentrations of pure Chl *a* from the blue-green algae *Anacystis nidulans* dissolved in 95% ethanol to evaluate the effect of acid strength and postacidification reaction time on the spectrophotometric determination of Chl *a*. Increasing acid strength resulted in more rapid stabilization of calculated Chl *a* concentration. At reaction times less than 120 s estimates of Chl *a* deviated from known concentrations by as much as 84.8%. The magnitude of error in the calculated Chl *a* values were dependent on acid strength and reaction time, which allowed us to develop predictive equations to correct Chl *a* measurements that were insufficiently acidified or read prior to reaction completion. We validated our predictive equations using benthic periphyton samples from northern Alaska and northwestern Vermont, U.S.A. Our results indicate that under-acidified samples with known reaction times can be easily corrected so results from different methods can be standardized. For future analyses we recommend acidifying ethanol-extracted algal samples to 0.008 mol HCl L^{-1} and allowing samples to react for 30–60 min to ensure accurate and consistent results.

2.0 Introduction

Precise and accurate quantification of algal chlorophyll *a* (Chl *a*) is critical to the study of aquatic ecosystems. The concentration of Chl *a* in periphyton and phytoplankton samples is widely used as a surrogate for algal biomass (Nusch 1980, Jeffrey et al. 1997) and primary production (Morin et al. 1999). The relationships between algal pigment concentration, biomass, metabolism, and nutrient uptake (Lehman 1981, Dodds et al. 2002) suggest that Chl *a* is also an important scaling metric that can be used to normalize rates of ecosystem function. For example, autotrophic production or nutrient assimilation normalized by Chl *a* content can highlight community (Arscott et al. 1998) or taxa-specific physiological responses to varying environmental conditions (Elrifi and Turpin 1987). However, seemingly minor methodological differences in spectrophotometric approaches between studies may introduce substantial variability in results (Wasmund et al. 2006) and alter the interpretation of long-term (Graff and Rynearson 2011) and spatial (Boyce et al. 2012) datasets.

Numerous methods have been utilized to determine the concentration of Chl *a* using ethanol solvents (Nusch 1980, Sartory and Grobbelaar 1984, Jespersen and Christoffersen 1987, Hansson 1988, Thompson et al. 1999). The lack of consensus among methods has led to extensive experimental work evaluating how extraction procedure (Porra and Grimme 1974, Sartory and Grobbelaar 1984, Porra 1990, Thompson et al. 1999, Wasmund et al. 2006), solvent type (Marker 1972, Arvola 1981, Bowles et al. 1985, Hagerthey et al. 2006), storage conditions (Reuss and Conley 2005, Wasmund et al. 2006, Graff and Rynearson 2011), and calculation equations (Ritchie 2006, Qin et al. 2013) affect Chl *a*

concentrations. However, few studies have used these findings to develop robust and standardized techniques for reliable and reproducible measurement of algal pigments (Graff and Rynearson 2011). This is especially the case when ethanol, a safer alternative to acetone (Ritchie 2006), is used as the extractant of choice.

The determination of Chl *a* relies on the conversion of Chl *a* into pheophytin *a* (Phe *a*) after being treated with hydrochloric acid (Lorenzen 1967). Conversion of Chl *a* to Phe *a* is initiated by protons from the dilute acid, which replace magnesium ions within the porphyrin ring of the Chl *a* molecule (Joslyn and Mackinney 1938). This chemical reaction causes a shift in peak absorbance within the red spectra from 664 nm (Chl *a*) to 665 nm (Phe *a*; Figure 1). The magnitude of this spectral shift is proportional to the concentration of Chl *a* and can therefore be used to calculate its concentration based on the known optical properties of pure Chl *a* in the extractant solvent.

Post-acidification reaction time is the specified time needed for complete conversion of Chl *a* to Phe *a* in a given sample. Algal pigments extracted using ethanol require stronger acid concentrations than methanol and acetone solvents in order to appropriately lower pH to an acceptable range for pigment determination (Moed and Hallegraeff 1978, Arvola 1981). According to Nusch (1980) sample acidification to 0.006 mol HCl L^{-1} results in complete absorbance shifts within one minute, whereas acidification to 0.0004 mol HCl L^{-1} results in absorbance shifts that take over three hours to complete. Levine et al. (1997) observed shifts in spectral absorbance that persisted for as long as 30 minutes after acidification when samples were acidified to 0.005 mol HCl L^{-1}.

Such large inconsistencies in the reaction time required for complete conversion to Phe *a*, as a function of the choice of sample acid concentration used, suggests that both acid strength and post-acidification reaction time are important factors to consider when measuring Chl *a* using ethanol solvents. Traditional monochromatic analysis of Chl *a* such as those described in Standard Methods for the Examination of Water and Wastewater (APHA 2012) call for samples to be acidified to 0.003 mol HCl L^{-1} with 90 s post-acidification reaction time. APHA (2012) highlights the importance of acid strength and post-acidification reaction time, however, the method does not provide any specific rationale as to why reaction time is critical to the quantification of algal Chl *a*. Moreover, despite being developed for use with 90% acetone, the APHA acidification procedure has been used for ethanol extractions, which could result in substantial underestimation of the Chl *a* concentration. Methods that recommend sample acidification with lower acid strength and similar 90 s reaction time using ethanol solvents (LINX II Methods unpubl., (Mulholland et al. 2008)) could potentially be even more susceptible to errors. The most widely cited ethanol-based method developed by Sartory and Grobbelaar (1984) calls for acidification to 0.0075 mol HCl L^{-1}, although several methods recommend even stronger final acid concentrations (Arvola 1981, Hansson 1988).

Differences among these methods and how they have been employed provide the motivation for this study. Our first objective was to evaluate how reaction time and acid strength influence the calculation of pigment concentration in samples extracted using 95% ethanol. We then used information from our initial investigation to develop a robust set of predictive equations to retroactively correct and standardize previous Chl *a* measurements

made using several acid concentrations across common post-acidification reaction times. Finally, we used benthic periphyton samples from northern Alaska and northwestern Vermont, USA to validate our predictive equations.

2.1 Materials and Procedures

2.1.1 Chl *a* Standard and Acid Preparation

While 90% and 95% ethanol are both suitable for the extraction of Chl *a* (Sartory and Grobbelaar 1984), we used 95% ethanol for this study because its concentration (v/v) is most similar to that used by (Wintermans and De Mots 1965) to develop specific absorption coefficients (96% ethanol). Experimental solvents were made on a volumetric basis using 95% anhydrous ethanol (Sigma E7023) and 5% deionized water.

Pure Chl *a* extracted from the freshwater blue-green algae *Anacystis nidulans* (Sigma Aldrich C1644) was combined with 95% ethanol to make a stock Chl *a* solution. To ensure the accuracy of the standard, solid Chl *a* crystals were carefully measured on a six-point microbalance (Mettler Toledo® XP26DR) and combined with 200 mL of 95% ethanol at room temperature (20ºC). The resulting stock solution contained 4.15 mg Chl *a* L^{-1}, which was diluted by mass in 40 mL borosilicate scintillation vials with 95% ethanol to create working standards containing 0.00, 1.09, 1.99, 3.00, and 3.98 mg Chl *a* L^{-1}. We targeted Chl *a* concentrations less than 4.0 mg Chl *a* L^{-1} for our standards based on the absorbance recommendations made by Lorenzen (1967), which states that pre-acidification peak absorbance values should range from 0.2 to 0.5. We developed our standards to fall within and below this range (Peak Abs. = 0.0 – 0.35 abs.) to test the sensitivity of our

spectrophotometer at low concentrations of Chl *a* typical for stream periphyton analyses. The stock solution and standards did not contain Phe *a* pigment (0.0 mg Phe *a* L^{-1}). All chlorophyll handling and subsequent spectrophotometric analyses were carried out in a dark room where the ambient photosynthetically active radiation was less than 0.25 μmol m^{-2} s^{-1} because photosynthetic pigments can degrade when exposed to light (Wasmund 1984). To minimize potential acid contamination, glassware was soaked in deionized water for 24 hours and rinsed with 95% ethanol solution prior to use.

Acid treatments were diluted on a volumetric basis using reagent grade hydrochloric acid (Fisher A144) and deionized water to 0.03, 0.10, 0.25, and 0.50 mol HCl L^{-1}. The addition of 0.10 mL of each acid treatment to 3.0 mL of ethanolic sample resulted in a range of target acid concentrations commonly used for ethanol-based analyses (Table 1).

2.1.2 Pigment Analysis and Calculations

Pigment analysis was carried out using a dual-beam ultraviolet-visible spectrophotometer (Shimadzu UV-2600) with a 1 cm light path cuvette holder. The spectral bandwidth of the instrument was set to 1.0 nm with a medium scan speed so repeated measurements could be made at multiple wavelengths.

Experimental concentrations of Chl *a* in 95% ethanol solutions were calculated for each scan based on the monochromatic equations originally developed by Lorenzen (1967)found in APHA (2012):

$$\text{Chl } a = [A \times K \times [(664_b - 750_b) - (665_a - 750_a)] \times V_e] / V_f \times l \qquad (1)$$

where Chl *a* is the pigment concentration (mg Chl *a* L^{-1}); A is the inverse absorption extinction coefficient equivalent to 11.99 mg Chl *a* cm L^{-1} (Wintermans and De Mots 1965); K, the absorption reduction factor of 2.43 (Lorenzen 1967); 664_b is the baseline absorbance at 664 nm before acidification; 750_b is absorbance at 750 nm before acidification; 665_a is the absorbance at 665 nm after acidification; 750_a is the absorbance at 750 nm after acidification; V_e is the volume of 95% ethanol used to extract the pigment (mL); V_f is the volume of sample filtered (mL); and *l* is the path length of the cuvette (cm).

Experimental concentrations of Phe *a* were calculated for each scan based on the monochromatic equations in APHA (2012):

$$\text{Phe } a = [A \times K \times [R \times (665_a - 750_a) - (665_b - 750_b)] \times V_e] / V_f \times l \quad (2)$$

where Phe *a* is the pigment concentration (mg Phe *a* L^{-1}); the maximum absorbance ratio, R, is 1.7 (Lorenzen 1967); and all other coefficients are as noted above.

The stock Chl *a* standard was used to calculate the observed inverse absorption extinction coefficient, $A_{observed}$ (mg Chl *a* cm L^{-1}); maximum absorbance ratio, $R_{observed}$; and absorption reduction factor, $K_{observed}$, as follows:

$$A_{observed} = (664_b - 750_b) / \text{Chl } a \qquad (3)$$

$$R_{observed} = (664_a - 750_a) / (665_b - 750_b) \qquad (4)$$

$$K_{observed} = R_{observed} / (R_{observed} - 1) \qquad (5)$$

2.1.3 Effect of Acid on pH of 95% Ethanol

To determine the effect of acidification on the pH of 95% ethanol, we measured the pH before and after the addition of each acid treatment using a calibrated Fisher AB15 pH probe. This analysis was conducted based on recommendations made by Moed and Hallegraeff (1978), who suggested that acidification to a pH of 2.6 to 2.8 is optimal for ethanolic extracts. Four replicate 1.5 mL aliquots of 95% ethanol were pipetted into 15 mL polypropylene conical vials and placed into a 20 ºC water bath to ensure consistent temperature between acid treatments and replicates. The glass pH probe was used to gently stir the ethanol solution until the pre-acidification pH stabilized, typically about 10-15 min. After pre-acidification pH measurements were recorded, each sample was acidified with 0.050 mL of each dilute hydrochloric acid treatment (Table 1) and post-acidification pH was measured following the same procedure. For each acid treatment, replicate post-acidification pH measurements were averaged and regressed against the $-\log_{10}$ transformed molar concentration of protons from the added hydrochloric acid to compare molar acid strength to previous recommendations made using pH. Linear regression analysis was conducted using JMP® Pro Version 12.0 (SAS Institute Inc.) statistical software (JMP®).

2.1.4 Effect of Reaction Time on Chl *a* Calculation

The effect of post-acidification reaction time on calculated Chl *a* and Phe *a* concentration was evaluated using repeated absorbance measurements following the addition of each acid treatment. Three (3) mL of 4.15 mg Chl *a* L^{-1} stock solution was pipetted into a 10.00 mm quartz cuvette (Hellma® QS) and the baseline absorbance was

recorded with respect to a quartz reference cuvette filled with 95% ethanol containing no Chl *a*. After baseline absorbance was determined, the sample containing Chl *a* was acidified using each of the four dilute acid treatments and immediately covered with Parafilm M® to prevent evaporative solvent losses. The acidified stock solution was mixed by inverting once (Riemann 1978), and returned to the spectrophotometer for at least one hour of repeated spectral readings. Chl *a* and Phe *a* concentrations were calculated using the absorbance measurements for each spectral reading and post-acidification timing was determined with respect to the 665 nm absorbance reading. A control sample not treated with acid was also scanned for one hour to evaluate whether the spectral composition of dissolved Chl *a* changed in response to repeated light exposure from the spectrophotometer. No changes above the photometric repeatability of the instrument were observed (< 0.001 Abs).

2.1.5 Effect of Pigment Concentration on Chl *a* Calculation

Using the Chl *a* standards, we evaluated the effect of pigment concentration on calculated Chl *a* after acidification with each acid treatment ranging from 0.001 to 0.016 mol HCl L^{-1} (Table 1). Our evaluation targeted 60, 90, and 120 s reaction times based on recommendations in Riemann (1978), APHA (2012), and Sartory (1982), respectively. To cover the full range of targeted reaction times the spectrophotometer was programed to take repeated measurements at 664, 665, and 750 nm wavelengths every 10 s during the 60 to 120 s period following acidification. The 90 s reaction time was identified as focal target time for this study because it represents the median recommended reaction time used for Chl *a* analyses. Additionally, APHA (2012) emphasizes the need to take post-acidification

readings at exactly 90 s to ensure accurate, consistent results, and although the 90 s reaction time associated with the APHA method was developed for 90% acetone, it has mistakenly been used for ethanol-extracted chlorophyll pigments.

For the 0.00, 1.09, 1.99, 3.00, and 3.98 mg Chl *a* L^{-1} standards, duplicate 3.0 mL aliquots were pipetted into 1.0 cm polystyrene cuvettes (Fisherbrand™ 14-955-125). Baseline absorbance values were measured with respect to a blank reference due to slight variations in absorbance among polystyrene cuvettes. After baseline absorbance values were determined, each sample was acidified using one of the four acid treatments, covered with parafilm, and inverted once before being returned to the spectrophotometer. Spectral readings were taken every 10 s during the 60 to 120 s period following acidification. Additional spectral scans were taken one hour (1 h) after acidification. The 1 h reaction time was determined during the previous experiment to be the amount of time needed for full stabilization in the 665a wavelength based on the accuracy limits of the spectrophotometer. Lab duplicates were averaged for each post-acidification reaction time, Chl *a* standard, and acid treatment.

2.1.6 Predictive Model Development

We used the results from analysis of the Chl *a* standards to develop a suite of predictive models that could be used to correct previous measurements of Chl *a* where acidification or post-acidification reaction time was inadequate. Mean calculated Chl *a* concentration for 60, 90, and 120 s reaction times were regressed against calculated 1 h Chl *a* and the known Chl *a* concentration of each standard using JMP®.

Model parameters specific to each reaction time and acid treatment were used to calculate predicted 1 h Chl *a* and predicted Chl *a* for any periphyton or phytoplankton sample extracted with 95% ethanol. For each acid treatment calculated Chl *a* concentrations measured with 60, 90, or 120 s post-acidification reaction times can be corrected as follows:

$$\text{Chl } a_{\text{predicted}} = \beta_0 + \text{Chl } a_{\text{observed}} \times \beta_1 \quad (6)$$

where, Chl $a_{\text{predicted}}$ is the predicted Chl *a* concentration (mg Chl *a* L^{-1}) and Chl a_{observed} is the concentration (mg Chl *a* L^{-1}) of the under-acidified sample with 60, 90, or 120 s reaction times, β_0 is the intercept parameter (mg Chl *a* L^{-1}), and β_1 is the slope parameter (unitless). Chl $a_{\text{predicted}}$ can be determined for both predicted Chl *a* and predicted 1 h Chl *a* concentrations depending on the parameters used. Predicted 1 h Chl *a* correction parameters were used to validate whether periphyton samples with early reaction times can be corrected to a stable (1 h) reaction time. The predicted Chl *a* correction parameters were used to ensure that insufficiently acidified samples could be standardized across multiple final acid treatments or reaction times.

2.1.7 Predictive Model Validation

Model validation was carried out using benthic periphyton samples collected from a clearwater tundra stream in northern Alaska (n=30) and from six suburban-agricultural streams in northwestern Vermont, USA (n=38). This comparison ensured that our predictive equations would correct algal-extracted Chl *a* from different regions and stream types. Algal samples were scrubbed from rock surfaces with a stainless steel brush and

stream water as described in Bowden et al. (1992). In the laboratory, 2-10 mL of the algae-water scrub mixture was filtered using a 25 mm Whatman GF/F filter. Filter tower vacuum pressure did not exceed 30 kPa below atmospheric pressure. Filters were removed from the tower, folded in half, and placed into a 15 mL polypropylene conical vial. Samples were stored frozen at -80 ºC for no more than three months prior to extraction using the hot ethanol method (Sartory and Grobbelaar 1984). Five milliliters (5 mL) of 95% ethanol were pipetted into each conical vial and samples were placed into a 78 ºC water bath for 5 min. After heating, the samples were chilled on ice and mixed vigorously for 10 to 15 s using a vortex mixer. Extraction continued for 24 h in a freezer at -20 ºC. Following extraction, samples were centrifuged for 15 min at 3000 rpm and extract supernatants were analyzed in polystyrene cuvettes as discussed above.

Extracted samples from both regions were acidified to 0.001 mol HCl L^{-1} and post-acidification measurements were taken with 90 s and 1 h reaction times. Validation of extracts acidified to 0.003 mol HCl L^{-1} was limited to the periphyton samples collected in Vermont, because replicates were not available from Alaska. Regression parameters were applied to 90 s calculated Chl *a* to determine predicted 1 h Chl *a* and predicted Chl *a* concentrations. Observed 1 h Chl *a* was then compared to the predicted 1 h Chl *a* to ensure that the equations could retroactively correct algal Chl *a* concentrations to longer reaction times. The 1 h reaction time represented a stable reaction time where minimal spectral shift based on the observed absorbance at 665a were observed. Finally, we used one-way analysis of variance (ANOVA) to test if predicted Chl *a* concentrations in samples acidified

to 0.001 mol HCl L^{-1} were significantly different from predicted Chl *a* in samples acidified to 0.003 mol HCl L^{-1}.

2.2 Assessment

2.2.1 Effect of Acid on pH of 95% Ethanol

Prior to acidification, the mean ± SD pH of the 95% ethanol among all four treatments (Table 1) and replicates (n=16) was 8.53 ± 0.05. The addition of acid resulted in mean post-acidification pH values of 3.09, 2.54, 2.18, and 1.92 for the samples containing 0.001, 0.003, 0.008 and 0.016 mol HCl L^{-1}, respectively (Figure 2). Standard deviations for all post-acidification pH values did not exceed 0.01.

Given the similar acid disassociation constants of water (pKa = 15.7) and ethanol (pKa = 15.9) (Olmstead et al. 1980) we wanted to confirm that the observed post-acidification pH and the $-\log_{10}$ transformed molar proton concentration of the hydrochloric acid in acidified samples closely followed a one-to-one relationship (Figure 2). Observed post-acidification pH was positively correlated to the $-\log_{10}$ transformed molar proton concentration for the four target acid concentrations studied ($df = 3$; $t = 23.83$; $p < 0.002$; $R^2 = 0.995$). A slight deviation in the slope of the modeled relationship between $-\log_{10}$ transformed acid concentration and observed pH could potentially be attributed to calibration errors in the pH probe. Our pH probe was calibrated using pH 4, 7, and 10 buffer solutions (YSI #3824) and the pH range observed in the acidified 95% ethanol was two orders of magnitude lower than our lowest calibration buffer.

Moed and Hallegraeff (1978) recommended extracting algal samples using 80% ethanol and then acidifying extracts to a pH of 2.6 to 2.8 to achieve optimal spectral shifts for pigment quantification. To reach the desired pH range, their acidification procedure called for two drops (~0.10 mL) of 0.4 mol HCl L^{-1} added to an 8 or 25 mL sample volume. This procedure would yield an estimated final acid concentration of 0.005 to as little as 0.002 mol HCl L^{-1} depending on the volume of the 'drop' (Figure 2). The relationship between $-\log_{10}$ transformed acid concentration and pH observed by Moed and Hallegraeff (1978) was not consistent with our results, which indicate that a final acid concentration of 0.003 to 0.002 mol HCl L^{-1} equates to a pH range of 2.6 to 2.8. Nusch (1980) reported that the optimal pH range of 2.6 to 2.8 could be achieved in samples extracted in 90% ethanol by acidifying to 0.006 mol HCl L^{-1}, yet our observations illustrate that acidification to 0.006 mol HCl L^{-1} correspond to a post-acidification pH of 2.3. Due to the lack of agreement between measured pH and final acid concentration among studies, we conclude that pH may not be the best indicator of whether a sample has been sufficiently acidified. We recommend that the molar hydrogen ion concentration (from hydrochloric acid) in the acidified sample should be used in lieu of pH to reliably represent the required acidification treatment condition for subsequent Chl *a* analyses.

2.2.2 Effect of Reaction Time on Pigment Calculation

Calculated Chl *a* and Phe *a* concentration changed substantially during the evaluation period depending on the acidification treatment (Figure 3). Higher acid treatment concentrations resulted in more constrained ranges of calculated Chl *a* and Phe *a*, whereas lower strength acid treatments resulted in larger ranges of observed pigment

concentration. This trend indicates that a subset of reactions may have been acid-limited. The lowest acid treatment resulted in Chl *a* that ranged from 0.69 to 3.84 mg Chl *a* L^{-1} and Phe *a* that ranged from 0.50 to 5.84 mg Phe *a* L^{-1} during the evaluation period. Observed Chl *a* concentration at 1 h was 7.5% lower than the known Chl *a* when acidified to lowest experimental treatment concentration of 0.001 mol HCl L^{-1}. Increasing the final acid concentration to 0.003 mol HCl L^{-1} (the APHA recommendation) led to more rapid stabilization of calculated pigment content, where Chl *a* and Phe *a* concentrations ranged from 2.75 to 4.06 mg Chl *a* L^{-1} and 0.12 to 2.34 mg Phe *a* L^{-1}, respectively. This APHA-equivalent acid treatment underestimated Chl *a* by 33.8 to 14.4% during the 60 to 120 s reaction times, respectively, and underestimated Chl *a* by 2.5% at 1 h.

Pigment concentrations stabilized rapidly when the sample was acidified to a final concentration of 0.008 mol HCl L^{-1}, the treatment recommended by Sartory and Grobbelaar (1984). Calculated Chl *a* in the sample ranged from 4.10 to 4.14 mg Chl *a* L^{-1}, and represented a deviation of less than 1.3%. At this acid treatment concentration, Phe *a* was also extremely close to the known concentration, ranging from -0.03 to 0.04 mg Phe *a* L^{-1} throughout the measurement period. Acidification to 0.016 mol HCl L^{-1} resulted in an immediate plateau of pigment concentration that exceeded known Chl *a* standard concentrations by 2.2 to 3.9%. Calculated Chl *a* and Phe *a* ranged from 4.26 to 4.31 mg Chl *a* L^{-1} and -0.31 to -0.21 mg Phe *a* L^{-1}, respectively. The highest acid treatment (0.016 mol HCl L^{-1}) had a mean Chl *a* concentration of 4.30 ± 0.01 mg Chl *a* L^{-1} for the entire evaluation period. The low coefficient of variation (CV < 0.3%) observed in calculated Chl *a* for the two highest acid treatment indicates that calculated concentrations remain

consistent for at least one hour after acid has reacted fully with the Chl *a* pigments. Therefore, we recommend longer reaction times of 30 to 60 minutes to improve measurement consistency and to ensure full pheophytinization when quantifying ethanol extracts of Chl *a*.

The wide range of calculated Chl *a* and Phe *a* concentrations in samples acidified to 0.001 mol HCl L^{-1} and 0.003 mol HCl L^{-1} is explained by rapid changes in absorbance at 665 nm as Chl *a* is converted to Phe *a*. This is because the equation developed by Lorenzen (1967) relies on the absorption reduction factor, K = R / (R-1), which assumes that the maximum ratio between 664_b and 665_a is R = 1.7 for Chl *a* containing no Phe *a*. When the absorbance measured at 665 nm is asymptotically approaching a stable value, the observed maximum ratio $R_{observed}$ will be lower than 1.7 until stability of all absorbance values is achieved. The stabilization period will also be reflected by increasing values for the absorption reduction factor ($K_{observed.}$). Incomplete reaction of HCl with Chl *a* was observed for samples acidified to 0.001 and 0.003 mol HCl L^{-1} in which $R_{observed}$ was less than R and $K_{observed}$ was greater than K (Table 2). The deviation between observed and empirical coefficients is the result of incorrect scaling of 664 and 665 nm absorbance values that can lead to the underestimation of Chl *a* and overestimation of Phe *a* concentration. This was not an issue for the sample acidified to 0.008 mol HCl L^{-1} for which the mean ± SD $R_{observed}$ and $K_{observed}$ across all spectrophotometric readings made from 60 s to 1 h (n=176) were 1.70 ± 0.00 and 2.43 ± 0.00, respectively. In the highest acidification treatment, $R_{observed}$ was greater than R and $K_{observed}$ was less than K. The variability in $R_{observed}$ and $K_{observed}$ coefficients indicate that particular combinations of reaction times

and acid concentrations are needed to best align observed coefficients with the empirical coefficients developed by Lorenzen (1967). Based on our findings, we recommend a target acid concentration of 0.008 mol HCl L^{-1} to achieve appropriate coefficients for Chl *a* calculation in 95% ethanol.

The inverse absorption extinction coefficient at 664 nm, $A_{observed}$, was also determined. $A_{observed}$ is not sensitive to acidification because it is calculated using absorbance values measured before acid is added to the ethanol extracted Chl *a*. Mean $A_{observed}$ was 12.07 ± 0.01 mg Chl *a* cm L^{-1} (n=4) which was slightly higher than the published value of 11.99 mg Chl *a* cm L^{-1} developed by Wintermans and De Mots (1965). The deviation between observed and empirical A coefficients was less than one percent and had minimal influence on the overall calculated Chl *a* concentration.

In addition to highlighting the importance of timing on pigment calculations for individual acidification treatments, our findings illustrate that the rate of conversion of Chl *a* to Phe *a* is dependent on the concentration of acid in the sample and that low acid strengths limit the rate of the reaction. Pioneering work by Joslyn and Mackinney (1938) demonstrated this same trend and concluded that chlorophyll pigments exhibit first-order reaction kinetics with respect to the concentration of acid. Because the reaction rate advances predictably for a given acid concentration, it should be possible to reliably calculate the concentration of Chl *a* at stable reaction time if the post-acidification reaction time is known.

2.2.3 Effect of Pigment Concentration on Calculated Chl *a*

We assessed the relationship between calculated and known Chl *a* concentrations to confirm that errors associated with reaction time and acid treatment occur independent of pigment concentration. For all Chl *a* standards tested, the calculated pigment concentrations at 60, 90, and 120 s displayed positive, linear relationships with known concentrations of Chl *a* as well as Chl *a* measured 1 h after acidification (Figure 4). When treated with the lowest acid concentration, the calculated Chl *a* underpredicted known values of all four standards. The extent of underestimation in the lowest acid treatment was alleviated as post-acidification read time increased, with mean ± SD calculated Chl *a* concentrations 84.8 ± 1.9%, 81.9 ± 2.3%, and 79.7 ± 2.4% lower than known values at 60, 90, and 120 s, respectively. Acidification to 0.003 mol HCl L^{-1} resulted in Chl *a* that underpredicted known concentrations by 32.7 ± 4.0%, 21.4 ± 3.3%, and 16.1 ± 2.2% for readings made 60, 90, and 120 s following acidification. As demonstrated previously, post-acidification reaction time did not have a pronounced influence on measured concentration when samples were acidified to 0.008 and 0.016 mol HCl L^{-1}. Sixty (60), 90, and 120 s reaction times resulted in 3.4 ± 0.5%, 3.0 ± 0.8%, and 3.1 ± 0.7% lower Chl *a* concentrations when samples were acidified to 0.008 mol HCl L^{-1}. Samples acidified to 0.016 mol HCl L^{-1} overpredicted Chl *a* by 1.5 ± 1.0% for all acid treatments and Chl *a* concentrations evaluated. Testing the effect of pigment concentration on calculated Chl *a* provides additional evidence to support that reaction between hydrochloric acid and Chl *a* proceed independent of pigment concentration.

Our findings also demonstrate that acidification to 0.003 mol HCl L^{-1} is more sensitive to calculation errors associated with reaction time than the other acid treatments studied. Samples acidified to 0.001 mol HCl L^{-1} experience a gradual decline in absorbance at 665a, which corresponds to slight increases in calculated Chl *a* concentration during the 60 to 120 second sampling window. On average, total change in calculated concentration during the 60 to 120 s reaction time period deviates from the known concentration by 5.1 ± 0.5% (Figure 4). When target acid concentration increases to 0.003 mol HCl L^{-1}, calculated concentration during the 60 to 120 s reaction time period changes much more rapidly and total change in calculated concentration deviates from the known concentration by 16.6 ± 2.0%. This means samples acidified to 0.003 mol HCl L^{-1} may be more sensitive to errors than samples acidified to 0.001 mol HCl L^{-1} if there is uncertainty regarding whether or not the post-acidification spectrophotometric reading is taken exactly at the prescribed reaction time. The increasing magnitude of error associated with reaction time uncertainty can be visualized by examining the 60 and 120 s regression lines for samples acidified to 0.001 and 0.003 mol HCl L^{-1} (Figure 4). We attribute timing uncertainty to the increased width of the 95% prediction interval observed on the 90 s calculated samples acidified to 0.003 mol HCl L^{-1}.

Acidification to 0.008 or 0.016 mol HCl L^{-1} both resulted in calculated Chl *a* concentrations that did not deviate substantially from known concentrations. In fact, the 0.016 mol HCl L^{-1} acid treatment showed slightly better alignment with the one-to-one line than standards acidified to 0.008 mol HCl L^{-1} (Figure 4c and 4d). This would suggest that acidification to 0.016 mol HCl L^{-1} is an adequate approach for determining pigment

concentration in pure Chl *a* extracts, however, increasing acid concentration in ethanol extracts of natural algal communities could lead to interferences by secondary pigments, such as chlorophyll *b* (Chl *b*) or chlorophyll *c* (Chl *c*) that could affect the determination of Chl *a*. When secondary photosynthetic pigments are present in an extracted algal sample their spectral properties may contribute to the absorbance measured at 664, 665, or 750 nm wavelengths and cause parallel identification (Ritchie 2006, Henderson 2015). Additionally, excess acid concentrations can form new compounds that may result in spectral interference and reduce the observed magnitude of post-acidification spectral shifts (Holm-Hansen and Riemann 1978, Riemann 1978). Because this experiment was conducted with pure Chl *a* extracts, it is possible that 0.016 mol HCl L^{-1} may not be the most appropriate acid treatment for mixtures of chlorophylls typical in natural periphyton or phytoplankton assemblages. Arvola (1981) found the acid concentration 0.01 mol HCl L^{-1} to be optimal for ethanol extracts of algae. At this acidification level, Arvola (1981) reports that deleterious spectral shifts, which occur at higher acid concentrations, are minimized. Similarly, Sartory (1982) recommended acidification to 0.006 to 0.009 mol HCl L^{-1} to avoid the formation of undesirable secondary pigments. Thus, we conclude that acidification to 0.008 mol HCl L^{-1} is the most conservative approach for determining Chl *a* in 95% ethanol because: 1) it is strong enough to cause rapid spectral shifts, 2) the resulting protonated pigment is stable for at least one hour, and 3) spectral measurements are therefore not confounded by the formation of secondary pigments.

2.2.4 Predictive Model Development

We used the relationships between known and calculated concentrations of the Chl *a* standards to develop predictive models to determine Chl *a* concentrations with stable reaction times and correct measurements from samples analyzed using different acid treatment conditions. The proportional deviations observed between calculated and known Chl *a* content discussed above resulted in 24 regression equations that can be used to determine predicted Chl *a* and predicted 1 h Chl *a* concentration (Table 3). Predicted Chl *a* and predicted 1 h Chl *a* were 3.9 to 5.9 times greater than observed Chl *a* with 60, 90, and 120 s reaction times when samples were acidified to 0.001 mol HCl L^{-1}. When acidified to 0.003 mol HCl L^{-1}, predicted Chl *a* concentrations were 1.1 to 1.5 times greater than observed Chl *a* concentrations. Because the 0.008 and 0.016 mol HCl L^{-1} acid treatments did not deviate by more or less than 5.0%, validation was only conducted on periphyton samples acidified to 0.001 and 0.003 mol HCl L^{-1} with 90 s reaction time.

2.2.5 Predictive Model Validation

Proof of concept – to validate the efficacy of our predictive models we sampled benthic periphyton from several streams in Vermont and Alaska, USA. Parameter estimates were applied to calculated Chl *a* with 90 s reaction time and the resulting predicted 1 h Chl *a* concentrations were compared to observed 1 h Chl *a* in order to determine if periphyton samples with early reaction times could be consistently corrected to a more stable predicted Chl *a* concentration (Figure 5). For both acid treatments tested the agreement between the predicted 1 h Chl *a* concentration and observed 1 h Chl *a* was excellent across a wide range

of Chl *a* concentrations (0.1 to 9.0 mg Chl *a* L^{-1}). Predicted 1 h Chl *a* was significantly correlated with observed 1 h Chl *a* when samples were acidified to 0.001 mol HCl L^{-1} and the slope of the regression line was 1.2% higher than the 1:1 line (df = 67; t = 3.01; $p < 0.001$; $R^2 = 0.956$). When acidified to 0.003 mol HCl L^{-1}, the slope of the line best describing the relationship between predicted 1 h Chl *a* and observed 1 h Chl *a* was only 3.3% higher than the 1:1 line (df = 37; t = 0.59; $p < 0.001$; $R^2 = 0.999$). Further, one-way ANOVA comparing mean predicted Chl *a* concentration in periphyton samples resulted in no significant difference between corrected pigment concentrations acidified to 0.001 and 0.003 mol HCl L^{-1} ($F_{1,74} = 0.30$; $p = 0.587$).

The strong alignment between predicted and observed 1 h Chl *a* confirms that our predictive models can be used to accurately determine Chl *a* concentrations at a more stable reaction time (1 h) as long as the original reaction time is precisely known. This assessment was carried out to ensure that Chl *a* samples previously analyzed using different acid treatments or post- acidification reaction times can be retroactively standardized to consistent methodological conditions. Given the range of the standard curve used to predict Chl *a* concentrations, we have the greatest certainty in predicted pigment concentrations extracted from natural algal assemblages that range from 0.1 to 4.0 mg Chl *a* L^{-1}. However, for both acid treatments four periphyton samples had pigment concentrations that exceeded the range of our standards. These samples were retained in the analysis to demonstrate that our predictive models can also be used to standardize conditions in ethanol pigment extracts with higher Chl *a* concentrations (4.0 to 9.0 mg Chl *a* L^{-1}) as long as the post-acidification reaction time is precisely known. Samples with higher Chl *a* concentrations

had greater variability when acidified to 0.001 mol HCl L^{-1}, likely due to a limiting stoichiometry of protons in the reaction mixture, which would result in the incomplete protonation of Chl *a* and underestimation of spectral shift values. We therefore urge caution when applying the presented predictive models to concentrations greater than 4.0 mg Chl *a* L^{-1}, which have been treated with similarly small additions of acid. Samples acidified to 0.003 mol HCl L^{-1} had excellent agreement throughout the entire range of concentrations encountered and showed no increase in variability when Chl *a* was greater than 4.0 mg Chl *a* L^{-1}.

The lack of significant differences in predicted concentrations between samples acidified to 0.001 and 0.003 mol HCl L^{-1} indicates that our predictive model can be used to standardize ethanol extracts of Chl *a* from multiple stream algal assemblages. Though our model validation focused on freshwater periphyton, our predictive models are suitable for retroactively correcting Chl *a* concentrations in phytoplankton and other algae, assuming that the pigment extraction into 95% ethanol is complete (e.g., sufficient Chl *a* was extracted for the analysis). For example, Levine et al. (1997) used ethanol to extract and quantify Chl *a* concentration in lake phytoplankton samples. Their approach called for 30 min reaction time when evaluating phytoplankton Chl *a* extracts to account for gradual spectrophotometric shifts in samples acidified to 0.005 mol HCl L^{-1}.

We have demonstrated that our predictive models can be used to standardize Chl *a* measurements in samples analyzed using different acid concentrations if post-acidification reaction times are known. However, it is important to consider the two limitations of our predictive models before applying them to past measurements of Chl *a* concentration.

First, our predictive equations are limited to the range of post-acidification reaction times and ethanol concentrations used to develop the models. Because our evaluation focused on the response of pigments extracted in 95% ethanol with 60, 90, and 120 s reactions times across four common final acid treatment concentrations, the predictive equations are restricted to the 12 combinations of reaction times and acid treatments described in Table 3. We anticipate similar linear relationships between observed and predicted Chl *a* concentrations for insufficiently acidified samples extracted in more dilute ethanol solvents (e.g., 80 and 90%), but additional testing is needed to confirm the suitability of our models at other ethanol concentrations. Further evaluation is also needed to develop predictive equations for samples with post-acidification reaction times greater than 60 to 120 s and at different acid strengths.

It is important to note the potential limitations of this approach beyond natural algal communities in which Chl *a* is the dominant photosynthetic pigment. As described in the previous section, the presence of secondary pigments in extracts of natural algal assemblages can confound the determination of Chl *a* due to interference or parallel identification. Our validation experiment demonstrates that the predictive equations accurately determine the Chl *a* concentration at a stable post-acidification reaction time in periphyton samples from well-oxygenated rivers. However, samples collected from algae or photosynthetic bacteria found in unique or extreme environmental conditions, such as poorly mixed anoxic waters, could be difficult to determine due to the abundance of other photosynthetic compounds (Henderson 2015). In order to effectively determine the concentration of multiple pigments, other approaches utilizing full spectral scans, such as

those developed by Ritchie (2006, 2008) could be used. Alternatively, more advanced analytical approaches, such as the separation of individual photosynthetic pigments using high-pressure liquid chromatography may be needed, particularly when comparing Chl *a* measurements in contrasting algal communities with variable photosynthetic pigment composition (Henderson 2015).

Despite the aforementioned limitations of our predictive models, the use of acidification to quantify algal Chl *a* remains one of the most widely used methods for routine monitoring of phytoplankton and periphyton communities. Increased use of ethanolic solvents will result in greater uncertainty unless careful attention is given to both acid strength and post-acidification reaction time. Our findings provide a standardized correction procedure for Chl *a* concentrations in previously measured extracts of algal pigments and ensure greater consistency for future analyses.

2.4 Discussion

Acid strength and post-acidification reaction time are two important factors that influence the determination of Chl *a* in 95% ethanol. Past studies that have acidified algal Chl *a* samples to a concentration below 0.008 mol HCl L^{-1} likely under-predicted Chl *a* concentrations, particularly in cases where post-acidification reaction times are less than 120 s. Based on our analysis, if samples were acidified to between 0.003 and 0.008 mol HCl L^{-1} we predict the observed Chl *a* concentrations to be 3 to 33% lower than the actual Chl *a* concentration. If samples were acidified to a lower acid treatment concentration, observed Chl *a* in the samples could be 33 to 85% lower than what was actually present.

Our analysis shows that deviations from the actual Chl *a* concentration are proportional to acid concentration as long as the post-acidification read time is consistent. Therefore, under-acidification of ethanol-extracted samples does not necessarily affect general trends between samples acidified in the same way, but could substantially underestimate absolute concentrations of reported Chl *a* and therefore the ability to reliably compare Chl *a* measurement across studies if protocols vary. If past samples were not properly acidified and post-acidification reaction times were not known or consistent among samples, significant uncertainty could proliferate in the dataset and call into question its validity or comparability.

Potential errors associated with acid strength and reaction time can also propagate through datasets if Chl *a* concentrations were used to normalize measurements of ecosystem function such as primary production or nitrogen assimilation. For example, if an under-acidified Chl *a* sample was used to normalize estimates of gross primary production for a particular algal culture for the development of photo-irradiance curves. The maximum production per unit Chl *a* could be overestimated by five times in samples acidified to 0.001 mol HCl L^{-1}. These issues could be especially problematic for large meta-analyses requiring the synthesis of Chl *a* data or when direct comparisons to past results are made (e.g., Hope et al. (2014)). Considering our results, these problems could be mitigated if the details of acid strength and post-acidification reaction times were provided.

Our work provides a comprehensive evaluation of the effect of acid on Chl *a* concentration, which will help improve the quality of future ecological research by increasing awareness among researchers of the importance of acid concentration and post-

acidification reaction time. Based on the large number of studies that rely on the measurement of Chl *a* in environmental samples, there exists an immediate need to reestablish correct procedures for its measurement. This will be particularly important in the context of large collaborative or multi-site research projects where the risk of inconsistent procedures for Chl *a* extraction acidifications are more likely to occur. Ultimately, ensuring consistent Chl *a* concentrations across acid treatments will allow for the accurate comparison of ecosystem level responses across studies.

2.5 Comments and Recommendations

For future analyses we recommend acidifying Chl *a* samples to 0.008 mol HCl L^{-1} as originally proposed by Sartory and Grobbelaar (1984). This acid strength offers rapid conversion of Chl *a* to Phe *a* as well as pigment calculation coefficients that are most consistent to those developed by Wintermans and De Mots (1965) and Lorenzen (1967). After acidification we recommend waiting 30 to 60 minutes before taking the post-acidification spectrophotometric reading because acidified absorbance at 665 nm remained stable throughout that time period. We advocate that researchers keep track of post-acidification reaction times and report both reaction time and acid concentration when describing analysis methods. This will help reduce the likelihood of methodological error propagation and allow for easier comparison among future studies. The predictive equations we developed can effectively correct samples that were not adequately acidified or read prior to completion of the reaction converting Chl *a* to Phe *a*. Our approach provides a framework to better understand the effect of acid and reaction time on Chl *a*

concentrations and can be easily applied to standardize Chl *a* measurements made using different procedural conditions.

2.6 Literature Cited

APHA. 2012. Method 10200 H Chlorophyll. In E. W. Rice, L. Bridgewater and A. P. H. Association [eds.], Standard methods for the examination of water and wastewater. American Public Health Association.

Arscott, D. B., W. B. Bowden, and J. C. Finlay. 1998. Comparison of epilithic algal and bryophyte metabolism in an Arctic Tundra Stream, Alaska. *J. Am. Benthol. Soc.* **17**: 210–227. doi:10.2307/1467963

Arvola, L. 1981. Spectrophotometric determination of chlorophyll *a* and phaeopigments in ethanol extractions. *Ann. Bot. Fenn.* **18**: 221–227.

Bowden, W. B., B. J. Peterson, J. C. Finlay, and J. Tucker. 1992. Epilithic chlorophyll *a*, photosynthesis, and respiration in control and fertilized reaches of a tundra stream. *Hydrobiologia* **240**: 121–131. doi:10.1007/BF00013457

Bowles, N. D., H. W. Paerl, and J. Tucker. 1985. Effective solvents and extraction periods employed in phytoplankton carotenoid and chlorophyll determinations. *Can. J. Fish. Aquat. Sci.* **42**: 1127–1131. doi:10.1139/f85-139

Boyce, D. G., M. Lewis, and B. Worm. 2012. Integrating global chlorophyll data from 1890 to 2010. *Limnol. Oceanogr. Methods* **10**: 840–852. doi:10.4319/lom.2012.10.840

Dodds, W. K., V. H. Smith, and K. Lohman. 2002. Nitrogen and phosphorus relationships to benthic algal biomass in temperate streams. *Can. J. Fish. Aquat. Sci.* **59**: 865–874. doi:10.1139/f02-063

Elrifi, I. R., and D. H. Turpin. 1987. Short-term physiological indicators of N deficiency in phytoplankton: a unifying model. *Mar. Biol.* **96**: 425–432. doi:10.1007/BF00412527

Graff, J. R., and T. A. Rynearson. 2011. Extraction method influences the recovery of phytoplankton pigments from natural assemblages. *Limnol. Oceanogr. Methods* **9**: 129–139. doi:10.4319/lom.2011.9.129

Hagerthey, S. E., J. William Louda, and P. Mongkronsri. 2006. Evaluation of pigment extraction methods and a recommended protocol for periphyton chlorophyll *a* determination and chemotaxonomic assessment. *J. Phycol.* **42**: 1125– 1136. doi:10.1111/j.1529-8817.2006.00257.x

Hansson, L. A. 1988. Chlorophyll a determination of periphyton on sediments: Identification of problems and recommendation of method. *Freshw. Biol.* **20**: 347–352. doi: 10.1111/j.1365-2427.1988.tb00460.x

Henderson, I. M. 2015. Ratios, proportions, and mixtures of chlorophylls: Corrections to spectrophotometric methods and an approach to diagnosis. *Limnol. Oceanogr. Methods* **13**: 617–629. doi:10.1002/lom3.10052

Holm-Hansen, O., and B. Riemann. 1978. Chlorophyll a determination: Improvements in methodology. *Oikos* **30**: 438–447. doi:10.2307/3543338

Hope, A., W. Mcdowell, and W. Wollheim. 2014. Ecosystem metabolism and nutrient uptake in an urban, piped head- water stream. *Biogeochemistry* **121**: 167–187. doi: 10.1007/s10533-013-9900-y

Jeffrey, S. W., R. F. C. Mantoura, and S. W. Wright. 1997. Phytoplankton pigments in oceanography: Guidelines to modern methods. UNESCO Publ.

Jespersen, A. M., and K. Christoffersen. 1987. Measurements of chlorophyll *a* from phytoplankton using ethanol as extraction solvent. *Arch. Hydrobiol.* **109**: 445–454. ISSN: 0003-9136/89/0109/0445

Joslyn, M. A., and G. Mackinney. 1938. The rate of conversion of chlorophyll to pheophytin. *J. Am. Chem. Soc.* **60**: 1132–1136. doi:10.1021/ja01272a037

Lehman, P. W. 1981. Comparison of chlorophyll *a* and carotenoid pigments as predictors of phytoplankton biomass. *Mar. Biol.* **65**: 237–244. doi:10.1007/BF00397117

Levine, S. N., A. D. Shambaugh, S. E. Pomeroy, and M. Braner. 1997. Phosphorus, nitrogen, and silica as controls on phytoplankton biomass and species composition in Lake Champlain (USA-Canada). *J. Great Lakes Res.* **23**: 131–148. doi:10.1016/S0380-1330(97)70891-8

Lorenzen, C. J. 1967. Determination of chlorophyll and pheopigments: Spectrophotometric equations. *Limnol. Oceanogr.* **12**: 343–346. doi:10.4319/lo.1967.12.2.0343

Marker, A. F. H. 1972. The use of acetone and methanol in the estimation of chlorophyll in the presence of phaeophytin. *Freshw. Biol.* **2**: 361–385. doi:10.1111/j.1365-2427.1972.tb00377.x

Moed, J. R., and G. M. Hallegraeff. 1978. Some problems in the estimation of chlorophyll *a* and phaeopigments from pre- and post-acidification spectrophotometric measurements. Int. Rev. *Gesamten Hydrobiol. Hydrogr.* **63**: 787– 800. doi:10.1002/iroh.19780630610

Morin, A., W. Lamoureux, and J. Busnarda. 1999. Empirical models predicting primary productivity from chlorophyll *a* and water temperature for stream periphyton and lake and ocean phytoplankton. *J. Am. Benthol. Soc.* **18**: 299– 307. doi:10.2307/1468446

Mulholland, P. J., and others. 2008. Stream denitrification across biomes and its response to anthropogenic nitrate loading. *Nature* **452**: 202–246. doi:10.1038/nature06686

Nusch, E. 1980. Comparison of different methods for chlorophyll and phaeopigment determination. *Arch. Hydrobiol*. **14**: 14–36. ISSN: 0071-1128/80/0014-0014

Olmstead, W. N., Z. Margolin, and F. G. Bordwell. 1980. Acidities of water and simple alcohols in dimethyl sulfoxide solution. *J. Am. Org. Chem.* **45**: 3295–3299. doi: 10.1021/jo01304a032

Porra, R. J. 1990. A simple method for extracting chlorophylls from the recalcitrant alga, *Nannochloris atomus*, without formation of spectroscopically-different magnesium-rhodochlorin derivatives. *Biochim. Biophys. Acta.* **1019**: 137–141. doi:10.1016/0005-2728(90)90135-Q

Porra, R. J., and L. H. Grimme. 1974. A new procedure for the determination of chlorophylls *a* and *b* and its application to normal and regreening Chlorella. Anal. *Biochem.* **57**: 255–267. doi:4817501

Qin, H., S. Li, and D. Li. 2013. An improved method for determining phytoplankton chlorophyll *a* concentration without filtration. *Hydrobiologia* **707**: 81–95. doi: 10.1007/s10750-012-1412-6

Reuss, N., and D. J. Conley. 2005. Effects of sediment storage conditions on pigment analyses. Limnol. Oceanogr. Methods **3**: 477–487. doi:10.4319/lom.2005.3.477

Riemann, B. 1978. Carotenoid interference in spectrophotometric determination of chlorophyll degradation products from natural populations of phytoplankton. *Limnol. Oceanogr.* **23**: 1059–1066. doi:10.4319/lo.1978.23.5.1059

Ritchie, R. J. 2006. Consistent sets of spectrophotometric chlorophyll equations for acetone, methanol and ethanol solvents. *Photosynth. Res.* **89**: 27–41. doi:10.1007/s11120- 006-9065-9

Ritchie, R. J. 2008. Universal chlorophyll equations for estimating chlorophylls *a*, *b*, *c*, and *d* and total chlorophylls in natural assemblages of photosynthetic organisms using acetone, methanol, or ethanol solvents. *Photosynthetica* **46**: 115–126. doi:10.1007/s11099-008-0019-7

Sartory, D. P. 1982. Spectrophotometric analysis of chlorophyll *a* in freshwater phytoplankton. M.S. thesis. Univ. of Free State.

Sartory, D., and J. Grobbelaar. 1984. Extraction of chlorophyll *a* from freshwater phytoplankton for spectrophotometric analysis. *Hydrobiologia* **114**: 177–187. doi:10. 1007/BF00031869

Thompson, R. C., M. L. Tobin, S. J. Hawkins, and T. A. Norton. 1999. Problems in extraction and spectrophotometric determination of chlorophyll from epilithic microbial biofilms: Towards a standard method. *J. Mar. Biol. Assoc. U.K.* **79**: 551–558. doi:10.1017/S0025315498000678

Wasmund, N. 1984. Problems of the spectrophotometric determination of chlorophyll. Acta Hydrochim. *Hydrobiol*. **12**: 255–272. doi:10.1002/aheh.19840120307

Wasmund, N., I. Topp, and D. Schories. 2006. Optimising the storage and extraction of chlorophyll samples. *Oceanologia* **48**: 125–144. http://www.iopan.gda.pl/oceanologia/

Wintermans, J. F. G. M., and A. De Mots. 1965. Spectrophotometric characteristics of chlorophylls *a* and *b* and their pheophytins in ethanol. *Biochim. Biophys. Acta* **109**: 448–453. doi:5867546

2.7 Acknowledgements

We would like to thank Joshua Beneš, Frances Iannucci, and Kyle Arndt for their assistance in the field and laboratory, Dr. Courtney Giles for her extensive technical review of the manuscript, and the researchers and technicians of the Toolik Field Station, Arctic LTER program, and Rubenstein Ecosystem Science Laboratory. In addition, we would like to thank the graduate students and principal investigators of the Scale, Consumers, and Lotic Ecosystem Rates (SCALER) project for their support and guidance throughout the production of this manuscript. Finally, we would like to thank three anonymous reviewers who provided insightful comments that helped clarify and strengthen our thesis. This material is based on work supported by the National Science Foundation under grant numbers EF-1065682, EF-1065267, and DEB/LTER-1026843. Any opinions, findings, and conclusions or recommendations expressed in this material are those of the authors and do not reflect the views of the National Science Foundation.

2.8 Tables

Table 2.1 Acid treatments used to achieve final acid concentration in Chl *a* samples.

Acid Treatment (mol HCl L^{-1})	TargetAcid Concentration (mol HCl L^{-1})	Acid Treatment Reference
0.03	0.001	LINX II Methods, 2004 (unpubl.)
0.10	0.003	APHA, 2012*
0.25	0.008	Sartory and Grobbelaar, 1984
0.50	0.016	

*APHA method was intended for 90% acetone.

Table 2.2 Observed maximum ratio (R_{obs}) and absorption reduction factor (K_{obs}) for stock Chl *a* solution containing 4.15 mg Chl *a* L^{-1} dissolved in 95% ethanol. Coefficients were calculated using absorbance values measured at 60, 90, 120 s and 1 h after acidification to each treatment condition.

Target Acid Conc. (mol H^+ L^{-1})	Target Time (s)	Measured Time (s)	R_{obs}	K_{obs}	A_{obs}
0.001	60	57	1.38	3.64	12.07
	90	90	1.49	3.03	12.07
	120	123	1.57	2.76	12.07
	3600	3600	1.68	2.47	12.07
0.003	60	58	1.38	3.64	12.07
	90	93	1.49	3.03	12.07
	120	127	1.57	2.76	12.07
	3600	3612	1.68	2.48	12.07
0.008	60	59	1.69	2.44	12.09
	90	87.5	1.70	2.44	12.09
	120	120	1.69	2.44	12.09
	3600	3600	1.70	2.42	12.09
0.016	60	61	1.74	2.35	12.06
	90	94	1.74	2.35	12.06
	120	116	1.74	2.35	12.06
	3600	3598	1.75	2.33	12.06

Table 2.3 Predictive model parameters used to correct and standardize previously observed concentrations of Chl *a* (Chl $a_{observed}$) in ethanol extracts of aquatic algae with 60, 90, or 120 s reaction times measured at one of four target acid treatments. Known Chl *a* parameter estimates predicts the Chl *a* concentration (Chl $a_{predicted} = \beta_0 + \text{Chl } a_{observed} \times \beta_1$) if Chl $a_{observed}$ was adequately acidified and permitted to reach reaction completion. Predicted 1 h Chl *a* parameter estimates are included for validation purposes and should not be used to correct past datasets. Predicted and observed Chl *a* concentrations are in units of mg Chl *a* L^{-1} and $df = 4$ for all regression equations.

Target Acid Conc. (mol H^+ L^{-1})	Target Time (s)	Mean Sample Time (s)	1h Chl *a* Parameter Estimates				Known Chl *a* Parameter Estimates			
			β_0	β_1	r^2	p	β_0	β_1	r^2	p
0.001	60	60 ± 0.9	0.098	5.192	0.994	<.001	0.131	5.927	0.991	<.001
	90	90 ± 1	0.104	4.315	0.994	<.001	0.139	4.926	0.992	<.001
	120	117 ± 1.3	0.098	3.888	1.000	<.001	0.132	4.439	1.000	<.001
0.003	60	60 ± 0.4	0.016	1.331	0.999	<.001	0.011	1.466	0.998	<.001
	90	90 ± 0.6	0.014	1.144	1.000	<.001	0.008	1.260	0.999	<.001
	120	116 ± 1.8	0.002	1.084	1.000	<.001	-0.005	1.193	1.000	<.001
0.008	60	60 ± 0.3	0.004	1.003	1.000	<.001	-0.009	1.042	1.000	<.001
	90	90 ± 0.3	0.001	1.001	1.000	<.001	-0.012	1.040	1.000	<.001
	120	116 ± 1	0.003	1.001	1.000	<.001	-0.010	1.040	1.000	<.001
0.016	60	60 ± 0.5	0.023	0.976	1.000	<.001	-0.011	0.993	1.000	<.001
	90	90 ±0.4	0.022	0.975	1.000	<.001	-0.012	0.993	1.000	<.001
	120	115 ± 0.4	0.023	0.976	1.000	<.001	-0.011	0.993	1.000	<.001

2.9 Figures

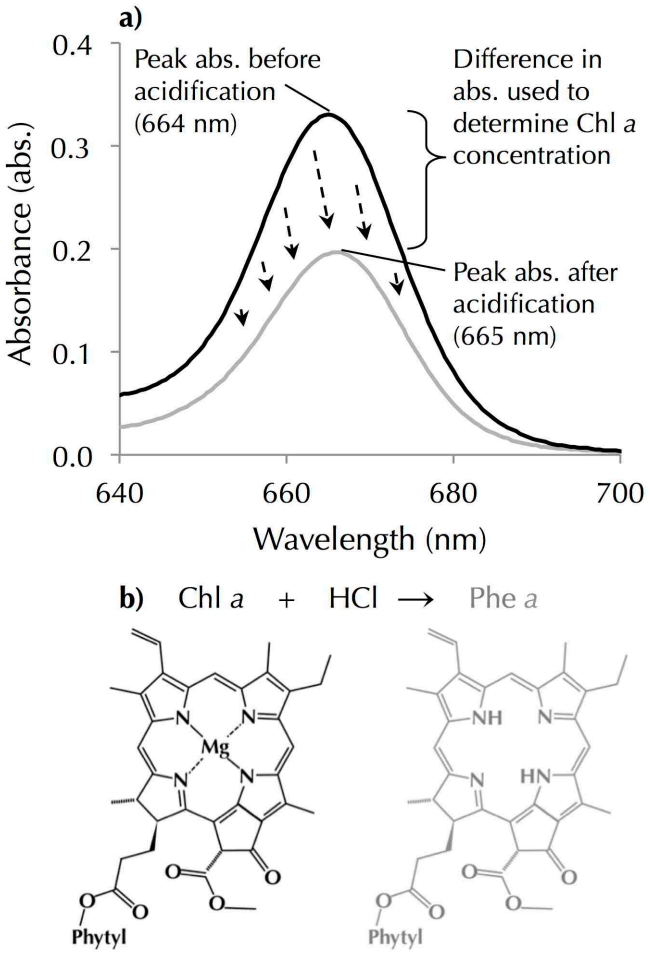

Figure 2.1 Conceptual diagram showing: a) red absorbance spectral shift of Chl *a* (black line) to Phe *a* (gray line) after the addition of dilute hydrochloric acid, and b) the chemical reaction whereby protons replace the magnesium ion in the center of the porphyrin ring to convert Chl *a* (black molecule) to Phe *a* (gray molecule).

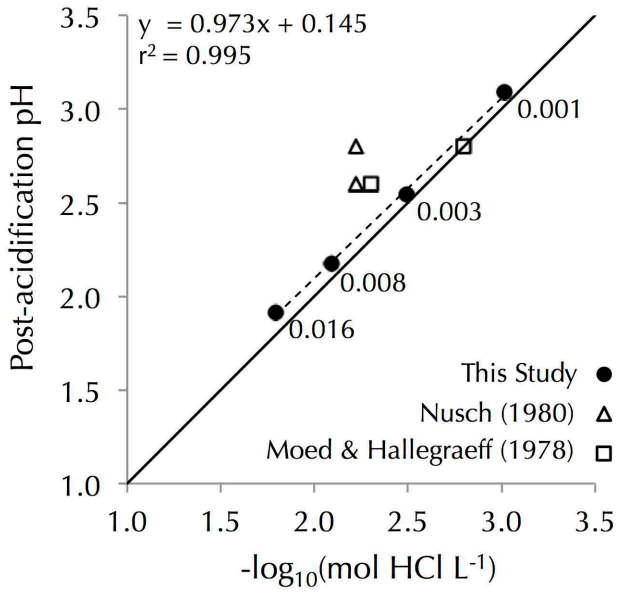

Figure 2.2 Scatterplot illustrating the relationship between mean observed postacidification pH of 95% ethanol and the -$\log_{10}$ transformed molar proton concentration of hydrochloric acid for each acid treatment. Text labels adjacent to the observed mean pH data points (closed circles) indicate the final molar concentration corresponding to each target acid concentration used in this study in units of mol HCl L^{-1}. Open square and triangle symbols denote estimated acidification recommendations based on pH described by Moed and Hallegraeff (1978) and Nusch (1980), respectively.

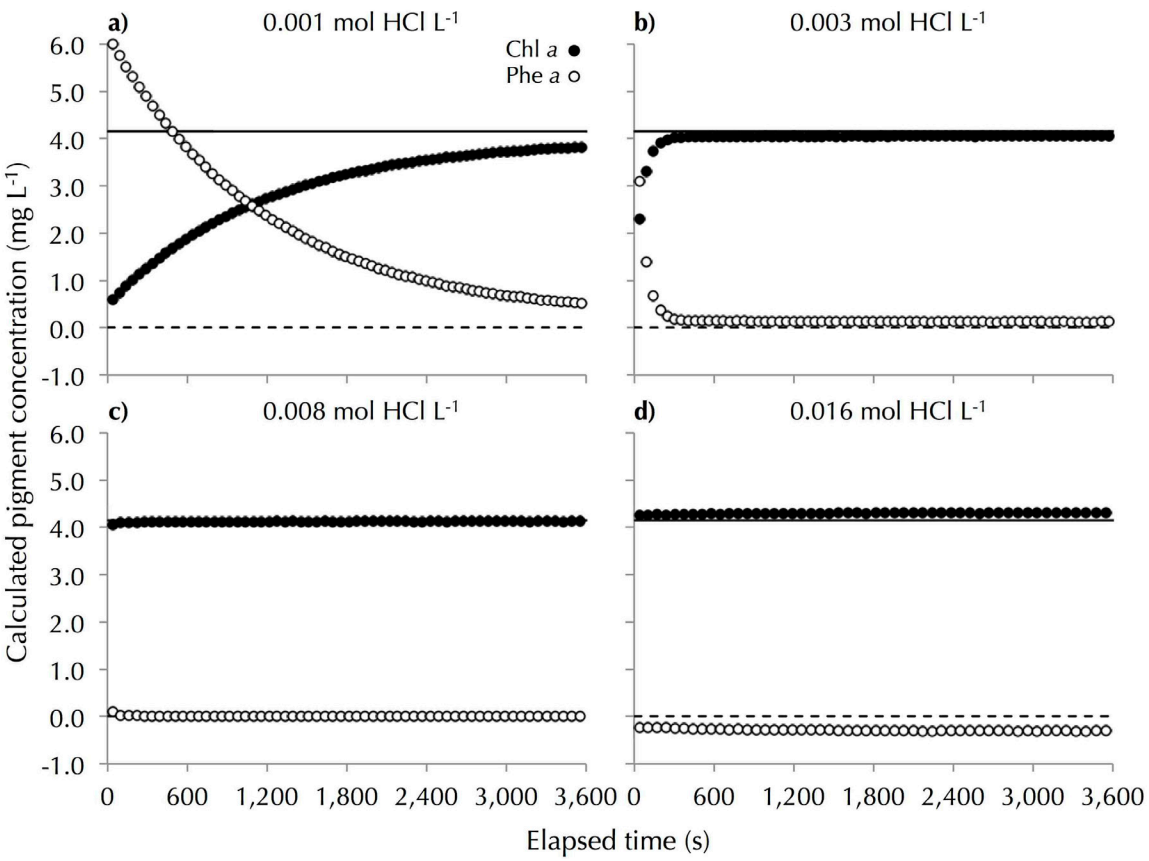

Figure 2.3 Effect of reaction time on calculated Chl *a* (closed circles) and Phe *a* (open circles) when stock chlorophyll solution is acidified to: a) 0.001 mol HCl L^{-1}, b) 0.003 mol HCl L^{-1}, c) 0.008 mol HCl L^{-1}, and d) 0.016 mol HCl L^{-1}. Solid lines represent the known concentration of Chl *a* (4.15 mg Chl *a* L^{-1}) and the dashed lines represent known concentration of Phe *a* (0.0 mg Phe *a* L^{-1}) in the stock chlorophyll solution which was made by dissolving pure Chl *a* from the blue-green algae *Anacystis nidulans* in 95% ethanol.

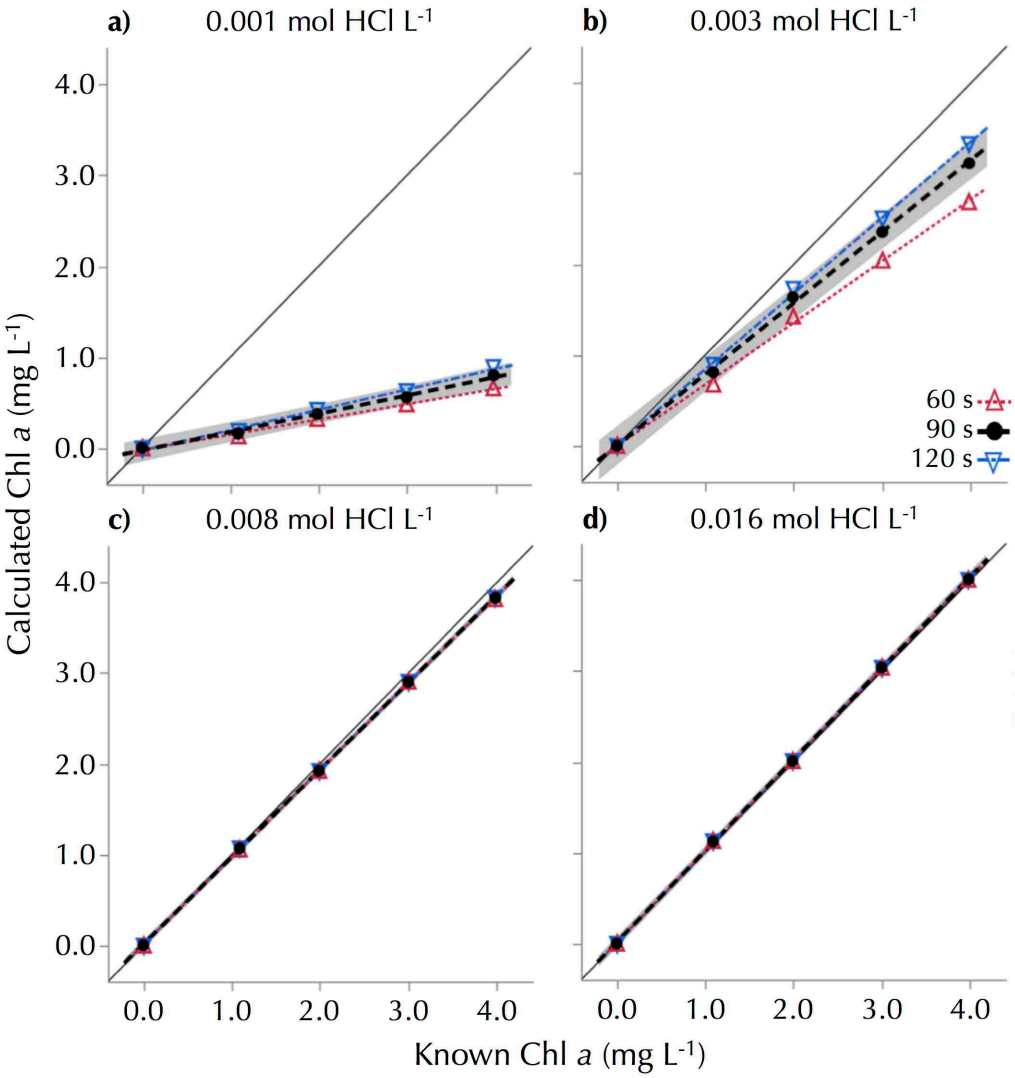

Figure 2.4 Effect of known Chl *a* concentration on calculated Chl *a* when standard solutions are acidified to: a) 0.001 mol HCl L^{-1}, b) 0.003 mol HCl L^{-1}, c) 0.008 mol HCl L^{-1}, and d) 0.016 mol HCl L^{-1} target acid concentrations. Solid circles with dashed line (black) denotes observed concentrations and linear model fit for samples read at 90 s, upward-pointing triangle with dotted line (red) denotes observed concentrations and linear model fit for samples read at 60 s, and downward-pointing triangle with dash-dot (blue) line illustrates observed concentrations and linear model fit for samples read at 120 s. Gray shaded area is 95% prediction interval for 90 s linear model and solid line is 1:1 relationship for reference.

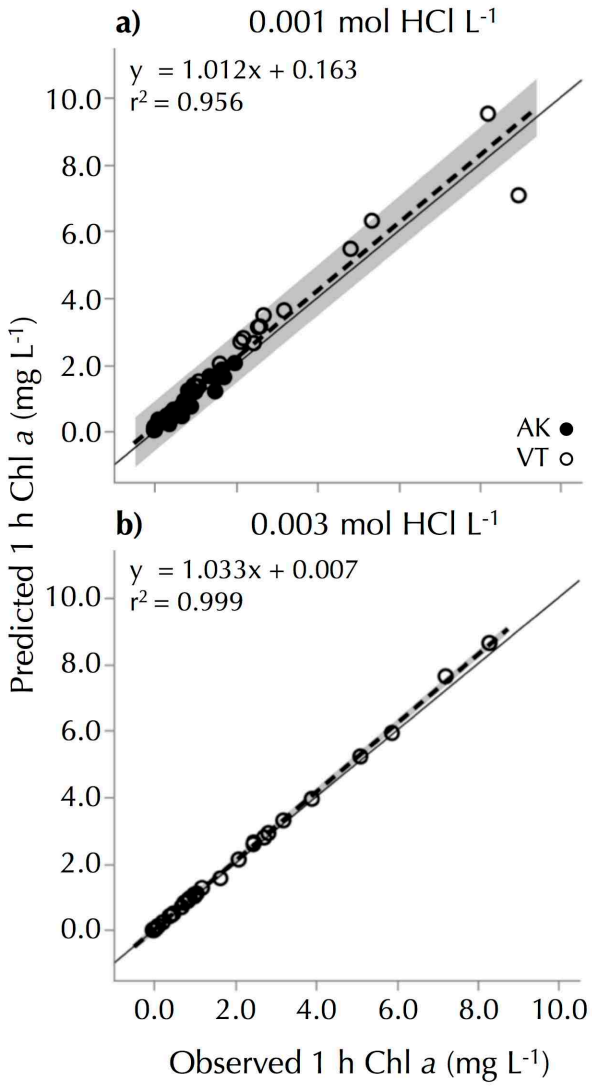

Figure 2.5 Scatterplots illustrating the relationships between predicted 1 h Chl *a* determined from periphyton samples with 90 s reaction time and observed 1 h Chl *a*. Predicted 1 h Chl *a* was compared to observed 1 h Chl *a* for samples acidified to: a) 0.001 mol HCl L^{-1} and b) 0.003 mol HCl L^{-1}. Open and closed circles indicate benthic periphyton samples collected from Vermont and Alaska, respectively. Dashed lines represent linear model fit for all combined samples. Gray shaded area is 95% prediction interval for the regression and solid line is 1:1 relationship for reference.

CHAPTER 3: EFFECT OF PARTICLE SIZE AND HETEROGENEITY ON SEDIMENT BIOFILM METABOLISM AND NUTRIENT UPTAKE SCALED USING TWO APPROACHES

ABSTRACT

Numerous studies have examined the effect of sediment particle size and distribution on com- munity structure, but few have focused explicitly on how physical habitat characteristics influence biogeochemical functions of freshwater biofilms. In this study, we evaluated the effect of particle size and heterogeneity on rates of biofilm metabolism and nutrient uptake in colonized and native sediments normalized using two different scaling approaches. Coarse, pebble- to cobble-sized sediments were sorted into four homogeneous particle size treatments plus one heterogeneous treatment. Each treatment was deployed, in replicate, within one riffle and one run habitat feature in three different high-latitude stream reaches with contrasting hydrological and physicochemical characteristics. A treatment of native, homogeneous sediment was also evaluated at each deployment location. After incubating for approximately five weeks, metabolism and nutrient uptake of biofilms in all treatments (n = 69) were measured in recirculating microcosm chambers. For each treatment, functional rates were normalized by projected surface area and sediment surface area scaling approaches, which account for the surface area in plan view (looking top-down) and the total surface area of all sediment particles, respectively. This comparison was designed to determine whether treatment effects were independent of increased surface area associated with smaller particle sizes or heterogeneous sediments. Community respiration and uptake of ammonium-nitrogen and phosphate-phosphorus by biofilms decreased significantly as the particle size of homogeneous treatments increased when normalized by projected surface area, but significantly increased with increasing particle size when normalized by sediment surface area. Sediment particle size had a limited influence on production rates evaluated across treatments. Heterogeneous and homogeneous treatments with similar median particle sizes did not differ significantly from one another for most biogeochemical functions measured. Our findings indicate that rates of biogeochemical function in heterogeneous habitats were directly related to the total sediment surface area available for biofilm colonization. The significant interactions between sediment surface area and rates of respiration and nutrient uptake suggest that information about the size and distribution of sediment particles could substantially improve our ability to predict and scale measurements of important biogeochemical functions in streams.

3.0 Introduction

Linking physical habitat heterogeneity to ecosystem structure and function is a central tenant of many theoretical and empirical ecological studies (Hynes 1970, Seiferling et al. 2014). Direct and indirect effects of habitat heterogeneity have been shown to promote biodiversity (Tews et al. 2004) and stimulate essential ecosystem functions (Cardinale et al. 2013, Lefcheck et al. 2015). In streams and rivers, restoration efforts have focused on the improvement of habitat heterogeneity through the manipulation of bed sediment distributions and addition of large woody debris (Laub et al. 2012). However, evidence from manipulated and natural river systems suggests that greater habitat heterogeneity does not always correspond to expected responses in ecosystem structure or function (Palmer et al. 2010, Hoellein et al. 2012). Disagreement between theory and observation highlights the need to better understand the mechanisms that link rates of ecosystem function to physical habitat characteristics of benthic sediments (Kovalenko et al. 2012).

Sediment biofilms are complex microbial, algal, and fungal assemblages that grow on the surface of benthic particles (Lock et al. 1984, Battin et al. 2016). Biofilms are a ubiquitous component of benthic ecosystems and are integral to the regulation of essential stream biogeochemical processes, such as nutrient uptake and metabolism (Palmer et al. 2000, Besemer 2015). Depending on the community composition, biofilms can be net heterotrophic or net autotrophic. Biofilms provide essential basal resources to invertebrate meiofauna and macrofauna (Lawrence et al. 2002, Majdi et al. 2012). While many studies have examined the effects of streambed sediment size and heterogeneity on the biodiversity

and function of macroinvertebrate communities (Wise and Molles 1979, Downes et al. 1998, Gayraud and Philippe 2003, Barnes et al. 2013), other studies have looked at the effect of meiofauna and macrofauna as sediment engineers that can influence the structure and function of benthic biofilms (Lawrence et al. 2002, Graba et al. 2014, Passarelli et al. 2014, Majdi et al. 2017). Few studies have explored the effect of physical sediment characteristics on the function of biofilms that colonize them (Claret and Fontvieille 1997, Cardinale et al. 2002, Hoellein et al. 2009).

The growth, composition, and maintenance of sediment biofilms are influenced by several physical controls, which vary at multiple spatial and temporal scales (Battin et al. 2016, Stegen et al. 2016). Three prominent, physical controls on biogeochemical dynamics in coarse-bottomed stream biofilms include size, depth, and distribution of benthic sediments. The distribution of sediments can affect the velocity and residence time of water within the hyporheic zone (Boulton et al. 2010). Increased residence times can create gradients of oxidation–reduction potential and microsites of anoxic waters (Briggs et al. 2015), which lead to greater variability in nutrient availability at small scales. Patchy hydrodynamic conditions attributed to deeper sediments have also been shown to promote more diverse biofilm community composition (Besemer et al. 2009), as well as greater ecosystem respiration (Haggerty et al. 2014). Moreover, the size of benthic sediments can affect the total surface area available for biofilm colonization because sediment surface area increases as particle size decreases (Boulton et al. 1998, Lottig and Stanley 2007). Because multiple physical factors contribute to the structure and function of biofilms,

additional experimental studies are needed to quantify the responses of biofilm communities to specific environmental factors (Besemer 2015).

The relationship between heterogeneous sediment particles and the total sediment surface area available for colonization has important implications for the interpretation of measurements of biofilm metabolism and nutrient uptake in stream ecosystems. Heterogeneous streambed sediments have greater sediment surface area available for biofilm colonization than homogeneous sediments of similar size due to more efficient grain packing. This presents a plausible mechanism for how heterogeneous habitats could be linked to increased ecosystem function (Palmer et al. 2010). Battin et al. (2016) noted that decreasing the particle size of one cubic meter of homogeneous sediment from 5 to 0.5 cm results, on average, in an order of magnitude increase to sediment surface area from 100 to 1000 m^2. Therefore, key processes driven by biofilms, such as nutrient uptake and metabolism, could potentially scale predictably with changes to particles size or heterogeneity. Considering that measurements of aquatic metabolism and nutrient uptake are commonly normalized using projected surface area, which scales observations relative to a square meter of stream bottom, it may be possible to gain a better understanding of ecosystem functional rates using relationships between sediment particle size and sediment surface area.

The objective of this study was to determine the effect of sediment particle size and heterogeneity on rates of key ecosystem functions using carefully controlled stream microcosm experiments. Raw rates of biofilm community metabolism and nutrient uptake were scaled by projected surface area and sediment surface area to test differences between

treatments using normalization approaches that account for surface area across two- (projected surface area) and three-dimensions (sediment surface area) (Figure 3.1). We hypothesized that sediment surface area would be a key driver of metabolism and nutrient uptake relative to other essential physical and biological components of benthic habitats, such as organic matter (OM) and algal chlorophyll a content. More specifically, we hypothesized that rates of respiration and nutrient uptake would be negatively correlated with coarse sediment particle size when normalized by projected area, because increased particle size results in decreases in total sediment surface area available for biofilm colonization. By the same logic, we hypothesized that heterogeneous sediment treatments would exhibit greater ecosystem function than homogeneous treatments when normalized by projected area, but show no differences when normalized by total sediment surface area. Lastly, we hypothesized that rates of gross primary production would not change with increasing particle size when expressed on a projected area basis because gross primary production is restricted to the upper, photosynthetically active area of the sediment.

3.1 Methods

3.1.1 Study Site

The experiment was carried out in Oksrukuyik Creek, a third-order, cobble-bottom stream located on the northern foothills of the Brooks Mountain Range, Alaska, USA. This study was part of a larger, inter-biome comparative study called Scale, Consumers, and Lotic Ecosystem Rates (SCALER). At its crossing with the Dalton Highway, the stream drains 71.6 km^2 of undisturbed tundra, which is underlain by continuous permafrost.

Experimental study sites were located 9 km upstream of the road crossing where the East and West tributaries flow into the Main Stem (Figure 3.2A). The two tributaries were selected because they have similar catchment areas but contrasting landscape characteristics (Whittinghill et al. 2014). The West Tributary site drains 5.5 km^2 of moist and dry acidic tundra vegetation complexes and contains no lakes, while the East Tributary site drains 8.1 km^2 of shrub and moist non-acidic tundra vegetation and contains a network of lakes, which account for 9.7% of the catchment area (Walker et al. 1994). The Main Stem site drains 36.3 km^2 and is located upstream of West Tributary and downstream of East Tributary.

The Oksrukuyik Creek flows freely from May to September and receives nearly 50 d of continuous daylight during the growing season. Annual precipitation in the region is typically <150 mm (Oswood et al. 1995), and the median daily discharge observed at the highway crossing summarized from the Arctic Long-Term Ecological Research (LTER) database averaged 670 L/s during the mid-June to mid-August gaging period from 1993 to 2013 (ARCTIC-LTER 2016). Surface waters in the Oksrukuyik Creek are phosphorus-limited (Harvey et al. 1998). Mean concentrations ± standard deviation (SD) of phosphate-phosphorus (PO_4-P) and ammonium-nitrogen (NH_4-N) from 2009 to 2013 (n = 43) were 3.9 ± 15.5 μg PO_4-P/L and 4.1 ± 3.8 μg NH_4-N/L, respectively (ARCTIC-LTER 2016). Benthic autotrophic communities in the region include numerous species of filamentous algae, bryophytes, and diatoms (Miller et al. 1992, Finlay and Bowden 1994, Harvey et al. 1998). Microbial communities below the surface water–sediment interface have multiple operational taxonomic units of prokaryotes including large proportions of *beta*- and

gamma- proteobacteria (Crump et al. 2012), which contain important genera of ammonium-oxidizing (nitrifying) bacteria and diazotrophs.

3.1.2 Study Design and Chamber Experimentation

Naturally occurring river sediments were used to prepare one heterogeneous and four different homogeneous sediment treatments, which were placed into plastic baskets based on median diameter (D_{50}). Sediments were acquired from a point bar located 5 km downstream of the West Tributary confluence (Figure 3.2A). The source location contained dry, well-sorted alluvium free of visible algae. Bar sediments were sieved to remove fines <8 mm and sorted into four homogeneous treatment classes (8–16, 23–32, 45–64, and 64–90 mm) using a gravelometer (Wildco, Yulee, Florida, USA). Sediments of each size class were placed into perforated plastic baskets (10 x 10 x 6 cm) so that each treatment had equal volumes. Forty-two baskets were filled so that seven baskets could be deployed in a riffle and run habitat feature within three separate streams (Figure 3.2B). Chamber experiments required three baskets, so that two experimental replicates could be conducted for each treatment at a given stream and habitat location. The heterogeneous treatment was created by placing one 45- to 64-mm-sized particle into a basket and filling the remaining space with equal volumes of the two smaller homogeneous sediment treatments. Median diameter (D_{50}) of each treatment was determined by measuring the b-axis of a subset of sediment particles to the nearest millimeter. Two hundred (200) individual grains were measured to determine the D_{50} of the three smallest pebble-sized treatments, and 70 particles were measured for the largest cobble-sized treatment (Wentworth 1922). The D_{50}

of the heterogeneous and native sediment treatments was also measured using a subset of 200 and 100 grains, respectively.

Seven baskets of each sediment treatment type were deployed in one riffle and one run habitat at each of the three study sites on three consecutive days in late June 2014 (Figure 3.2B). Suitable habitat locations were identified using previous transect surveys of physical stream characteristics in the area (Rüegg et al. 2015b), and baskets were deployed in locations, that best matched the median conditions of each contrasting reach. Riffle transects contained turbulent, fast-flowing water with visible white water caused by shallow water depth. Run transects contained moderate-to-deep, swift-flowing water with herringbone-patterned ripples on the water surface. Native stream sediments were removed from the benthic layer to a depth of 10 cm, and the space was filled with treatment baskets configured in a seven-by-five basket grid pattern. The grid was oriented long ways with respect to the flow of water, and individual baskets were arranged using a stratified approach by row that included one basket of each treatment (Figure 3.2B). Displaced native sediments similar in size to the largest homogeneous treatment were placed adjacent to basket grids to be used as experimental controls on colonization. Native sediment and the largest homogeneous treatments were not placed in baskets due to irregularities in particle shape.

Sediment treatments were colonized in riffle habitats for an average standard deviation (SD) of 33 ± 0.6 days and in run habitats for and 38 ± 1.5 days. Hydrological and meteorological conditions were monitored during the colonization period. Stream stage and temperature were continuously recorded at each site using HOBO U20 pressure

transducers (Onset Computer, Bourne, Massachusetts, USA), and discharge was determined using dilution gaging methods (Kilpatrick and Cobb 1985). Meteorological inputs were also recorded in a central location adjacent to the Main Stem site using a HOBO RG-3 tipping bucket rain gage and an Odyssey photosynthetically active radiation (PAR) sensor (Dataflow Systems, Christchurch, New Zealand). All probes and sensors recorded stream conditions at five-minute intervals. Following colonization, baskets were carefully removed and transported back to the Toolik Field Station. Baskets were stored in the dark on wet ice prior to analysis.

We evaluated benthic community metabolism and net nutrient uptake in clear acrylic recirculating chambers (Rüegg et al. 2015a). Chambers were housed in two, water-filled incubation tanks (300 L) equipped with adjustable 1000-watt high-pressure sodium grow lights (Hydrofarm Northwest, Portland, Oregon, USA) and 1/3 horsepower chiller pumps (Aqua Logic, San Diego, California, USA). Light conditions were recorded using an LI-1500 logger with an LI-190R PAR sensor (LICOR, Lincoln, Nebraska, USA). Tank water was chilled to 5 °C to regulate chamber temperature to similar conditions observed in the upper 10 cm of an arctic stream bottom during summer months and to prevent degassing of dissolved oxygen (DO). All replicates were processed consecutively in one day. Six chambers were divided between the two tanks and filled with three randomly selected baskets of each colonized treatment type. For the native and largest sized homogeneous sediment treatment, three or four individual sediment particles were used to fill the 300 cm^2 basket area. Chambers were filled with a known volume of water from the Oksrukuyik Creek (~10 L) and sealed. Mean ± standard error (SE) NH_4-N and PO_4-P

concentrations in the water were 4.1 ± 0.2 µg NH_4-N/L and 2.90 ± 0.07 µg PO_4-P/L, respectively. A calibrated DO probe (YSI ProODO) was threaded into each chamber to ensure no air bubbles, and the recirculation rate was adjusted to 0.1 m/s (Rüegg et al. 2015a).

Community respiration (CR) and net community production (NCP) were evaluated by recording the change in chamber water DO over time in the absence and presence of light, respectively. To evaluate CR, incubation tanks were covered to eliminate light and DO and temperature were recorded every 10 s for a period of 35–45 min. At the end of the CR measurement period, darkening covers were removed and NCP was measured using a similar procedure in full light. The duration of dark and light periods was kept under 45 min each to minimize nutrient depletion and to maximize changes in DO (Cardinale et al. 2002).

Net uptake of NH_4-N and PO_4-P was evaluated during NH_4-N-enriched conditions (N-enrichment) and NH_4-N plus PO_4-P-enriched conditions (N+P-enrichment). Separate stock solutions contained 144.3 mg NH_4-N/L (Fisher A661) and 9.54 mg PO_4-P/L (Fisher P285). For the N-enrichment experiment, 3.0 mL of the stock ammonium solution was injected into each chamber to increase the NH_4-N by 10 times background concentration (~43.3 µg NH_4-N/L). Six samples were taken 2, 6, 12, 20, 30, and 40 min after the initial injection using acid-washed 60-mL syringes (BD 309653). Each aliquot was immediately filtered (25-mm Whatman GF/F) into a new, clean, 60-mL high-density polyethylene bottle. After 42 min, we injected 1.5 mL of stock phosphate solution into the chambers and repeated the sampling procedure to determine the net uptake of NH_4-N and PO_4-P under

N+P-enriched conditions. A 10:1 N-to-P ratio (molar) was targeted based on work by Harvey et al. (1998), which found increased productivity in the Oksrukuyik Creek across all trophic levels during whole-stream fertilization experiments conducted at this ratio.

Nutrient samples were immediately frozen (-20 °C) for subsequent analysis, and grow lights were turned off to minimize biofilm chlorophyll a (Chl *a*) production. Sediment treatments were carefully removed from the chambers, placed into plastic bags, and stored in the dark, on wet ice, prior to sample analysis (<12 h). The remaining chamber water was poured through a 1-mm sieve to separate fine benthic OM (FBOM <1 mm) and coarse benthic OM (CBOM >1 mm) fractions.

3.1.3 Sample Analysis

Biofilms were removed by meticulously scrubbing each individual sediment grain using stainless steel brushes and tap water (Bowden et al. 1992). The smallest homogeneous treatment and the heterogeneous treatment were representatively subsampled by mass due to the large number of individual particles. For these treatments, approximately one-half (52 ± 14% SD) of the total sediment grains were scrubbed. Two aliquots (2– 10 mL) of the resulting biofilm–water mixture were filtered through 25-mm glass fiber filters (Whatman GF/F). One filter was frozen (-80°C) for subsequent Chl *a* analysis, and the others were dried (60 °C) for quantification of biofilm OM (biofilm OM). Chamber FBOM and CBOM subsamples were filtered (47-mm Whatman GF/F) and dried (60 °C). Biofilm OM, FBOM, and CBOM were evaluated for ash-free dry mass (AFDM). Samples and filters were first dried for 24 h (60 °C), weighed for dry mass, ashed in a

muffle furnace for 4 h (500 °C), and re-weighed for ash mass. Ash-free dry mass was calculated as the difference between dry mass and ash mass (Steinman et al. 2006). Filters for Chl *a* pigment analysis were extracted using hot ethanol (90%; Sartory and Grobbelaar 1984). Extracted pigments were acidified to 0.008 mol HCl/L and allowed to react with the acid for 30–60 min prior to spectrophotometric determination (Parker et al. 2016). Prior to analysis, chamber water samples were thawed in a 20 °C water bath and evaluated for NH_4-N and PO_4-P simultaneously to avoid re-freezing samples. All water nutrient analyses were conducted in triplicate. NH_4-N was measured on a Lachat FIA+ 8000 using QuikChem Method 10-107-06-2O (Hach Instruments, Loveland, Colorado, USA). This method is similar to the sodium salicylate method originally developed by (Verdouw et al. 1978), except that it uses lower concentrations of sodium salicylate (144 g/L) and sodium hypochlorite (0.32%). Sodium nitroprusside (3.5 g/L) was also used to intensify color development at 660 nm. We measured PO_4-P on a UV-2600 spectrophotometer (Shimadzu Scientific Instruments, Columbia, Maryland, USA) using the molybdenum blue method (Parsons et al. 1984). The mean reported value from laboratory triplicates was used for subsequent data evaluation.

The total surface area of sediment particles in each treatment (the sediment surface area) was determined using the mass–area approach developed by (Cooper and Testa 2001). First, 375 individual sediment grains from the homogeneous treatments were wrapped with aluminum foil. The foil was removed and weighed, and the surface area of each grain was determined using a standard curve relating foil mass to foil surface area (Tait et al. 1994). A relationship between sediment surface area and mass of individual

sediment particles was developed and used to predict total sediment surface area (cm^2) for each treatment ($t = 258.4$, $df = 374$, $p<0.0001$, Figure 3.3). After treatments were scrubbed, individual grains were weighed to the nearest tenth of a gram and sediment surface area was calculated as:

$$\text{Sediment Surface Area } (cm^2) = \sum_{i=1}^{n} 3.619 \times M_i{}^{0.665} \quad (1)$$

where, M_i is mass of an individual sediment grain in grams; n is the total number of sediment grains in each treatment. Sediment surface areas were adjusted to reflect the additional surface area contributed by the baskets, which was calculated using a digital scanner and the WinFOLIA™ leaf area processing tool (Regent Instruments Inc., Canada).

3.1.4 Calculation of Community Metabolism and Nutrient Uptake

Rates of metabolism and nutrient uptake for all experimental replicates (2), treatments (6), habitats (2), and sites (3, $n = 72$ total) were calculated using the fit linear model (fitlm) function in Matlab® R2014b (Mathworks Inc.). Three chambers from the Main Stem were compromised due to nutrient contamination and omitted from subsequent analysis ($n = 69$). Regression slopes were used to determine the rate of DO, NH_4-N, and PO_4-P concentration change for each experimental phase (mg/L/h). Dark and light regression slopes were multiplied by chamber water volume to calculate the raw CR (CR_{raw}) and raw NCP (NCP_{raw}) expressed as a mass flux (mg O_2/h). Raw community gross primary production (GPP_{raw}) was calculated by summing CR_{raw} and NCP_{raw} (Bott 2006). Raw rates of NH_4-N uptake ($N_{N\text{-}raw}$) and PO_4-P uptake ($P_{N\text{-}raw}$) for the N-enrichment period and raw rates of NH_4-N uptake ($N_{N+P\text{-}raw}$) and PO_4-P uptake ($P_{N+P\text{-}raw}$) for the N+P-

enrichment period were calculated by multiplying the regression slopes by the water volume adjusted for the mean losses from the two sampling phases (0.18 and 0.54 L, respectively). Raw rates were divided by the total sediment surface area and separately by the 0.03 m^2 constant projected area of the three treatment baskets. Subscripts denote sediment area-normalized rates ($_{sed}$) and projected area-normalized rates ($_{proj}$) of uptake and metabolism. Functional rates are expressed as mean values ± 1 SE unless otherwise noted.

3.1.5 Data Evaluation and Statistical Approach

We evaluated sediment treatment particle size and sediment surface area to test the efficacy of our manipulation. One-way analysis of variance (ANOVA) was used to determine whether particle size and sediment surface area were significantly different among homogeneous, heterogeneous, and native treatment types. We conducted a post hoc Tukey honest significant difference (HSD) test for particle size and sediment surface area to evaluate differences among individual treatments. Chl *a* and OM fractions were also summarized by treatment across sites and habitats. Post hoc multiple comparison results are reported as mean values ± SE. Variables were tested for normality using the Shapiro-Wilk W test, and analyses were conducted on natural log- or square root-transformed data, as necessary. Chl *a* and FBOM were natural log-transformed, CBOM was square root-transformed, and sediment surface area was untransformed.

A stepwise multiple linear regression model with Bayesian information criterion (BIC, minimum likelihood) was used to evaluate the effect of sediment surface area relative

to other community characteristics. Bayesian information criteria offers a robust approach for confirmatory analysis and variable selection (Aho et al. 2014). Multiple linear regression models included appropriately transformed estimates of Chl *a*, CBOM, FBOM, biofilm OM, and sediment surface area. Variables identified in the models with lowest BIC were assumed to best predict raw rates of uptake and metabolism. Delta BIC (Δ_{BIC}) was used to determine the lost model performance due to the removal of the sediment surface area variable. All statistical tests were considered significant at a = 0.05 and were performed using JMP Pro version 12.0 (SAS Institute Inc., Cary, North Carolina, USA) statistical software unless otherwise noted.

3.2 Results

3.2.1 Colonization Conditions

Mean discharge for the Main Stem, East Tributary, and West Tributary sites during colonization was 1,059 ± 2.8, 203 ± 2.8, and 197 ± 2.9 L/s, respectively. Mean water temperatures in the Main Stem, East Tributary, and West Tributary were 11.05 ± 0.02, 12.07 ± 0.02, and 7.92 ± 0.02 °C, respectively. During the five-week deployment period, mean daily PAR ± SD was 366.9 ± 169.9 μmol/s/m^2 and precipitation totaled 13.8 cm. Two precipitation events produced over 2 cm of rainfall in 24 h. These events resulted in high flows that overtopped the riverbanks. High discharge caused some losses to the smallest homogeneous sediment treatments and heterogeneous sediment treatments. Approximately 25% and 8% of the surface area was lost from riffle habitats for the smallest homogeneous sediment treatments and heterogeneous treatments, respectively.

3.2.2 Effect of Particle Size and Heterogeneity on Surface Area and Biofilm Characteristics

Median particle sizes (D_{50}) of colonized homogeneous treatments were 13, 31, 54, and 84 mm. The D_{50} of the heterogeneous and native treatments was 29 and 84 mm, respectively. Homogeneous particle size treatments were significantly different (F = 1162.0, df = 969, $P < 0.001$) and post-hoc tests indicated that all treatments differed significantly from one another ($P < 0.05$; Figure 3.4A). As intended, mean particle size of the 31-mm homogeneous sediment treatment (32.6 ± 0.7 mm) did not differ significantly from the heterogeneous treatment (33.2 ± 0.7 mm; $P > 0.05$). Similarly, native sediment treatments (84.6 ± 1.0 mm) did not differ significantly from the 84-mm homogeneous treatment class (84.7 ± 1.1 mm; $P > 0.05$).

Particle size had a significant effect on sediment surface area in a three-basket treatment ($F = 220.6$, $df = 71$, $P < 0.001$). Sediment surface area decreased with increasing particle size from 0.09 to 0.82 m^2, which was 3–27 times greater than the constant, 0.03 m^2, projected surface area (Figure 3.4B). Sediment surface area was significantly different across each treatment ($P < 0.05$) except the 84-mm and native treatments ($P > 0.05$), which did not differ significantly. Mean sediment surface area of the heterogeneous treatment (0.48 ± 0.02 m^2) was significantly greater than sediment surface area of the 31-mm homogeneous treatment (0.36 ± 0.02 m^2, $P < 0.05$).

Biofilm Chl *a* mass was generally consistent among particle sizes, yet sediment treatment had a significant effect on biofilm Chl *a* mass ($F = 2.8$, $df = 71$, $P < 0.001$; Figure

3.4C). Post hoc tests indicated significant differences between the native and 84-mm treatments ($P < 0.05$), but no significant differences among other treatments ($P > 0.05$). Sediment treatment also had a significant effect on OM (Figure 3.4D). Treatment explained 33 percent of the variance in FBOM mass ($F = 6.8$, $df = 71$, $P < 0.001$), 47% of the variance in CBOM mass (F=11.6,df=71,P<0.001), and 62% of the variance in biofilm OM mass ($F = 21.8$, $df = 71$, $P < 0.001$). For FBOM, significant differences were observed among all treatments except the 84-mm treatment, which had significantly less mean mass (0.038 ± 0.005 g AFDM). Comparisons of CBOM mass by sediment treatment showed that the 13-, 31-, 54-mm, and heterogeneous treatments were significantly greater than the 84-mm treatment ($P < 0.05$), and the CBOM of the native sediments was significantly less than that of the 13- and 54-mm homogeneous treatments ($P < 0.05$). There were no significant differences in biofilm OM among treatments except in the native treatment, which was seven times greater than the colonized treatments ($P < 0.05$).

3.2.3 Effect of Particle Size and Heterogeneity on Biofilm Metabolism

Mean chamber temperature ± SD during metabolism experiments in the temperature-controlled incubators was 8.3 ± 1.1 °C. Biofilm CR_{proj} ranged from 0.003 to 67.0 mg $O_2/h/m^2$, and CR_{sed} ranged from 0.001 to 18.0 mg $O_2/h/m^2$. The greatest mean respiration rates occurred in native sediment treatments where mean CR_{proj} and CR_{sed} were 47.1 ± 3.7 mg $O_2/h/m^2$ and 12.7 ± 1.0 mg $O_2/h/m^2$, respectively (Figure 3.5A). Mean CR_{sed} of the heterogeneous and 31-mm homogeneous treatments was 2.2 ± 0.3 mg $O_2/h/m^2$ and 2.6 ± 0.4 mg $O_2/h/m^2$, respectively. The heterogeneous treatment had a mean CR_{proj} of 36.0 ± 4.8 mg $O_2/h/m^2$, which was 4.4 mg $O_2/h/m^2$ greater than the CR_{proj} of the 31-mm

homogeneous treatment (31.6 ± 4.6 mg O_2/h/m^2). The heterogeneous and 31-mm homogeneous treatments did not differ significantly when CR was scaled using either normalization approach ($P > 0.05$). Rates of CR_{proj} and CR_{sed} were significantly correlated with D_{50} particle size for the four homogeneous sediment treatments evaluated, but the two normalization approaches had opposite relationships. As particle size increased, CR_{proj} significantly decreased ($F = 20.6$, $df = 44$, $P < 0.001$). In contrast, increased particle size resulted in increased CR_{sed} ($F = 4.8$, $df = 44$, $P = 0.034$).

During light phases of chamber metabolism and nutrient uptake measurements, mean PAR ± SD at the surface of the chambers was 575.4 ± 21.7 l µmol/s/m^2. Rates of GPP_{proj} ranged from 0.003 to 200.1 mg O_2/h/m^2, and rates of GPP_{sed} ranged from 0.001 to 36.8 mg O_2/h/m^2 (Figure 3.5B). Native sediments had the greatest rate of production among the treatments evaluated. Mean GPP_{proj} and GPP_{sed} of native treatments were 79.5 ± 7.7 mg O_2/h/m^2 and 21.3 ± 2.1 mg O_2/h/m^2, respectively. Observed mean GPP_{proj} of the 31-mm homogeneous treatment was 11.8 mg O_2/h/m^2 greater than the heterogeneous treatment, which had a mean GPP_{proj} of 59.3 ± 18.5 mg O_2/h/m^2. The 31-mm homogeneous treatment also had greater rates of GPP_{sed} than the heterogeneous treatment. Mean GPP_{sed} for the homogeneous and heterogeneous treatments was 5.9 ± 1.8 mg O_2/h/m^2 and 3.6 ± 1.1 mg O_2/h/m^2, respectively. For homogeneous treatments, sediment particle size had a weak, albeit significant, relationship with the GPP_{proj} where D_{50} explained 9% of the variance in productivity ($F = 4.3$, $df = 44$, $P = 0.046$; Figure 3.5B).

On average, rates of biofilm NCP_{proj} and NCP_{sed} were net autotrophic for all treatments evaluated (Figure 3.5C). NCP_{proj} ranged from -25.3 to 147.9 mg O_2/h/m^2, and

NCP_{sed} ranged from -4.2 to 18.8 mg $O_2/h/m^2$. Native sediment treatments had the lowest mean NCP_{proj} of 6.7 ± 4.9 mg $O_2/h/m^2$, while the 54-mm homogeneous treatment had the greatest NCP_{proj} of 46.6 ± 19.6 mg O_2/h. Mean NCP_{sed} was greatest in the native treatment and lowest in the 84mm homogeneous treatment. NCP_{sed} of the two treatments was 8.7 ± 1.5 mg $O_2/h/m^2$ and 1.4 ± 0.9 mg $O_2/h/m^2$, respectively. For both normalization approaches, the heterogeneous treatment did not differ significantly from the 31-mm homogeneous treatment ($P > 0.05$), which had greater net autotrophy. Particle size had no significant effect on NCP_{proj} and NCP_{sed} for the colonized sediment treatments included in the linear model ($P > 0.05$; Figure 3.5C).

3.2.4 Effect of Particle Size and Heterogeneity on Biofilm Nutrient Uptake

Mean chamber temperature ± SD during nutrient uptake experiments in the temperature-controlled incubators was 9.5 ± 0.8°C, and PAR conditions remained comparable to metabolic experiments. Net biofilm NH_4-N uptake during the N-enrichment experiments ranged from 0.21 to 8.15 mg NH_4-N/h/m^2 and 0.06 to 1.49 mg NH_4-N/h/$m^2$when normalized by projected area ($N_{N\text{-}proj}$) and sediment surface area ($N_{N\text{-}sed}$), respectively (Figure 3.6A). The 13-mm homogeneous treatment had the greatest mean $N_{N\text{-}proj}$ of 4.91 ± 0.56 mg NH_4-N/h/m^2, and the native treatment had the greatest mean $N_{N\text{-}proj}$ of 0.77 ± 0.12 mg NH_4-N/h/m^2. When normalized by projected surface area, mean $N_{N\text{-}proj}$ of the heterogeneous treatment (0.15 ± 0.08 mg NH_4-N/h/m^2) was 25% less than that of the 31-mm homogeneous treatment (0.20 ± 0.10 mg NH_4-N/h/m^2), and the two projected area-normalized treatments did not differ significantly ($P > 0.05$). Mean $N_{N\text{-}sed}$ for the heterogeneous treatment was 0.23 ± 0.02 mg NH_4- N/h/m^2. The heterogeneous uptake was

18% less than the mean $N_{N\text{-}sed}$ uptake observed in the 31-mm homogeneous treatment (0.28 ± 0.04 mg NH_4-N/h/m^2), and the two also did not differ significantly ($P > 0.05$). There were significant differences in NH_4-N uptake in homogeneous treatments for both normalization approaches during the N-enrichment period (Figure 3.6A). D_{50} explained 18% of the variance in projected area-normalized uptake ($N_{N\text{-}proj}$, $F = 9.4$, $df = 44$, $P = 0.004$) and 33% of the variance in sediment area-normalized uptake ($N_{N\text{-}sed}$, $F = 21.5$, $df = 44$, $P < 0.001$). Projected and sediment surface area normalization approaches resulted in opposite relationships between particle size and NH_4-N uptake. $N_{N\text{-}proj}$ decreased as particle size increased, while $N_{N\text{-}sed}$ increased.

Net biofilm PO_4-P exchange during the N-enrichment experiments ranged from --- 0.56 to 1.64 mg PO_4-P/h/m^2 and -0.13 to 0.18 mg PO_4-P/h/m^2 when normalized by projected area ($P_{N\text{-}proj}$) and sediment surface area ($P_{N\text{-}sed}$), respectively (Figure 3.6C). The mean net uptake was greatest in the 54-mm homogeneous treatment, which had a $P_{N\text{-}proj}$ of 0.29 ± 0.19 mg PO_4-P/h/m^2. The 84-mm homogeneous treatment had the greatest mean $P_{N\text{-}sed}$ of 0.08 ± 0.02 mg PO_4-P/h/m^2. $P_{N\text{-}sed}$ of heterogeneous sediment treatment did not differ significantly from the 31-mm homogeneous treatment during the N-enrichment period ($P > 0.05$). Similarly, native sediment treatments were not significantly different than the 84-mm treatment for both uptake rates during the N-enrichment ($P > 0.05$). Particle size had a significant effect on the variance of sediment area-normalized PO_4-P uptake ($P_{N\text{-}sed}$) during the experimental period ($F = 16.7$, $df = 44$, $P < 0.001$), but no significant effect on projected area-normalized uptake ($P_{N\text{-}proj}$, $P > 0.05$; Figure 3.6C).

The addition of PO_4-P to an enriched NH_4-N environment, the N+P-enrichment, resulted in decreased ammonium uptake for all treatments evaluated. Net biofilm NH_4-N uptake during N+P-enrichment experiments ranged from -1.91 to 7.63 mg NH_4-N/h/m^2 and -0.12 to 1.14 mg NH_4-N/h/m^2 when normalized by projected area ($N_{N+P\text{-}proj}$) and sediment surface area ($N_{N+P\text{-}sed}$), respectively (Figure 3.6B). When normalized by projected area, the greatest net uptake was observed in the 13-mm homogeneous treatment (2.37 ± 0.36 mg NH_4-N/h/m^2). The 84-mm homogeneous treatment had the greatest net $N_{N+P\text{-}sed}$ of 0.55 ± 0.08 mg NH_4-N/h/m^2. Nitrogen uptake in the 31-mm homogeneous and heterogeneous treatments did not differ significantly for both normalization approaches during the N+P-enrichment uptake experiments ($P > 0.05$). Particle size had no significant effect on $N_{N+P\text{-}proj}$ ($P > 0.05$), but it did have a significant, positive effect on $N_{N+P\text{-}sed}$ ($F = 29.3$, $df = 44$, $P < 0.001$).

The addition of PO_4-P to an enriched ammonium environment resulted in increased PO_4-P uptake for all treatments and normalization approaches evaluated. Net biofilm uptake during the N+P-enrichment experiments ranged from 0.51 to 4.16 mg PO_4-P/h/m^2 and 0.08 to 0.62 mg PO_4-P/h/m^2 when normalized by projected area ($P_{N+P\text{-}proj}$) and sediment surface area ($P_{N+P\text{-}sed}$), respectively (Figure 3.6D). The greatest projected surface area-normalized uptake rate was observed in the 13-mm homogeneous treatment, which had a mean $P_{N+P\text{-}proj}$ of 3.07 ± 0.14 mg PO_4-P/h/m^2. The greatest sediment areanormalized uptake rate was observed in the

native treatment, which had a mean $P_{N+P\text{-}proj}$ of 0.41 ± 0.02 mg PO_4-P/h/m^2. Mean $P_{N+P\text{-}sed}$ uptake of the 31-mm homogeneous treatment (0.21 ± 0.02 mg PO_4-P/h/m^2) was 40% greater than that of the heterogeneous treatment (0.15 ± 0.01 mg PO_4-P/h/m^2), but no significant differences in PO_4-P uptake were observed ($P < 0.05$). Native sediment treatments did not differ significantly from the 84-mm homogeneous treatment for all nutrient uptake rates and normalization approaches except $P_{N+P\text{-}sed}$, where the mean rate of uptake in the native treatment (0.41 ± 0.02 mg PO_4-P/h/m^2) was greater than in the homogeneous treatment (0.30 ± 0.04 mg PO_4-P/h/m^2). D_{50} particle size had a significant effect on $P_{N+P\text{-}proj}$ ($F = 49.6$, $df = 44$, $P < 0.001$) and $P_{N+P\text{-}proj}$ ($F = 16.2$, $df = 44$, $P < 0.001$).

3.2.5 Effect of Sediment Surface Area on Biofilm Function

Multiple linear regression analysis was conducted using a stepwise model selection procedure to identify the importance of sediment surface area relative to the other characteristics. Due to significant differences in biofilm OM in the native sediment treatments, this evaluation was limited to colonized heterogeneous and homogeneous treatments. Multiple linear models explained 55%, 84%, and 87% of the variance in raw rates of community respiration (CR_{raw}), gross primary production (GPP_{raw}), and net community production (NCP_{raw}), respectively (Table 1). Chamber Chl *a* had the greatest effect on model fit for all three metabolic rates. The Δ_{BIC} was greater for NCP_{raw} and CR_{raw} than for GPP_{raw}, an indication that sediment surface area has a greater effect on the prediction of respiration rates than on rates of production. Net NH_4-N nutrient uptake was predominately controlled by Chl *a* mass on the sediment biofilms, especially during the

N+P-enrichment addition (Table 1). Our models explained 39% and 42% of the variance in uptake for the N- and N+P-enrichment periods, respectively. Poor model performance was observed for the ambient PO_4-P uptake during the N-enrichment period. Sediment surface area alone only explained 6% of the variance in uptake. Sediment surface area, Chl *a*, and CBOM explained 75% of the variance in PO_4-P uptake during the N+P-enrichment period, where Δ_{BIC} was greatest among all functional rates measured.

3.3 Discussion

We tested how the function of biofilm communities differs with respect to coarse sediment particle size and heterogeneity in riffle and run habitats of streams with contrasting hydrological and physicochemical characteristics. To accomplish this, we evaluated metabolic and nutrient uptake rates of stream biofilms across a range of median particle sizes using both projected area- and sediment surface area-normalized data. Community respiration and nutrient uptake were sensitive to changes in sediment particle size, while rates of gross primary production and NCP were more strongly correlated with mass of Chl *a* associated with the projected surface area. Our findings are consistent with previous studies that have examined the effect of various habitat characteristics on stream biofilm community processes (Kemp and Dodds 2002, Webster et al. 2003, Hoellein et al. 2009, Kendrick and Huryn 2015), and offer additional perspective to the existing paradigm that links heterogeneous physical habitats to increased rates of ecosystem function (Cardinale et al. 2002, Palmer et al. 2010). Our results revealed no clear link between heterogeneous physical habitats and rates of biogeochemical function in biofilms when normalized by sediment surface area. This finding promotes a mechanistic framework

whereby elevated function can be explained by increased sediment surface area scaled across equal habitat volumes.

3.3.1 Effect of Particle Size and Heterogeneity on Biofilm Metabolism

We hypothesized that rates of respiration would be negatively correlated with coarse sediment size due to decreases in total sediment surface area. This hypothesis was confirmed by the significant decrease in biofilm CR_{proj} with increasing particle size in homogeneous treatments. The significant interaction between sediment particle size and rates of CR_{proj} suggests that conventional assessments of stream biofilm community function using projected area normalization approaches may reflect differences in total available sediment surface area for colonization rather than functional differences between habitats. Cobble-sized sediment particles measured using chamber techniques and projected surface area normalization approaches from an adjacent arctic river had a CR_{proj} of 21.7 ± 4.2 mg $O_2/h/m^2$ (Kendrick and Huryn 2015). Although CR_{proj} rates were comparable to our 54and 84-mm homogeneous treatments, the potential for confounding results due to variation in particle size was not discussed.

Contrary to our hypothesis that rates of CR_{sed} would not differ across different particle sizes, CR_{sed} increased with increasing particle size in homogeneous treatments. Variable respiration rates between different substrata have been previously acknowledged by Hoellein et al. (2009), who quantified rates of metabolism and nitrate uptake using substrate surface area and biofilm biomass scaling approaches. The significant, positive relationship between CR_{sed} and sediment surface area suggests that biofilms on larger

sediment particles may be more active than biofilms colonized on smaller particles (i.e., greater productivity per unit chlorophyll a; data not shown). This pattern could also be attributed to better circulation of water through larger particle size treatments. However, the effect of flow through interstitial space on biofilm function is not currently known (Battin et al. 2016) and offers an exciting opportunity for future research.

The observed productivity of colonized sediment biofilms provides some support to our hypothesis that primary production would be similar across all treatments due to similar projected area for biofilm autotroph colonization. Although particle size had a weak, albeit significant, effect on mean GPP_{proj} in the colonized homogeneous sediment treatments from riffle and run habitats, the trend across the 13to 54mm treatments was not significant ($F = 0.006$, $df = 34$, $P = 0.939$). The significant relationship is the result of low GPP_{proj} observed in the 84mm homogeneous treatment (Figure 3.5C). Both Chl *a* and the GPP_{proj} were lowest for the 84-mm treatment across all sites and habitats, which could be attributed to not placing the largest homogeneous sediment treatments into plastic baskets during colonization.

Decreased rates of CR and GPP as well as lower biofilm OM observed in the colonized sediments suggest that our manipulated homogeneous and heterogeneous treatments did not fully mature during the deployment period. Native sediments had a sevenfold increase in biofilm OM over the colonized treatments and significantly greater rates of respiration and primary production depending on the colonized treatment. Although the rates of CR and GPP were greater in the native treatments, the NCP did not differ from the colonized treatments. This indicates that mature biofilms have greater

carbon turnover than younger biofilms, but their net effect on an ecosystem is similar. Greater biofilm mass observed on the native sediments corresponds well with the legacy effects concept developed by Kendrick and Huryn (2015), whereby bed ice during the spring freshet protects arctic stream biofilm communities from scour and allows them to develop over several seasons.

3.3.2 Effect of Particle Size and Heterogeneity on Nutrient Uptake

The NH_4-N uptake rates during our N+P-enrichment supported our hypothesis that nutrient uptake would decrease as particle size increased. Whole-stream measurements of net $N_{N\text{-}proj}$ uptake observed in a nearby arctic stream ranged from approximately 0.9–1.8 mg NH_4-N/m^2/h (Peterson et al. 2001). Net uptake rates in the nearby system were 1.3–5.5 times lower than the uptake rates observed in this study. However, Peterson et al. (2001) utilized whole-stream isotopic tracer methods to determine the rate of uptake, which could account for some differences in observed net uptake between the two nearby stream sites. Our observed rates of $P_{N+P\text{-}proj}$ uptake were also comparable to previous whole-stream estimates from a nearby tundra river, which had a mean $P_{N+P\text{-}proj} \pm$ SD of 1.2 ± 1.0 mg PO_4P/m^2/h (Peterson et al. 1993). The projected area-normalized estimates of phosphorus uptake we observed were less than threefold higher than previous whole-stream estimates.

Although our estimates are within the expected range of values observed in nearby arctic river systems, those studies did not explicitly consider the relationships between uptake rates and sediment particle size. Kemp and Dodds (2002) examined ammonium uptake rates across multiple substrata in prairie streams. They found epilithic periphyton

biofilms and FBOM to contribute substantially to the net ammonium uptake. The rates of $N_{N\text{-}proj}$ uptake they measured, in a more productive temperate system, were up to three times greater than the rates observed in this study. Additionally, our results indicate that FBOM mass does not have a significant effect on the ammonium uptake under N-enriched or N+P-enriched conditions. Lottig and Stanley (2007) examined the effect of benthic sediment on dissolved phosphorus concentrations in headwater streams in central Wisconsin. Their findings indicated phosphorus uptake of sand-size substrate was nearly double that of coarser rock and gravel-size sediment similar to what we evaluated in the present study. Lottig and Stanley (2007) found that sands had limited biotic uptake and were dominated by abiotic sorption, while larger rock and gravel sediments had near equal contributions of abiotic and biotic uptake. However, their measurements were expressed per unit sediment mass and were not directly comparable to our measurements of P uptake. Given the coarse nature of benthic sediments in our study system and the observed biofilm colonization, we conclude that the net uptake measured can be attributed largely to biotic processes on the colonized biofilms.

We also anticipated that the addition of phosphate to an N-enriched system would result in elevated NH_4-N uptake. However, we observed that the addition of PO_4-P resulted in a suppression of NH_4-N uptake across all treatments evaluated for $N_{N+P\text{-}proj}$. An inhibition of nitrate-nitrogen uptake by the presence of ammonia in freshwater algae has been well documented (Ohmori et al. 1977) as well as the inhibition of primary production by addition of ammonium (Elrifi and Turpin 1986). But, to the best of our knowledge, no study has demonstrated suppression of NH_4-N uptake by PO_4-P addition. An important

caveat to our findings is that our experimental additions were linked in time series; therefore, the ambient concentration of the ammonium in the chamber during the addition of phosphate was much lower than during the onset of the ammonium only uptake experiment. Additional testing is needed to fully evaluate whether PO_4-P can temporarily suppress the ammonium uptake of freshwater biofilms. Nevertheless, the suppression of NH_4-N uptake by the addition of phosphate has important implications for streams where impacts due to eutrophication are likely.

3.3.3 Effect of Sediment Surface Area on Biofilm Functions

Our results indicate that sediment surface area is a critical habitat characteristic that contributes to several important ecosystem functions. This finding has important implications for understanding the role of physical habitat heterogeneity on ecosystem function, which is supported by the comparison of heterogeneous and 31-mm homogeneous sediment treatments when normalized using the two normalization approaches. For example, mean CR_{proj} and $N_{N\text{-}proj}$ were greater in the heterogeneous treatment than in the 31-mm homogeneous treatment, but the 31-mm treatment had greater CR_{sed} and $N_{N\text{-}sed}$ than the heterogeneous treatment. The additional sediment surface area associated with heterogeneous habitats needs to be more explicitly considered when examining functional rates in stream and river reaches with different physical habitat types. Warfe et al. (2008) called for more focused evaluation of habitat heterogeneity using various structural metrics. Our findings support a simple approach whereby habitat complexity can be accounted for by quantifying the total sediment surface area for colonization.

Our results were somewhat contrary to the findings described by Cardinale et al. (2002), who attributed elevated rates of community primary production and respiration to increased habitat heterogeneity. Cardinale et al. (2002) manipulated the sediment distribution in an entire stream reach and used chamber measurements of ceramic tiles to test how ecosystem function differed between treatments. Their approach was effective at highlighting the direct response of sediment biofilms independent of additional community factors such as FBOM and CBOM. However, tile-colonizing biofilms may not be representative of the complex biofilm community found on natural river sediments. Our evaluation of colonized benthic sediment treatments provides evidence that habitat heterogeneity was important, but the overall response was less apparent. This could be attributed to the larger spatial grain of our chamber measurements. Aubeneau et al. (2016) examined the effect of biofilm colonization on solute dynamics in heterogeneous and homogeneous experimental streams. They found that the accumulation of biofilm mats on the streambed surface systematically modified the condition of the flow conditions within the stream. Therefore, we suspect that streams that are prone to develop large biofilm mats are less likely to show increased functional rates in relation to decreasing particle size or increasing heterogeneity, but rather a shift in control of these functional rates from sediment to physical habitat-control to biofilm-control over time.

3.4 Conclusion

In conclusion, our observations are consistent with the framework put forth by Battin et al. (2016), which describes freshwater biofilms as microbial skin. As particle size decreases, sediment surface area increases, thus increasing the total area available for

microbial colonization within a given habitat. We found that sediment surface area significantly contributed to the performance of each raw metabolism multivariate model evaluated as well as the N-enriched nitrogen. Sediment surface area was the most important variable to the model performance for phosphorus uptake. The multiple linear regression analysis highlights the importance of sediment surface area relative to other drivers of biofilm community metabolism. In an unexpected result, we observed a weak, positive relationship between biogeochemical functions and particle size expressed on a total sediment area basis. This may be a consequence of better circulation of water around larger versus smaller particles, which should be further investigated. The conditions of our experiments (homogeneous particle sizes in controlled environments) were clearly artificial, but illustrate a point that may have wider applicability in stream biogeochemical modeling. Specifically, an expression of stream function on the basis of projected area allows for lateral spatial heterogeneity but ignores three-dimensional spatial heterogeneity—the sediment surface area. Our results show that there are predictable relationships between projected surface area and important stream ecosystem functions (metabolism and nutrient uptake) that can be related to particle size. Particle size in streams is a function of other, discernible environmental factors in the ecosystem (e.g., slope, stream order, local geology). Therefore, it may be possible to connect these discernible factors to predict general particle size distributions in stream networks in a way that would allow us to refine estimates of important ecosystem processes.

3.5 Literature Cited

Aho, K., D. Derryberry, and T. Peterson. 2014. Model selection for ecologists: the worldviews of AIC and BIC. Ecology 95:631-636.

ARCTIC-LTER. 2016. Arctic Long-Term Ecological Research Streams and Rivers Database. Accessed December 2016. http://arc-lter.ecosystems.mbl.edu/arctic-lter-streams-and-rivers.

Aubeneau, A. F., B. Hanrahan, D. Bolster, and J. Tank. 2016. Biofilm growth in gravel bed streams controls solute residence time distributions. Journal of Geophysical Research: Biogeosciences 121:1840-1850.

Barnes, J. B., I. P. Vaughan, and S. J. Ormerod. 2013. Reappraising the effects of habitat structure on river macroinvertebrates. Freshwater Biology 58:2154-2167.

Battin, T. J., K. Besemer, M. M. Bengtsson, A. M. Romani, and A. I. Packmann. 2016. The ecology and biogeochemistry of stream biofilms. Nat Rev Micro 14:251-263.

Besemer, K. 2015. Biodiversity, community structure and function of biofilms in stream ecosystems. Research in Microbiology 166:774-781.

Besemer, K., G. Singer, I. Hödl, and T. J. Battin. 2009. Bacterial community composition of stream biofilms in spatially variable-flow environments. Applied and environmental microbiology 75:7189-7195.

Bott, T. L. 2006. Chapter 28: Primary Production and Community Respiration.in F. R. Hauer and G. A. Lamberti, editors. Methods in Stream Ecology: Second Edition. Elsevier, Burlington, MA.

Boulton, A. J., T. Datry, T. Kasahara, M. Mutz, and J. A. Stanford. 2010. Ecology and management of the hyporheic zone: stream-groundwater interactions of running waters and their floodplains. Journal of the North American Benthological Society 29:26-40.

Boulton, A. J., S. Findlay, P. Marmonier, E. H. Stanley, and H. M. Valett. 1998. The functional significance of the hyporheic zone in streams and rivers. Annual Review of Ecology and Systematics 29:59-81.

Bowden, W. B., B. J. Peterson, J. C. Finlay, and J. Tucker. 1992. Epilithic chlorophyll-a, photosynthesis, and respiration in control and fertilized reaches of a tundra stream. Hydrobiologia 240:121-131.

Briggs, M. A., F. D. Day-Lewis, J. P. Zarnetske, and J. W. Harvey. 2015. A physical explanation for the development of redox microzones in hyporheic flow. Geophysical Research Letters 42:4402-4410.

Cardinale, B. J., K. Gross, K. Fritschie, P. Flombaum, J. W. Fox, C. Rixen, J. van Ruijven, P. B. Reich, M. Scherer-Lorenzen, and B. J. Wilsey. 2013. Biodiversity simultaneously enhances the production and stability of community biomass, but the effects are independent. Ecology 94:1697-1707.

Cardinale, B. J., M. A. Palmer, C. M. Swan, S. Brooks, and N. L. Poff. 2002. The influence of substrate heterogeneity on biofilm metabolism in a stream ecosystem. Ecology 83:412-422.

Claret, C., and D. Fontvieille. 1997. Characteristics of biofilm assemblages in two contrasted hydrodynamic and tophic contexts. Microbial Ecology 34:49-57.

Cooper, C. M., and S. Testa. 2001. A quick method of determining rock surface area for quantification of the invertebrate community. Hydrobiologia 452:203-208.

Crump, B. C., L. A. Amaral-Zettler, and G. W. Kling. 2012. Microbial diversity in arctic freshwaters is structured by inoculation of microbes from soils. ISME J 6:1629-1639.

Downes, B. J., P. S. Lake, E. S. G. Schreiber, and A. Glaister. 1998. Habitat structure and regulation of local species diversity in a stony, upland stream. Ecological Monographs 68:237-257.

Elrifi, I. R., and D. H. Turpin. 1986. Nitrate and ammonium induced photosynthetic suppression in N-limited *Selenastrum minutum*. Plant Physiology 81:273-279.

Finlay, J. C., and W. B. Bowden. 1994. Controls on production of bryophytes in an arctic tundra stream. Freshwater Biology 32:455-465.

Gayraud, S., and M. Philippe. 2003. Influence of Bed-Sediment Features on the Interstitial Habitat Available for Macroinvertebrates in 15 French Streams. International Review of Hydrobiology 88:77-93.

Graba, M., S. Sauvage, N. Majdi, B. Mialet, F. Y. Moulin, G. Urrea, E. Buffan-Dubau, M. Tackx, S. Sabater, and J.-M. Sanchez-Perez. 2014. Modelling epilithic biofilms combining hydrodynamics, invertebrate grazing and algal traits. Freshwater Biology 59:1213–1228.

Haggerty, R., M. Ribot, G. A. Singer, E. Martí, A. Argerich, G. Agell, and T. J. Battin. 2014. Ecosystem respiration increases with biofilm growth and bed forms: Flume measurements with resazurin. Journal of Geophysical Research: Biogeosciences 119:2220-2230.

Harvey, C. J., B. J. Peterson, W. B. Bowden, A. E. Hershey, M. C. Miller, L. A. Deegan, and J. C. Finlay. 1998. Biological responses to fertilization of Oksrukuyik Creek, a tundra stream. Journal of the North American Benthological Society 17:190-209.

Hoellein, T. J., J. L. Tank, S. A. Entrekin, E. J. Rosi-Marshall, M. L. Stephen, and G. A. Lamberti. 2012. Effects of benthic habitat restoration on nutrient uptake and ecosystem metabolism in three headwater streams. River Research and Applications 28:1451-1461.

Hoellein, T. J., J. L. Tank, E. J. Rosi-Marshall, and S. A. Entrekin. 2009. Temporal variation in substratum-specific rates of N uptake and metabolism and their contribution at the stream-reach scale. Journal of the North American Benthological Society 28:305-318.

Hynes, H. 1970. The ecology of running waters. University of Toronto Press, Toronto, Ontario.

Kemp, M. J., and W. K. Dodds. 2002. The influence of ammonium, nitrate, and dissolved oxygen concentrations on uptake, nitrification, and denitrification rates associated with prairie stream substrata. Limnology and Oceanography 47:1380-1393.

Kendrick, M. R., and A. D. Huryn. 2015. Discharge, legacy effects and nutrient availability as determinants of temporal patterns in biofilm metabolism and accrual in an arctic river. Freshwater Biology 60:2323-2336.

Kilpatrick, F. A., E. D. Cobb, and G. Survey. 1985. Measurement of discharge using tracers. Department of the Interior, U.S. Geological Survey. https://pubs.er.usgs.gov/publication/twri03A16

Kovalenko, K. E., S. M. Thomaz, and D. M. Warfe. 2012. Habitat complexity: approaches and future directions. Hydrobiologia 685:1-17.

Laub, B. G., D. W. Baker, B. P. Bledsoe, and M. A. Palmer. 2012. Range of variability of channel complexity in urban, restored and forested reference streams. Freshwater Biology 57:1076-1095.

Lawrence, J. R., B. Scharf, G. Packroff, and T. R. Neu. 2002. Microscale evaluation of the effects of grazing by invertebrates with contrasting feeding modes on river biofilm architecture and composition. Microbial Ecology 44:199–207.

Lefcheck, J. S., J. E. K. Byrnes, F. Isbell, L. Gamfeldt, J. N. Griffin, N. Eisenhauer, M. J. S. Hensel, A. Hector, B. J. Cardinale, and J. E. Duffy. 2015. Biodiversity enhances ecosystem multifunctionality across trophic levels and habitats. Nat Commun 6.

Lock, M. A., R. R. Wallace, J. W. Costerton, R. M. Ventullo, and S. E. Charlton. 1984. River Epilithon: Toward a Structural-Functional Model. Oikos 42:10-22.

Lottig, N. R., and E. H. Stanley. 2007. Benthic sediment influence on dissolved phosphorus concentrations in a headwater stream. Biogeochemistry 84:297-309.

Majdi, N., B. Mialet, S. Boyer, M. Tackx, J. Leflaive, S. Bouletreau,L.Ten-Hage,F.Julien,R.Fernandez, and E. Buffan-Dubau. 2012. The relationship between epilithic biofilm stability and its associated meiofauna under two patterns of flood disturbance. Freshwater Science 31:38–50.

Majdi, N., I. Threis, and W. Traunspurger. 2017. It's the little things that count: meiofaunal density and production in the sediment of two headwater streams. Limnology and Oceanography 62:151–163.

Miller, M. C., P. Deoliveira, and G. G. Gibeau. 1992. Epilithic diatom community response to years of PO4 fertilization - Kuparuk River, Alaska (68 N Lat.). Hydrobiologia 240:103-119.

Ohmori, M., K. Ohmori, and H. Strotmann. 1977. Inhibition of nitrate uptake by ammonia in a blue-green alga, Anabaena cylindrica. Archives of Microbiology 114:225-229.

Oswood, M. W., L. K. Miller, and J. G. Irons III. 1995. River and stream ecosystems of Alaska.in C. E. Cushing, K. W. Cumming, and G. W. Minshall, editors. Ecosystems of the World 22: River and Stream Ecosystems. Elsevier, Amsterdam.

Palmer, M. A., A. P. Covich, S. Lake, P. Biro, J. J. Brooks, J. Cole, C. Dahm, J. Gibert, W. Goedkoop, K. Martens, J. Verhoeven, and W. J. Van De Bund. 2000. Linkages between aquatic sediment biota and life above sediments as potential drivers of biodiversity and ecological processes. Bioscience 50:1062-1075.

Palmer, M. A., H. L. Menninger, and E. Bernhardt. 2010. River restoration, habitat heterogeneity and biodiversity: a failure of theory or practice? Freshwater Biology 55:205-222.

Parker, S. P., W. B. Bowden, and M. B. Flinn. 2016. The effect of acid strength and postacidification reaction time on the determination of chlorophyll a in ethanol extracts of aquatic periphyton. Limnology and Oceanography: Methods 14:839-852.

Parsons, T. R., Y. Maita, and C. M. Lalli. 1984. 1.6 - Determination of Phosphate. Pages 22-25 in T. R. P. M. M. Lalli, editor. A Manual of Chemical & Biological Methods for Seawater Analysis. Pergamon, Amsterdam.

Passarelli, C., F. Olivier, D. M. Paterson, T. Meziane, and C. Hubas. 2014. Organisms as cooperative ecosystem engineers in intertidal flats. Journal of Sea Research 92:92–101.

Peterson, B. J., L. Deegan, J. Helfrich, J. E. Hobbie, M. Hullar, B. Moller, T. E. Ford, A. Hershey, A. Hiltner, G. Kipphut, M. A. Lock, D. M. Fiebig, V. McKinley, M. C. Miller, J. R. Vestal, R. Ventullo, and G. Volk. 1993. Biological responses of a tundra river to fertilization. Ecology 74:653-672.

Peterson, B. J., W. M. Wollheim, P. J. Mulholland, J. R. Webster, J. L. Meyer, J. L. Tank, E. Martí, W. B. Bowden, H. M. Valett, A. E. Hershey, W. H. McDowell, W. K. Dodds, S. K. Hamilton, S. Gregory, and D. D. Morrall. 2001. Control of Nitrogen Export from Watersheds by Headwater Streams. Science 292:86-90.

Rüegg, J., J. D. Brant, D. M. Larson, M. T. Trentman, and W. K. Dodds. 2015*a*. A portable, modular, self-contained recirculating chamber to measure benthic processes under controlled water velocity. Freshwater Science 34:831-844.

Rüegg, J., W. K. Dodds, M. D. Daniels, K. R. Sheehan, C. L. Baker, W. B. Bowden, K. J. Farrell, M. B. Flinn, T. K. Harms, J. B. Jones, L. E. Koenig, J. S. Kominoski, W. H. McDowell, S. P. Parker, A. D. Rosemond, M. T. Trentman, M. Whiles, and W. M. Wollheim. 2015*b*. Baseflow physical characteristics differ at multiple spatial scales in stream networks across diverse biomes. Landscape Ecology 31:119-136.

Sartory, D., and J. Grobbelaar. 1984. Extraction of chlorophyll a from freshwater phytoplankton for spectrophotometric analysis. Hydrobiologia 114:177-187.

Seiferling, I., R. Proulx, and C. Wirth. 2014. Disentangling the environmental-heterogeneity species-diversity relationship along a gradient of human footprint. Ecology 95:2084-2095.

Stegen, J. C., J. K. Fredrickson, M. J. Wilkins, A. E. Konopka, W. C. Nelson, E. V. Arntzen, W. B. Chrisler, R. K. Chu, R. E. Danczak, S. J. Fansler, D. W. Kennedy, C. T. Resch, and M. Tfaily. 2016. Groundwater-surface water mixing shifts ecological assembly processes and stimulates organic carbon turnover. Nat Commun 7.

Steinman, A. D., G. A. Lamberti, and P. R. Leavitt. 2006. Chapter 17: Biomass and Pigments of Benthic Algae.in F. R. Hauer and G. A. Lamberti, editors. Methods in Stream Ecology: Second Edition. Elsevier, Burlington, MA.

Tait, C. K., J. L. Li, G. A. Lamberti, T. N. Pearsons, and H. W. Li. 1994. Relationships between Riparian Cover and the Community Structure of High Desert Streams. Journal of the North American Benthological Society 13:45-56.

Tews, J., U. Brose, V. Grimm, K. Tielbörger, M. C. Wichmann, M. Schwager, and F. Jeltsch. 2004. Animal species diversity driven by habitat heterogeneity/diversity: the importance of keystone structures. Journal of Biogeography 31:79-92.

Verdouw, H., C. J. A. Van Echteld, and E. M. J. Dekkers. 1978. Ammonia determination based on indophenol formation with sodium salicylate. Water Research 12:399-402.

Walker, M. D., D. A. Walker, and N. A. Auerbach. 1994. Plant communities of a tussock tundra landscape in the Brooks Range Foothills, Alaska. Journal of Vegetation Science 5:843-866.

Warfe, D. M., L. A. Barmuta, and S. Wotherspoon. 2008. Quantifying habitat structure: surface convolution and living space for species in complex environments. Oikos 117:1764-1773.

Webster, J. R., P. J. Mulholland, J. L. Tank, H. M. Valett, W. K. Dodds, B. J. Peterson, W. B. Bowden, C. N. Dahm, S. Findlay, S. V. Gregory, N. B. Grimm, S. K. Hamilton, S. L. Johnson, E. Marti, W. H. McDowell, J. L. Meyer, D. D. Morrall, S. A. Thomas, and W. M. Wollheim. 2003. Factors affecting ammonium uptake in streams - an inter-biome perspective. Freshwater Biology 48:1329-1352.

Wentworth, C. K. 1922. A scale of grade and class terms for clastic sediments. Journal of Geology 30: 377–392.

Whittinghill, K. A., J. C. Finlay, and S. E. Hobbie. 2014. Bioavailability of dissolved organic carbon across a hillslope chronosequence in the Kuparuk River region, Alaska. Soil Biology and Biochemistry 79:25-33.

Wise, D. H., and M. C. Molles. 1979. Colonization of artifical substrates by stream insects: Influence of susbtrate size and diversity. Hydrobiologia 65:69-74.

3.6 Acknowledgements

We would like to thank Frances Iannucci, Ford Ballantyne, and Chao Song for their assistance in the field and laboratory, and the researchers and technicians of the Toolik Field Station, Arctic LTER program, and Rubenstein Ecosystem Science Laboratory. In addition, we would like to thank the graduate students and principal investigators of the Scale, Consumers, and Lotic Ecosystem Rates (SCALER) project for their support and guidance throughout the production of this manuscript. Finally, we would like to thank the anonymous reviewers who provided insightful comments that helped clarify and strengthen our thesis. This material is based on work supported by the National Science Foundation under grant numbers EF-1065682, EF1065267, and DEB/LTER-1026843. Any opinions, findings, and conclusions or recommendations expressed in this material are those of the authors and do not reflect the views of the National Science Foundation.

3.6 Tables

Table 3.1 Stepwise multivariate analysis of variance models that best predict functional rates of colonized sediment biofilms. Bayesian information criterion (BIC) used to select most parsimonious model that minimizes the number of significant effects variables while maximizing predictive power. Δ_{BIC} indicates lost model performance due to the removal of sediment surface area variable. Significant effects variables are ordered relative to their contribution to overall model fit.

Ecosystem Rate	DFE	Adj. R2	RMSE	Ratio	BIC	ΔBIC	Significant Effect Variables (p<0.05)
Metabolism (mg O2 h-1)							
CRraw	53	0.55	0.35	23.6	57.3	8.6	CRraw = -0.18*Chla - 0.87*SA - 0.69*CBOM - 0.59
GPPraw	53	0.84	0.77	97.4	148.2	1.4	GPPraw = 1.12*Chla + 0.97*FBOM - 1.56*SA + 6.86
NCPraw	53	0.87	0.57	79.0	114.0	13.8	NCPraw = 0.96*Chla + 0.78*FBOM - 2.21*SA + 5.49
N Uptake (mg NH4-N h-1)							
NN-raw	54	0.39	0.04	19.0	-186.8	6.2	NN-raw = 0.02*Chla + 0.09*SA + 0.11
NN+P-raw	55	0.42	0.04	41.6	-208.4	n/a	NN+P-raw = 0.25*Chla + 0.11
P Uptake (mg PO4-P h-1)							
PN-raw	55	0.06	0.01	4.5	-345.4	n/a	PN-raw = -0.15*SA + 0.01
PN+P-raw	53	0.75	0.01	56.4	-306.7	33.1	PN+P-raw = 0.07*SA + 0.01*Chla + 0.03*CBOM + 0.05

Chla = LN[Chl a (mg)]; SA = Sediment Surface Area (m2); CBOM = sqrt[CBOM (g)]; FBOM = LN[FBOM (g)]

3.7 Figures

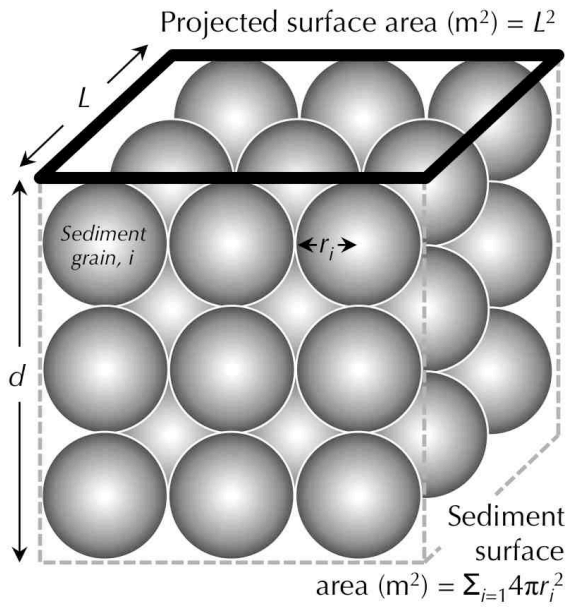

Figure 3.1 Conceptual diagram comparing projected surface area (black parallelogram) and sediment surface area normalization approaches (gray spheres). Projected surface area ignores the depth, size, and distribution of benthic sediments, whereas sediment surface area accounts for the surface area of each individual sediment grain, i.

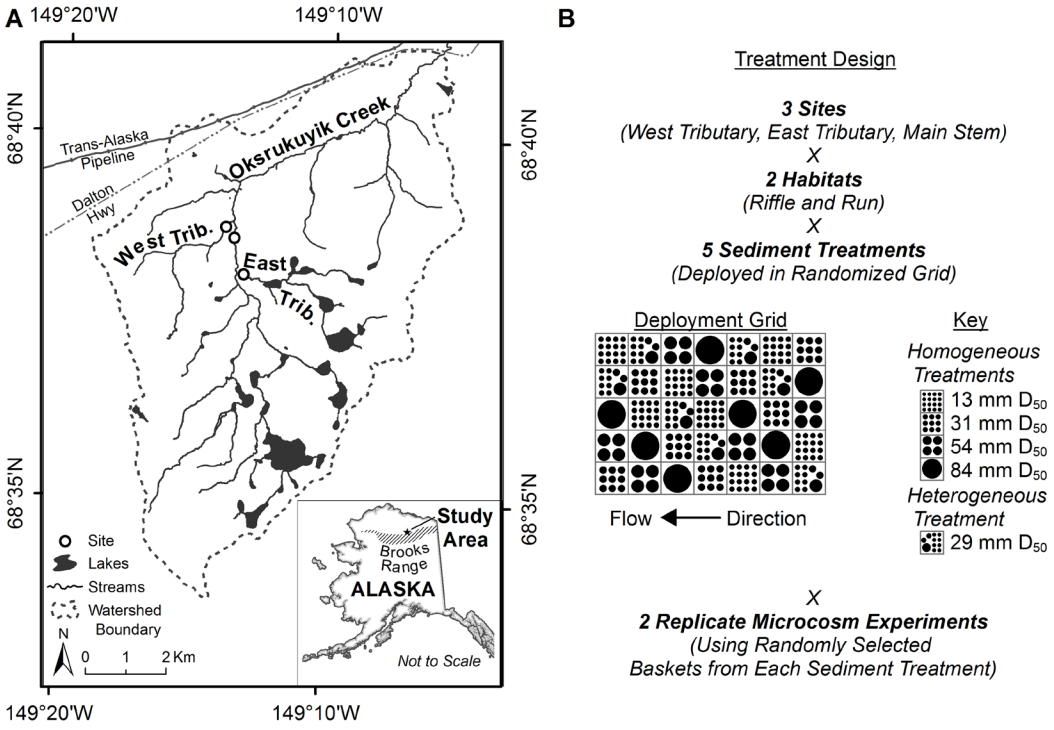

Figure 3.2 (A) Location of the East Tributary, West Tributary, and Main Stem deployment sites within the Oksrukuyik Creek study area located on the northern slope of the Brooks Range, Alaska (USA). (B) Treatment design and sediment deployment grid layout.

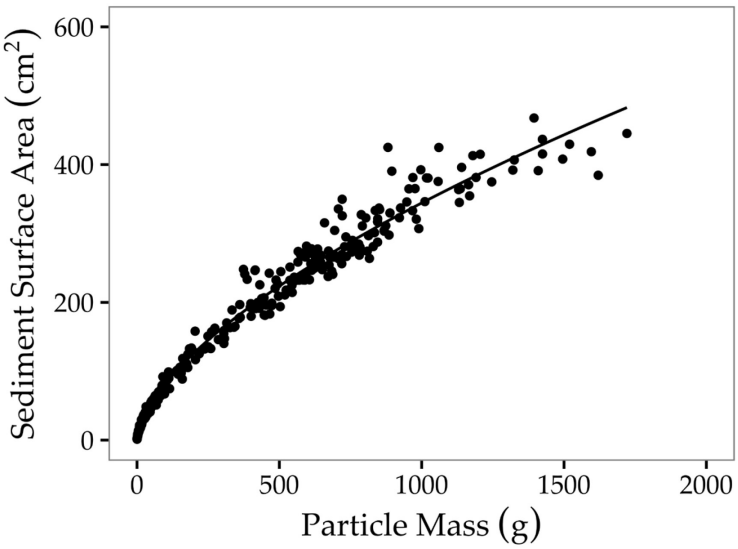

Figure 3.3 Scatterplot illustrating the relationship between individual sediment particle mass (M), in grams, and sediment surface area (SA), in cm^2, of the 375 sediment grains wrapped in aluminum foil to create the predictive relationship between sediment grain mass and SA. Power function used to determine sediment surface area, SA (cm^2) = $3.619 9M^{0.665}$ ($t = 258.4$, $df = 374$, $P < 0.0001$, $r^2 = 0.994$).

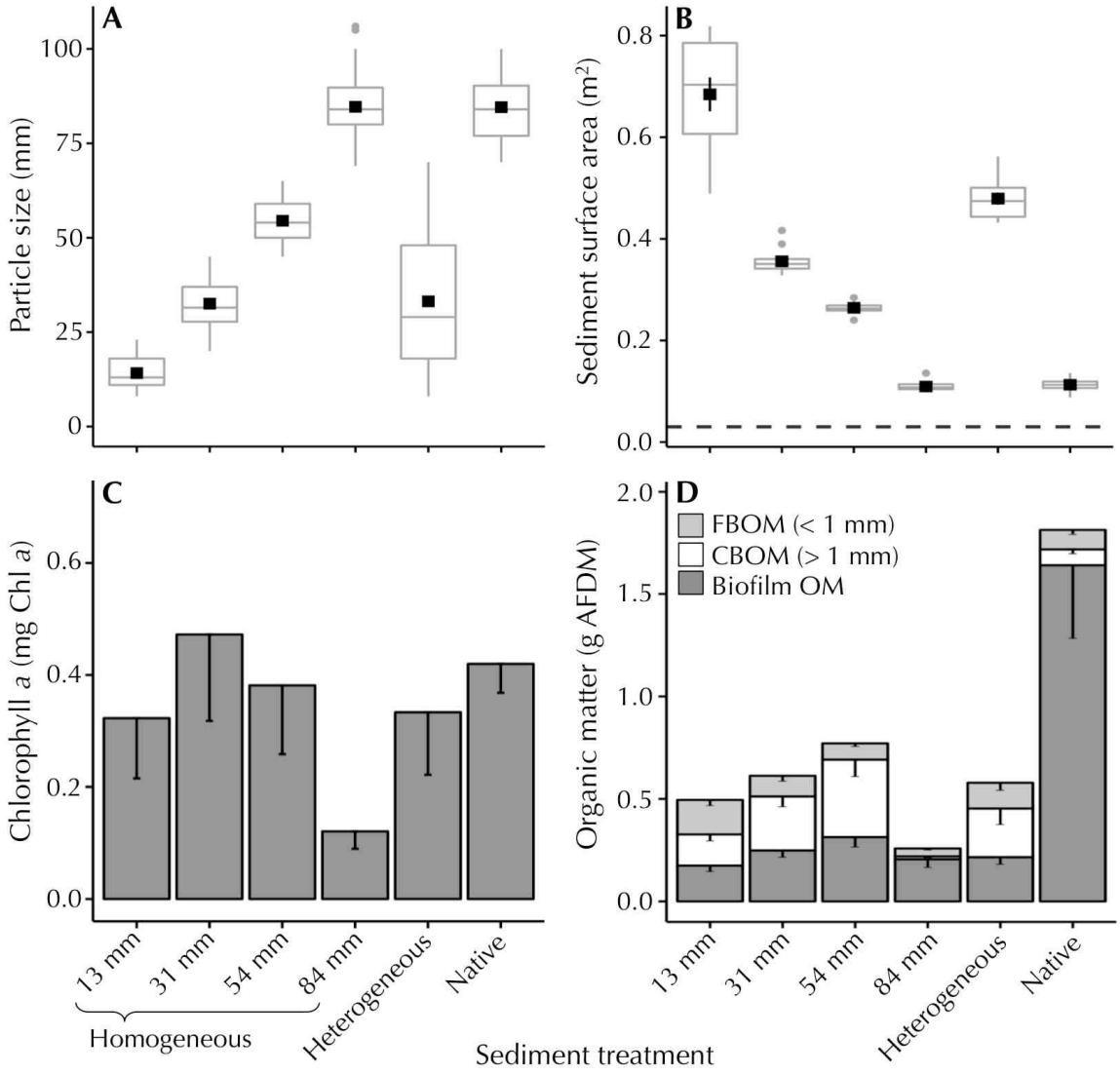

Figure 3.4 (A) Particle size, (B) sediment surface area, (C) chlorophyll a, and (D) organic matter (OM) fractions for the six sediment treatments evaluated across all sites and habitats. Boxplots illustrate interquartile range with centerline denoting median value and black squares indicating mean ± standard error (SE). Bar plots illustrate the mean ± SE mass of Chl *a* and OM for each treatment. For visualization purposes, bar plot error bars are displayed only in the negative (-) direction.

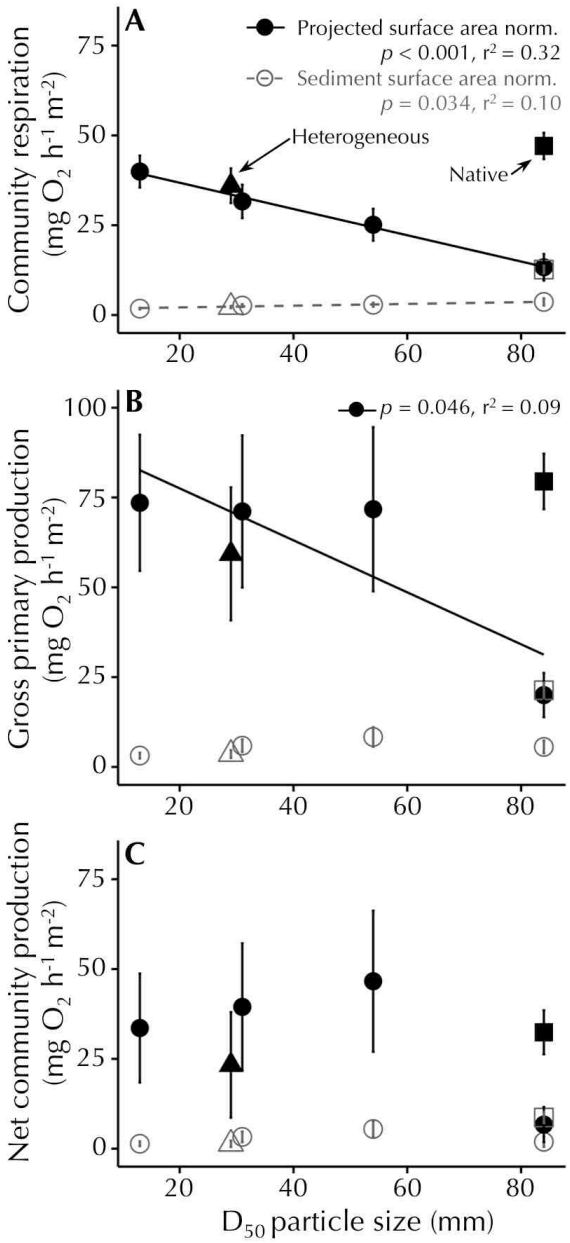

Figure 3.5 Scatterplots illustrating the relationship between sediment particle size and mean ± standard error rates of (A) community respiration, (B) gross primary production, and (C) net community production for sediment biofilms across all sites, habitats, and experiments. Solid points denote functional rates normalized by projected surface area, and open points denote functional rates normalized by sediment surface area. Homogeneous (circles), heterogeneous (triangles), and native (squares) sediment treatments are identified by shape. Significant linear regressions are labeled accordingly.

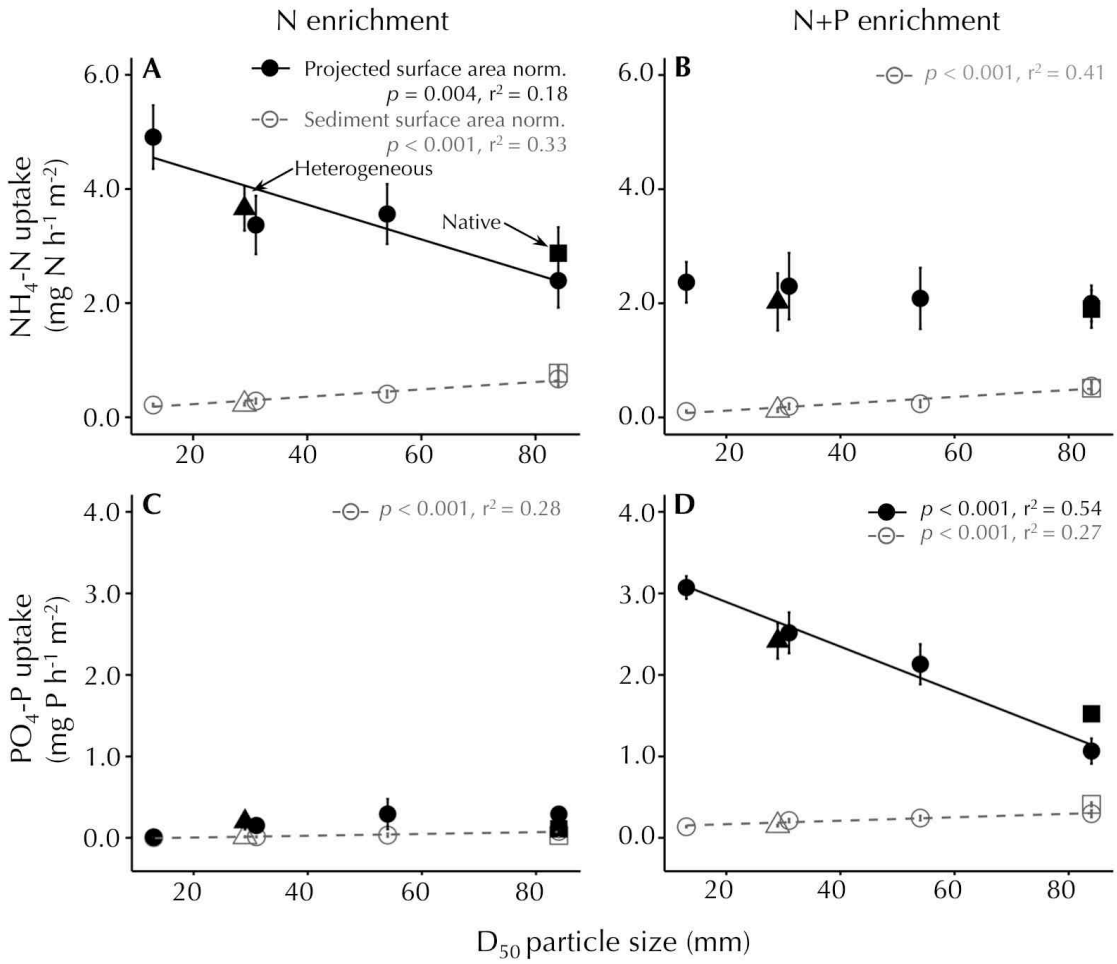

Figure 3.6 Scatterplots illustrating the relationship between sediment particle size and mean ± standard error rates of (A) NH_4-N uptake during the N-enrichment period, (B) NH_4-N uptake during the N+P-enrichment period, (C) PO_4-P uptake during the N-enrichment period, and (D) PO_4-P uptake during the N+P-enrichment period across all sites, habitats, and experiments. Solid points denote functional rates normalized by projected surface area, and open points denote functional rates normalized by sediment surface area. Homogeneous (circles), heterogeneous (triangles), and native (squares) sediment treatments are identified by shape. Significant linear regressions are labeled accordingly.

CHAPTER 4: THE PRESENCE OF LAKES, CATCHMENT VEGETATION, AND PRECIPITATION REGIME STRONGLY PREDICT STREAM ORGANIC NUTRIENT CONCENTRATIONS AND INFORMS FUTURE CHANGES TO CARBON AND NITROGEN DYNAMICS IN ARCTIC INLAND

ABSTRACT

The effects of catchment characteristics on stream macronutrient concentrations were evaluated using a synoptic water sampling approach across an Artic watershed that contained tributaries with and without intervening lakes. Stream water was sampled in 19 primary stations (n=9 with lakes; n=10 without) across five separate events to test the effect of lake presence and median event discharge at the watershed outlet on dissolved nutrient concentration (n=95). Concentrations of dissolved organic carbon (DOC) and other inorganic nutrients were significantly greater in streams without lakes than in streams in with lakes. DOC, total dissolved nitrogen (TDN), and soluble reactive phosphorus concentrations increased significantly as a function of discharge at the watershed outlet for each synoptic event. Although the variance of nutrient concentrations in streams with lakes was less than the variance in streams without, no significant interaction effects between median discharge and lake presence were noted ($p>0.05$). The absence of significant interaction effects indicates that the presence of lakes in the network does not alter the response of nutrient concentrations in stream to changes in flow condition. The lack of significant interaction effects enabled the development of a single predictive linear model for each nutrient using data from the 19 primary stations. Candidate model variables included landscape characteristics, hydrological characteristics, and the distribution of vegetation cover types at reach and watershed levels. Selected predictive models explained between 20% and 76% of the variance of the inorganic and organic nutrients measured, except dissolved organic phosphorus, which could not be predicted. DOC and dissolved organic nitrogen (DON) models were driven by antecedent precipitation and watershed vegetation cover type while inorganic nutrients were driven primarily by antecedent precipitation, landscape characteristics and reach vegetation cover types, suggesting that inorganic and organic nutrients have different scales of influence within a catchment. Model validation, conducted using additional stations sampled from separate synoptic events, indicated that the developed models most reliably predicted concentrations of DOC, DON, and TDN. Model validation and sensitivity analysis was conducted to examine model efficacy relative to measured stream nutrient concentrations associated with drought conditions in the watershed and understand how projected increases to the Arctic precipitation regime over the next century influence stream nutrient concentrations. Drought conditions resulted in increased organic nutrient concentrations. A 50% increase in precipitation resulted in significant increases to DOC, DON, and TDN concentrations in the network for extreme precipitation events. The developed models contribute to existing and future understanding of the changing Arctic and lend new confidence to the prediction of nutrient dynamics in streams where lakes are present.

4.0 Introduction

Relating catchment characteristics to in-stream conditions is particularly challenging in certain regions where lakes are prevalent features on the landscape, such as in the Arctic (Jones 2010a). Studies have shown how landscape features influence lake chains connected by streams (Kling et al. 2000, Leavitt et al. 2006, Sadro et al. 2012, McDonald and Lathrop 2017), as well as the broader inclusion of lakes as important features along the stream continuum (Lottig et al. 2011, Lottig et al. 2013, Powers et al. 2014, Xu and Xu 2018). Although a number of important conceptual frameworks have been developed to describe the influence of landscape characteristics on biological or biogeochemical conditions in streams (Vannote et al. 1980, Ward and Stanford 1983, Poole 2002, Jones 2010a, Xenopoulos et al. 2017), there are few examples of quantitative, predictive models that incorporate the presence of lakes within the stream network as a key variable that influences stream biogeochemical conditions. Given the increased focus on hydrologic connectivity in the aquatic sciences (Covino 2017, Larsen et al. 2017), a more comprehensive understanding of how catchment characteristics and the presence of lakes affect concentrations of stream nutrients across a range of hydrologic conditions is needed to inform the fate and transport of organic and inorganic nutrients in inland waters (Cole et al. 2007, Raymond et al. 2016).

Arctic streams drain a carbon-rich landscape (Schuur et al. 2015, Olefeldt et al. 2016) and nitrogen and phosphorus typically act as key limiting nutrients in high-latitude terrestrial (Shaver and Chapin 1995, Mack et al. 2004, McLaren et al. 2017) and aquatic environments (Peterson et al. 1985, Peterson et al. 1993, Harvey et al. 1998). Lakes

comprise approximately 6% of the Pan-Arctic land surface area (Paltan et al. 2015). In the Alaskan Arctic, lakes represent approximately 3.8% of land area, while streams and rivers represent 0.3 to 2% (Allen and Pavelsky 2018). Arctic streams and lakes are integrally involved in the cycling, release and/or transport of carbon (Cory et al. 2014, Tranvik et al. 2018), nitrogen, and phosphorus (Frey et al. 2007, McNamara et al. 2008, Khosh et al. 2017) from the terrestrial environment to the atmosphere or ocean. Tranvik et al. (2009) found 22% of the carbon entering an arctic lake to be deposited or released to the atmosphere and 78% to exit through downstream streams. Kling et al. (2000) found increasing DOC concentration from lake inlets to outlets in a stream-lake network while streams showed decreasing concentration from upstream to downstream. This suggests that lakes could act as both sinks and sources for organic and inorganic nutrients along a stream-lake network. The reservoir effect of lakes in stream networks is well known and it is reasonable to expect that the increase in hydrologic retention with lakes will also alter the biogeochemical signal of water passing through the lake-stream network. Goodman et al. (2011) found lakes to alter the magnitude, timing, and variability in carbon sources due to hydrological buffering.

The patterns of macronutrient concentrations in streams and lakes are also dependent on a variety of other landscape characteristics, such as land cover (Soranno et al. 2015), hydrologic condition (Guo et al. 2018), antecedent moisture (Davis et al. 2014), disturbance [e.g., fire (Larouche et al. 2015)], and underlying geology (Whittinghill and Hobbie 2011). The spatial scale and the arrangement of landscape characteristics may also affect the distribution of inorganic and organic nutrients (Cui et al. 2018). Land-water

interactions across the reach area or within a water body corridor may be more or less important than the cumulative effect of watershed characteristics in the upgradient watershed. For example, Cui et al. (2018) and Sliva and Dudley Williams (2001) both found cumulative watershed characteristics to be stronger predictors of water quality than corridor or reach variables.

Current global models of climate-induced changes to terrestrial and aquatic systems rely heavily on remotely sensed data (Pettorelli et al. 2016, Turak et al. 2017) as do similar models of the Arctic region (Pastick et al. 2018). Nevertheless, the ability to predict nutrient concentrations and other functional processes in streams is difficult due to their spatial and temporal heterogeneity (Dong et al. 2017). Griffin et al. (2018) successfully used satellite remote sensing data to predict chromophoric dissolved organic matter, which was used to predict dissolved organic carbon (DOC) concentrations in major Alaskan rivers. Röman et al. (2018) used remotely sensed landscape characteristics to predict losses of total nitrogen and phosphorus from high-latitude catchments in Finland. The model developed by Röman et al. (2018) incorporated the proportion of lakes across mixed land use basins, which indicates the presence of lakes could be an important characteristic used to predict dissolved inorganic and organic nutrients in other regions. In the Arctic, catchment characteristics of particular interest include antecedent precipitation and vegetation cover type. Precipitation in the Arctic is anticipated to increase by as much as 50% over the next century (Kattsov et al. 2007, Bintanja and Selten 2014, Bintanja and Andry 2017). With increased precipitation comes increased soil moisture, which has been linked to other widespread changes in arctic vegetation cover, such as increased shrubification (Elmendorf

et al. 2012, Myers-Smith et al. 2015, Ackerman et al. 2017) or decreased terrestrial productivity in the form of arctic browning (Phoenix and Bjerke 2016, Lara et al. 2018, Pastick et al. 2018). Therefore, a robust predictive tool to determine the response of stream nutrient conditions based on lake presence, antecedent precipitation, and vegetation cover type would contribute to existing and future models of the changing Arctic and lend new confidence to the prediction of nutrient dynamics where lakes are present.

The objectives of this study were twofold. The first objective was to evaluate whether the presence or absence of lakes affects stream inorganic and organic nutrient concentrations over a range of hydrologic conditions in an arctic watershed. Specifically, this objective sought to identify whether interaction effects between flow regime and the presence of lakes could be identified. The second objective was to determine if lake presence or absence, vegetation type, and antecedent precipitation could be used to predict the distribution of organic and inorganic nutrient concentrations across a gradient of Arctic streams with and without intervening lakes. We hypothesized that streams with lakes would have decreased inorganic nutrient concentration and increased organic nutrients within a stream-lake network and that changes in nutrient concentration would be less pronounced at greater discharges in streams with lakes due to hydrologic buffering. We also hypothesize that landscape watershed characteristics could be used to develop models that reliably describe macronutrient availability in arctic streams.

4.1 Method

4.1.1 Study Site

This study was located in the Oksrukuyik Creek, a third-order, cobble-bottom stream located on the northern foothills of the Brooks Range in Alaska, USA (**Figure 4.1**). The Oksrukuyik Creek has been monitored as part of the Arctic Long Term Ecological Research (LTER) program for several decades (Harvey et al. 1998). The stream also became a core aquatic site of the National Ecological Observatory Network (NEON) in 2017.

At its crossing with the Dalton Highway (N68°41'16", W149°5'43"), the Oksrukuyik Creek drains 71.6 km^2 of undisturbed tundra underlain by continuous permafrost. The southern and eastern portions of the watershed are comprised of a substantial stream-lake network. In total, the watershed lake area is approximately four percent. Given its location at the foothills of the Brooks Range, the watershed contains a diverse array of tundra flora communities. Flowing freely from May to September, Oksrukuyik Creek receives nearly 50 night-less days during the growing season. Annual precipitation in the region is typically less than 150 mm (Oswood et al. 1995) and the July to mid-August median discharge (Q_{50}) was 550 L s^{-1} from 1998 to 2015 (ARCTIC-LTER 2016).

4.1.2 Synoptic Study Design

Surface water nutrient concentrations were evaluated using a synoptic sampling study design whereby multiple stations were sampled in rapid succession to minimize potential temporal variation in water quality condition and maximize spatial coverage. A stratified station selection process was used to identify locations based on the presence or absence of upgradient lakes and position in the watershed. Nineteen primary stations were identified throughout the watershed to achieve near-balanced distribution of sampling stations with lakes present (n=9) and without lakes present (n=10) (**Figure 4.1**). The 19 primary stations (S01-S19) were sampled in their entirety across five synoptic events (n=95). This core dataset was used to test the effect of lakes on inorganic and organic nutrient concentrations across a variety of discharge events and for predictive model development using catchment characteristics. Supplemental stations were used to validate the developed models. The validation dataset (n=146) was comprised of all supplemental stations sampled from 2012 to 2014. A drought-sampling event from 2015, the driest summer on record for Oksrukuyik Creek, was also used in the assessment of the predictive models. This event was evaluated using a separately because conditions were outside of those observed in the model development datasets. During the 2015 drough synoptic event, the discharge recurrence interval at the LTER gauging station was in the 10^{th} percentile and large portions of the Oksrukuyik Creek were hydrologically disconnected from surface flows.

The first synoptic event on 5 August 2012 targeted the 19 primary stations. Subsequent synoptic sampling events for both primary and supplemental stations were conducted in July or August one or more days during periods of consistent discharge. The intensity of supplemental station sampling was based on resource availability, as conducting network-scale monitoring in a remote setting poses logistical and fiscal challenges. The largest synoptic event occurred on 18 July 2014 when 86 stations were sampled in less than seven hours. **Table 4.1** summarizes synoptic event characteristics and distribution of stations amongst streams with and without lakes present for the 12 synoptic events.

4.1.3 Sample Collection and Analysis

Field samples were collected using new or acid washed 1 L high-density polyethylene (HDPE) grab bottles, which were triple rinsed with stream water prior to collection. Grab bottles were stored in insulated bags prior to field or laboratory filtration using pre-combusted, 25 mm Whatman GF/F filter (pore size ~0.7μm). Approximately 5–10mL of water was filtered into a new, clean, 60 mL HDPE bottle, which was then capped, shaken, and emptied three times before filling. Time between collection and freezing the samples was typically less than 6 hours.

Sample analysis was conducted in accordance with Arctic LTER protocols (ARCTIC-LTER, 2015). Laboratory triplicates were analyzed for dissolved organic carbon (DOC), total dissolved nitrogen (TDN), ammonium-nitrogen (NH_4-N), and soluble reactive phosphorus (SRP). Nitrate/nitrite-nitrogen (NO_x-N) was analyzed in duplicate and

a single laboratory sample was evaluated for total dissolved phosphorus (TDP). DOC and TDN were measured using a Shimadzu TOC-5000. NH_4-N and NO_x-N were measured on a Lachat FIA+ 8000 (Hach® Instruments, Loveland, CO) using QuikChem Method 10-107-06-2O and QuikChem Method 31-107-04-1-E, respectively. TDP and PO_4-P were measured on a UV-2600 spectrophotometer (Shimadzu Scientific Instruments, Columbia, MD) using the molybdenum blue method (Parsons et al. 1984). The aliquots analyzed for TDP were digested using a potassium persulfate ($K_2S_2O_8$) solution in an autoclave at 105 °C for 90 minutes. The mean reported value from laboratory replicates was used for subsequent data evaluation.

Dissolved inorganic nitrogen (DIN) was calculated as the sum of NH_4-N and NO_x-N for a given sample. Dissolved organic nitrogen (DON) and dissolved organic phosphorus (DOP) were calculated as the difference between TDN and DIN and TDP and SRP, respectively. Values below detection were reported as one-half the mean method detection limit observed for each of the analytical sampling days.

4.1.4 GIS and Remote Sensing Evaluation

Geographic information systems (GIS) and remotely sensed data were used to characterize sub-catchments within the Oksrukuyik Creek watershed at each sampling station. Variables were assessed across two main categories: 1) landscape and hydrologic characteristics and 2) vegetation cover types (**Table 4.2**).

Landscape and hydrological characteristics were obtained using a mix of automated and manual spatial assessment techniques. First, the cumulative upslope drainage areas for

each station were delineated using 0.5 m digital elevation models (DEMs) created by the Polar Geospatial Center (PGC) from DigitalGlobe, Inc. imagery using the Hydrology toolset in ArcGIS Release 10.4.1. (Environmental Systems Research Institute (ESRI). Redlands, CA.). Stream order (Strahler 1954), lake presence/absence, and upstream distance to lakes were assessed manually using stream centerlines, lake features, and aerial imagery obtained from Toolik Field Station GIS and Remote Sensing. Stream slope was obtained by intersecting the stream centerline with 0.5 m contours created from the PGC DEM. The distance between contours corresponding to 1 or 2 m of elevation change upslope was used to calculate an estimate of stream slope. For the 2012 and 2015 study years, antecedent precipitation data was obtained from the Environmental Data Center at the Toolik Field Station (EDC, 2015), and for 2013 and 2014 similar data was obtained from a temporary meteorological station deployed within Oksrukuyik Creek watershed (Parker et al. 2018). The sum of 7-day precipitation for each event was used to estimate the potential antecedent moisture conditions. Arctic LTER discharge records from 1998 to 2015 were obtained to determine the median discharge at the gauging location for each synoptic event (ARCTIC-LTER 2016). Discharge recurrence intervals (e.g., Q_{10}) were calculated using 17 years of data for the study period (3 July–11 August).

Vegetation cover used in the evaluation was originally developed by Walker et al. (1994), further validated by Muller et al. (1998), and updated to align with the circumpolar Arctic vegetation map (Walker et al. 2005). Although vegetation cover mapping continues to improve in the region and across the arctic ((Walker et al. 2017), this vegetation cover scheme was selected due to its high spatial resolution (1:25,000 scale), robust field

validation, and widespread use in other regional studies. The 11 vegetation complexes were simplified to minimize model parameterization. Snowbeds were consolidated into the barren land cover type, dry acidic and non-acidic tundra were consolidated into dry tundra cover type, moist acidic and non acidic tundra were consolidated into moist tundra cover type, shrub tundra and riparian shrubland were consolidated into shrub cover type, and rich and poor fens were consolidated into fen cover type. Open water features remained unchanged. Land cover types were expressed as percentage of total reach (r) and watershed (w) areas (**Supplemental Figure 4.1**). Reach area was chosen over corridor buffering approaches because corridor buffer distances are often arbitrarily selected and have been found to explain less variance in water quality models than characteristics scaled by cumulative upslope watershed area (Sliva and Dudley Williams 2001, Cui et al. 2018).

4.1.5 Statistical Analyses

Statistical analyses were carried out on transformed datasets from the primary and supplemental synoptic stations. Inorganic and organic nutrient concentrations were $\log_{10}$ transformed and explanatory variables were untransformed. The primary station dataset was used for hypothesis testing and predictive model development (n=95), the validation dataset was used to test the efficacy and sensitivity of the predictive models (n=146), and the drought sampling dataset was used to explore the potential influence of extrapolating beyond the conditions of the model development dataset during periods of hydrological discontinuity (n=34). Chemical analysis of SRP and DOP from station S11 of the primary dataset on 3-7 August 2013 was compromised and omitted from statistical testing and model development (n=94). Analysis of TDP and DOP in supplemental stations S27 from

3-7 August 2013 and S74 from 8 July 2014 (n=144), and analysis of NH_4-N, SRP, TDP, and DOP in drought-sampling station S17 (n=33) were also compromised and omitted from validation assessment.

The effects of lake presence or absence and discharge condition on $\log_{10}$ transformed inorganic and organic nutrient concentrations were evaluated using a two-way ANOVA. The evaluation was constrained to the primary stations to ensure a balanced study design. A full factorial assessment was used to determine whether inorganic and organic nutrient concentrations respond differently to changing flow conditions in streams with and without lakes present. Synoptic events were categorically grouped by the following discharge recurrence intervals: one event occurred at median discharge conditions, three during slightly elevated discharge in the 65th to 70th percentile, and one during a period of extreme discharge in the 95th percentile. Significant two-way interaction effects of lake presence and event discharge would indicate that separate models might be needed to characterize nutrient concentrations in streams with and without lakes present.

The relationships between each explanatory and dependent variables were evaluated using Pearson's r coefficient prior to model development. The correlation matrix and ANOVA analysis was used to identify potential explanatory variables with multicolinearity. The presence of multicolinearity can result in decreased statistical power, parameter estimate inaccuracy, or masking or exclusion of significant predictor variables (Graham 2003).

Linear models using catchment characteristics were developed based on the primary stations with the aid of the automated model selection and multi-model inference tool *glmulti* (Calcagno and de Mazancourt 2010) in the *R* environment (R Core Team, 2018). All 18 explanatory variables obtained through GIS and remote sensing data sources were selected as candidate variables used to predict $\log_{10}$ transformed nutrient concentration with a linear model. The model fitting procedure considered only main effects. Bayesian information criteria (BIC) minimization drove candidate model selection. Given the large number of candidate models in the full heuristic evaluation (over 250,000), limits on model complexity were considered to help refine key drivers of inorganic and organic nutrient concentrations. The number of model variables was incrementally increased from one to eight. Model complexity beyond eight variables was not considered due to increased potential of multicolinearity of explanatory variables.

Further assessment of potential multicolinearity was carried out using the variance inflation factor (VIF) thresholds. VIF thresholds refined *glmulti*-identified candidate models and aided in the selection of a single predictive model for each nutrient. VIFs were calculated for all explanatory variables of each optimized candidate model at a given level of complexity. If a variable within a candidate model had a VIF>3 it was removed. Subsequent reductions in model complexity were made until all variable VIFs≤3. This approach was similar to that discussed by Zuur et al. (2010).

The selected candidate models were then used to predict inorganic and organic nutrient concentrations using the supplemental station dataset. Observed nutrient concentrations were compared to predicted concentrations using a linear regression similar

to the approach described by Piñeiro et al. (2008). Concentrations from the drought synoptic event were also used to assess the ability of the model to predict concentrations during extreme dry periods. Model fits were evaluated on the basis of the r^2 and the root mean squared difference (RMSD) of each model (units of Log_{10} μg L^{-1}). The antecedent precipitation sensitivity assessment was conducted to estimate changes in watershed nutrient concentrations based on the current understanding of future climate regimes in the Arctic, which are anticipated to have as much as 150% more precipitation over the next century (Bintanja and Selten 2014). Percent land cover vegetation type was held constant during the precipitation sensitivity assessment. The effect of 100%, 125% and 150% increases to precipitation was evaluated for the 7-day antecedent precipitation that corresponded to the three separate discharge event types: 10 mm (~Q50th), 30 mm (~Q70th), and 90mm (Q95th) using ANOVA.

4.2 Results

4.2.1 Effect of Lake Presence and Discharge Event Type on Stream Nutrient Concentrations

Results of the two-way ANOVA of lake presence and median discharge on nutrient concentration are illustrated in **Figure 4.2**. Significant main effects were noted for both median event discharge type and lake presence for DOC, TDN and SRP (**Table 4.3**). NH_4-N, DIN, and TDP were significantly influenced by lake presence, but not median event discharge type. No significant interaction effects were noted for the nutrients evaluated. Where the effects of lake presence were significant, streams without lakes had greater

concentration of inorganic and organic nutrients than streams with lakes. Concentrations of DOC, TDN, and SRP all increased significantly with increasing median discharge. Concentrations of NO_x-N in streams were lower where lakes were present, decreased with increasing discharge event type, and remained invariant in streams without lakes.

4.2.2 Multicolinearity of Model Variables

Evaluation of catchment characteristics was carried out to determine potential for multicolinearity (**Figure 4.3**). Fifty (50) percent of the explanatory variables evaluated were significantly correlated. Vegetation cover types had the greatest incidence of significant correlations due to having a combined sum of 100 percent at a given station for the six reach and watershed cover types. The sum of 7-day precipitation was not correlated with any other explanatory variable, and all other explanatory variables were significantly correlated with at least one or more covariates. The strongest correlation was observed between lakes presence number and distance to upstream lakes (r=-0.99, p<0.05).

4.2.3 Model Development

Catchment characteristics were effective predictors of the inorganic and organic stream nutrients measured, except DOP (**Table 4.4**). Seventy-six (76) percent of the variance in DOC concentration was explained by the linear combination of the sum of 7-day precipitation and percent watershed open water, barren land, and dry tundra (p<0.001). The model fit for DON was also significant (p<0.001, r^2=0.64). Catchment characteristics explained the greatest amount of variance in NO_x-N concentrations (p<0.001, r^2=0.62). Apart from the sum of 7-day precipitation, none of the explanatory variables responsible

for the prediction of DOC and DON contributed significantly to the optimized model fits for inorganic nutrients. Rather, inorganic nutrient models were comprised of reach-area vegetation cover types and other localized hydrological variables.

Models for inorganic nutrients NH_4-N, NO_x-N, and SRP included more explanatory variables than models for organic nutrients. DIN and NO_x-N were the only models that did not include the sum of 7-day precipitation as an explanatory variable. The percentage of open water was the most prevalent lake-related explanatory variable. Open water area significantly contributed to the DOC, DON, and TDP models. Inorganic nutrients had fewer explanatory variables associated with lakes. Lake presence and percent watershed shrub or reach shrub area were not identified as significant explanatory variables in any of the optimized models.

4.2.4 Catchment Characterization Model Validation

Validation of each optimized model was conducted using the supplemental stations and drought synoptic sampling event. **Table 4.5** summarizes results from the linear model fits of observed on predicted concentrations for each nutrient evaluated. Although the model fits for inorganic nutrients in the supplemental data sets were significant, less of the variance was explained than was the case for the original, synoptic data sets. Variance among the supplemental stations that was explained by the predictive models was less than 10% for NH_4-N, DIN, SRP, and TDP. The poor model fit was also evident in the greater RMSD between observed and predicted values. RMSD for NH4-N, DIN, SRP, and TDP

were 58%, 38%, 41% and 15% greater for supplemental stations than primary stations, respectively.

The concentrations predicted for supplemental stations explained 46%, 29%, 21% and 19% of the variance in observed DOC, DON, NO_x-N, and TDN concentrations, respectively. Models for these nutrients were investigated further in subsequent sensitivity assessment. Among retained models, observed versus predicted concentration slopes were less than one (**Table 4.5**). The best relationship between observed and predicted values for the supplemental stations was for DOC (slope=0.68; **Figure 4.4A**; **Table 4.5**). The overall model fit for DON was similar but not as strong (r^2=0.29; **Figure 4.4B**; **Table 4.5**). Of the four models retained, TDN had the least variance explained (r^2=0.19; **Figure 4.4C**; **Table 4.5**). NO_x-N had the highest RMSD of all supplemental station models and the 95th percentile prediction intervals of the linear model illustrate this uncertainty (**Table 4.5**; **Figure 4.4D**). Explanatory variables used to predict NO_x-N remain unchanged across precipitation events.

The relationship between observed and predicted nutrient concentrations for drought sampling was also evaluated. RMSD was greater during drought sampling in all models. Slopes of predicted on observed relationships for DOC and DON under drought conditions were greater than one (**Figure 4.4A** and **Figure 4.4B**), indicating greater organic nutrient concentrations were observed during periods of hydrologic disconnection. The relationship between observed and predicted TDN concentration was not significant during the drought-sampling event (**Figure 4.4C**). Overall variance explained in drought sampling models decreased relative to other models for DOC (r^2=0.27) and TDN (r^2=0.01), but

increased for DON (r^2=0.66) and NO_x-N (r^2=0.48; **Table 4.5**). Generally, higher NO_x-N concentrations were observed throughout the drought sampling (**Figure 4.4D**).

4.2.5 Model Sensitivity – Future Changes to Nutrient Concentrations

The sensitivity assessment conducted on 7-day antecedent precipitation for a given event indicates that increases to watershed DOC, DON, and TDN concentrations will be most pronounced for extreme precipitation events. Sum of 7-day precipitation events corresponding to the Q50th, Q70th and Q95th discharge events were examined across three projected precipitation scenarios: no change (100%), 25% increase (125%), and 50% increase (150%). All other catchment characteristics were held constant. No sensitivity assessment was carried out on NO_x-N due to the lack of hydrological explanatory variables. Due to the positive parameter estimate and log transformed nutrient concentration the response of DOC concentration to increasing nutrient concentration increased exponentially. Concentrations were significantly greater across all three-discharge recurrences under current conditions (**Figure 4.5**). The increasing sum of 7-day precipitation had no appreciable effect on the 10 mm and 30 mm events. However, changes brought on by increases to extreme precipitation (90 mm) resulted in significant increases to watershed DOC, DON, and TDN concentrations.

4.3 Discussion

4.3.1 Effect of Lake Presence and Discharge Event Type on Stream Nutrient Concentrations

This study investigated the effect of lake presence and event discharge type on inorganic and organic dissolved macronutrient concentrations in an Arctic watershed. We hypothesized 1) that streams with lakes would have decreased inorganic nutrient concentrations and increased organic nutrient concentrations, and 2) that changes in nutrient concentration would be less pronounced at greater discharges in streams with lakes due to hydrologic buffering.

Contrary to our first hypothesis, both inorganic (NH_4-N, DIN, SRP) and organic (DOC) stream nutrient concentrations were significantly greater at stations with no lakes present (**Table 4.3**). This indicates potential for lakes to be sinks for both inorganic and organic nutrients across a stream-lake network as well as for lakes to buffer the impacts of precipitation on nutrients due to increased residence times. Mechanisms driving the decreased nutrient concentrations in streams with lakes include greater residence time and increased biotic uptake (Kalinin et al. 2016); dilution with oligotrophic pelagic waters in the mixing zone (Goodman et al. 2011); or abiotic mechanisms, such as photolytic degradation (Cory et al. 2014); sorption, precipitation, and deposition (Clow et al. 2015); or, a greater water-air interface surface area for nitrogen losses (Grant et al. 2018). The findings we observed across all primary stations are consistent with Lottig et al. (2011), who found streams to have significantly greater TDP than lakes. Kling et al. (2000) found

that lakes were responsible for the consumption of dissolved NO_3-N in a nearby Artic stream-lake network (I-series); however, no significant difference in NO_x-N concentration were observed between streams with and without lakes in this study. Lottig et al. (2011) did not find significant differences in TDN and DOC between streams and lakes; however, other inorganic nutrients were not measured. A longitudinal examination of the nutrient concentrations moving down a stream-lake network, as implemented by Sadro et al. (2012) and Kling et al. (2000), may provide additional insight into specific patterns of inorganic and organic nutrient concentrations with and without lakes present.

Although some evidence of hydrologic buffering was observed in streams with lakes, there were no significant interaction effects between lake presence and discharge event type to support our second hypothesis (**Table 4.3**). Rather, concentrations of nutrients with significant main effects for both variables using the two-way ANOVA (DOC, TDN, and SRP) behaved similarly in their response to changing discharge event types in streams with lakes and without lakes present (**Figure 4.2A, Figure 4.2C, Figure 4.2H**). The similar pattern could indicate that abiotic and biotic mechanisms controlling nutrient delivery during increased flows are similar between streams with and without lakes for DOC, TDN, and SRP. The minimal effect of discharge event type on the remaining nutrients (DON, NH_4-N, NO_x-N, DIN, TDP, and DOP) indicates that hydrological processes that cause changes in concentration may be happening during different flow periods not captured by this study (i.e., the spring freshet), if at all.

The presence of a strong lake thermocline during the July and August study period permitting stream water to flow over the lakes surface with minimal mixing may contribute

to the absence of any significant interaction effects across the discharge events studied. Kalinin et al. (2016) found mixing dynamics to play a large role in the residence time of water and nutrients moving into and out of lakes. If thermal conditions are appropriate, water density differentials can lead to rapid transport of surface waters across lakes. Goodman et al. (2011) found strong hydrologic buffering to occur in alpine lakes during spring runoff periods. However, as the season progressed towards summer baseflow conditions, the lakes transitioned from a DOC sink to a DOC source. Coefficients of variation for streams with lakes tended to be less than streams without lakes indicating that lakes impose some buffering to concentration. These findings are similar to those observed by Goodman et al. (2011) who observed 40% to 90% greater coefficient of variation in lake outlets than lake inlets for organic matter. Nevertheless, given the evaluation period and hydrologic events monitored in this study, hydrological buffering that results in significant interaction effects was not apparent.

4.3.2 Efficacy of Model for Predicting Organic and Inorganic Nutrient Concentrations

Our study successfully demonstrated that stream nutrient concentrations could be reliably predicted using catchment characteristics. Based on validation performance, DOC, DON, and TDN were suitably validated, whereas inorganic nutrients were unable to be validated using other synoptic events. Organic nutrients were also less heavily parameterized models than inorganic nutrients and driven largely by antecedent precipitation and watershed characteristics; whereas inorganic nutrients contained more reach level characteristics. Several factors contributed to the favorable predictability of organic nutrients versus inorganic nutrients. The lability of inorganic nutrients is one

possible factor that resulted in poor model performance. Nutrient spiraling length, or the distance a nutrient travels before biogeochemical update removes it from the water column, for NH_4-N in the arctic streams was found to be less than 100 m (Peterson et al. 2001), whereas NO_x-N and PO_4-P were found to be 556 m and 87 m, respectively (Snyder and Bowden 2014). Additional factors influencing the difficulty predicting inorganic nutrients could be attributed to the strong internal control of biological processes. Mulholland et al. (2008) found that stream biota and chemistry control nitrate removal; however, Grant et al. (2018) determine that stream turbulence constrains the rate at which nitrate is removed from streams. Given the short uptake length and that nitrogen and phosphorus are co-limiting nutrients in the Oksrukuyik Creek (Harvey et al. 1998), inorganic nutrients are likely taken up cycled by stream biogeochemical processes at a rate that exceeds landscape level inflows.

The predictability of organic nutrients is likely attributed to greater spiraling length and the presence of larger, less labile source pool across the landscape when compared to inorganic nutrients. Terrestrial sources of organic carbon are abundant within the Arctic (Schuur et al. 2015, Olefeldt et al. 2016). Oxidation of dissolved organic carbon (DOC) in aquatic systems is largely controlled by two mechanisms: photochemical degradation and microbial mineralization (Tranvik et al. 2009). In arctic systems, Cory et al. (2014) found photochemical degradation to be the dominant mechanisms responsible for DOC oxidation, removing as much as 90%; however, given the high concentrations this still results in residual DOC that may be more recalcitrant. Bertuzzo et al. (2017) noted that the change of lability of organic carbon compounds as residence time in a watershed increases

poses a limitation to understanding and scaling carbon dynamics. In several large riverine systems with discharge ranging from 16,000 to 83,900 L s^{-1}, Hall et al. (2016) found organic carbon spiraling lengths to range from 38 to 1193 km. Similar physical and biologically mediated processes are likely to influence DON dynamics and enable greater predictability than inorganic compounds. Gradual photochemical mineralization of DON to ammonia (Jeff et al. 2012) occurs in the aquatic environment and the subsequent nitrification (Snyder and Bowden 2014) can lead to its removal. Far fewer studies have documented the dynamics of DON across stream and lake systems, which offers an exciting opportunity for future research.

The sensitivity evaluation conducted on the organic nutrients and TDN indicated the importance of extreme meteorological events. During extreme meteorological events, the greatest concentrations of organic nutrient concentrations were observed in Oksrukuyik creek waters. Similarly, under 50% increases to the anticipated precipitation regime, significant changes to the concentrations of DOC, DON, and TDN were observed. Empirical data from the Oksrukuyik Creek watershed measured by Khosh et al. (2017) found the high discharge during the spring and fall seasons to have the greatest DON and DOC concentrations. The findings from their study align well with the results of our predictive models for organic nutrients.

These developed models have several limitations. The vegetation cover types, although widely used in regional studies, are constrained to ~710 km^2 area of the upper Kuparuk River valley. Taking the modeling framework and implementing a synoptic sampling approach across larger areas with the use of the recently developed Circumpolar

Arctic Vegetation Classification mapping (Walker et al. 2017) will provide critical estimates of the role of Arctic streams in the global carbon cycle. Additional validation across larger spatial extents and in other watersheds is needed. Our findings provide further support as to the importance of extreme meteorological events as drivers of change to nutrient concentrations in streams and should also be further studied.

4.4 Conclusion

This work contributes to existing and future understanding of the changing Arctic and lends new confidence to the behavior and prediction of nutrient dynamics in streams where lakes are present. The greater concentrations of DOC and other inorganic nutrients in streams without lakes than in streams in with lakes provide additional evidence to the importance of lakes for biogeochemical processing within stream networks. Further, increased nutrient concentration as a function of increased outlet discharge and lack of significant interaction effects for DOC, TDN, and SRP highlights how streams with and without lakes present respond similarly to elevated discharge conditions. For these nutrients, the abiotic and biotic mechanisms controlling delivery during increased flows are likely similar, which enable prediction using unified models. The utility of catchment characteristics to predict in nutrient concentrations in streams with and without lakes present was demonstrated. Organic nutrient models were driven by antecedent precipitation and watershed vegetation cover type while inorganic nutrients were driven primarily by antecedent precipitation, landscape characteristics and reach vegetation cover types. This suggests that inorganic and organic nutrients have different scales of influence within a catchment. The concentration of more recalcitrant organic nutrients more heavily

controlled by cumulative watershed-level landscape characteristics whereas labile inorganic nutrients are likely controlled by in-stream processes. Drought conditions resulted in increased organic nutrient concentrations that could be delivered downstream during periods increased precipitation following low water. In the Arctic precipitation rates are expected to increase by as much as 50% in the coming century. A projected precipitation increase of 50% resulted in significant increases to DOC, DON, and TDN concentrations in the network. The magnitude of increased concentrations was greatest for extreme precipitation events indicating the importance of understanding nutrient delivery at periods of high catchment discharge. The modeling approach developed can be used to help constrain and refine our understanding of organic nutrients within streams with and without lakes present and help scale measurements of watershed nutrient inputs and outputs.

4.5 Literature Cited

Ackerman, D., D. Griffin, S. E. Hobbie, and J. C. Finlay. 2017. Arctic shrub growth trajectories differ across soil moisture levels. Global Change Biology 23:4294-4302.

Allen, G. H., and T. M. Pavelsky. 2018. Global extent of rivers and streams. Science 361:585-588.

ARCTIC-LTER. 2016. Arctic Long-Term Ecological Research Streams and Rivers Database. Accessed December 2016. http://arc-lter.ecosystems.mbl.edu/arctic-lter-streams-and-rivers.

Bertuzzo, E., A. M. Helton, R. O. Hall, and T. J. Battin. 2017. Scaling of dissolved organic carbon removal in river networks. Advances in Water Resources 110:136-146.

Bintanja, R., and O. Andry. 2017. Towards a rain-dominated Arctic. Nature Climate Change 7:263.

Bintanja, R., and F. M. Selten. 2014. Future increases in Arctic precipitation linked to local evaporation and sea-ice retreat. Nature 509:479.

Calcagno, V., and C. de Mazancourt. 2010. glmulti: An R Package for Easy Automated Model Selection with (Generalized) Linear Models. 2010 34:29.

Cole, J. J., Y. T. Prairie, N. F. Caraco, W. H. McDowell, L. J. Tranvik, R. G. Striegl, C. M. Duarte, P. Kortelainen, J. A. Downing, J. J. Middelburg, and J. Melack. 2007. Plumbing the global carbon cycle: Integrating inland waters into the terrestrial carbon budget. Ecosystems 10:171-184.

Cory, R. M., C. P. Ward, B. C. Crump, and G. W. Kling. 2014. Sunlight controls water column processing of carbon in arctic fresh waters. Science 345:925-928.

Covino, T. 2017. Hydrologic connectivity as a framework for understanding biogeochemical flux through watersheds and along fluvial networks. Geomorphology 277:133-144.

Cui, L., W. Li, C. Gao, M. Zhang, X. Zhao, Z. Yang, Y. Lei, D. Huang, and W. Ma. 2018. Identifying the influence factors at multiple scales on river water chemistry in the Tiaoxi Basin, China. Ecological Indicators 92:228-238.

Davis, C. A., A. S. Ward, A. J. Burgin, T. D. Loecke, D. A. Riveros-Iregui, D. J. Schnoebelen, C. L. Just, S. A. Thomas, L. J. Weber, and M. A. St. Clair. 2014. Antecedent Moisture Controls on Stream Nitrate Flux in an Agricultural Watershed. Journal of Environmental Quality 43:1494-1503.

Dong, X., A. Ruhí, and N. B. Grimm. 2017. Evidence for self-organization in determining spatial patterns of stream nutrients, despite primacy of the geomorphic template. Proceedings of the National Academy of Sciences 114:E4744-E4752.

Elmendorf, S. C., G. H. R. Henry, R. D. Hollister, R. G. Björk, N. Boulanger-Lapointe, E. J. Cooper, J. H. C. Cornelissen, T. A. Day, E. Dorrepaal, T. G. Elumeeva, M. Gill, W. A. Gould, J. Harte, D. S. Hik, A. Hofgaard, D. R. Johnson, J. F. Johnstone, I. S. Jónsdóttir, J. C. Jorgenson, K. Klanderud, J. A. Klein, S. Koh, G. Kudo, M. Lara, E. Lévesque, B. Magnússon, J. L. May, J. A. Mercado-Dı´az, A. Michelsen, U. Molau, I. H. Myers-Smith, S. F. Oberbauer, V. G. Onipchenko, C. Rixen, N. Martin Schmidt, G. R. Shaver, M. J. Spasojevic, Þ. E. Þórhallsdóttir, A. Tolvanen, T. Troxler, C. E. Tweedie, S. Villareal, C.-H. Wahren, X. Walker, P. J. Webber, J. M. Welker, and S. Wipf. 2012. Plot-scale evidence of tundra vegetation change and links to recent summer warming. Nature Climate Change 2:453.

Environmental Data Center EDC Team. 2015. Meteorological monitoring program at Toolik, Alaska. Toolik Field Station, Institute of Arctic Biology, University of

Alaska Fairbanks, Fairbanks, AK 99775. http://toolik.alaska.edu/edc/abiotic_monitoring/data_query.php

Frey, K. E., J. W. McClelland, R. M. Holmes, and L. C. Smith. 2007. Impacts of climate warming and permafrost thaw on the riverine transport of nitrogen and phosphorus to the Kara Sea. Journal of Geophysical Research: Biogeosciences 112.

Goodman, K. J., M. A. Baker, and W. A. Wurtsbaugh. 2011. Lakes as buffers of stream dissolved organic matter (DOM) variability: Temporal patterns of DOM characteristics in mountain stream‐lake systems. Journal of Geophysical Research: Biogeosciences 116.

Graham, M. H. 2003. Confronting multicolinearity in ecological multiple regression. Ecology 84:2809-2815.

Grant, S. B., M. Azizian, P. Cook, F. Boano, and M. A. Rippy. 2018. Factoring stream turbulence into global assessments of nitrogen pollution. Science 359:1266-1269.

Griffin, C., J. McClelland, K. Frey, G. Fiske, and R. Holmes. 2018. Quantifying CDOM and DOC in major Arctic rivers during ice-free conditions using Landsat TM and ETM+ data.

Guo, Y., C. Song, W. Tan, X. Wang, and Y. Lu. 2018. Hydrological processes and permafrost regulate magnitude, source and chemical characteristics of dissolved organic carbon export in a peatland catchment of northeastern China. Hydrol. Earth Syst. Sci. 22:1081-1093.

Hall, R. O., J. L. Tank, M. A. Baker, E. J. Rosi-Marshall, and E. R. Hotchkiss. 2016. Metabolism, gas exchange, and carbon spiraling in rivers. Ecosystems 19:73-86.

Harvey, C. J., B. J. Peterson, W. B. Bowden, A. E. Hershey, M. C. Miller, L. A. Deegan, and J. C. Finlay. 1998. Biological responses to fertilization of Oksrukuyik Creek, a tundra stream. Journal of the North American Benthological Society 17:190-209.

Jeff, S., K. Hunter, D. Vandergucht, and J. Hudson. 2012. Photochemical mineralization of dissolved organic nitrogen to ammonia in prairie lakes. Hydrobiologia 693:71-80.

Jones, N. E. 2010. Incorporating lakes within the river discontinuum: longitudinal changes in ecological characteristics in stream-lake networks. Canadian Journal of Fisheries and Aquatic Sciences 67:1350-1362.

Kalinin, A., T. Covino, and B. McGlynn. 2016. The influence of an in‐network lake on the timing, form, and magnitude of downstream dissolved organic carbon and nutrient flux. Water Resources Research 52:8668-8684.

Kattsov, V. M., J. E. Walsh, W. L. Chapman, V. A. Govorkova, T. V. Pavlova, and X. Zhang. 2007. Simulation and Projection of Arctic Freshwater Budget Components by the IPCC AR4 Global Climate Models. Journal of Hydrometeorology 8:571-589.

Khosh, M. S., J. W. McClelland, A. D. Jacobson, T. A. Douglas, A. J. Barker, and G. O. Lehn. 2017. Seasonality of dissolved nitrogen from spring melt to fall freezeup in Alaskan Arctic tundra and mountain streams. Journal of Geophysical Research: Biogeosciences 122:1718-1737.

Kling, G. W., G. W. Kipphut, M. M. Miller, and W. J. O'Brien. 2000. Integration of lakes and streams in a landscape perspective: the importance of material processing on spatial patterns and temporal coherence. Freshwater Biology 43:477-497.

Lara, M. J., I. Nitze, G. Grosse, P. Martin, and A. D. McGuire. 2018. Reduced arctic tundra productivity linked with landform and climate change interactions. Scientific Reports 8:2345.

Larouche, J. R., B. W. Abbott, W. B. Bowden, and J. B. Jones. 2015. The role of watershed characteristics, permafrost thaw, and wildfire on dissolved organic carbon biodegradability and water chemistry in Arctic headwater streams. Biogeosciences 12:4221-4233.

Larsen, L. G., J. Ma, and D. Kaplan. 2017. How Important Is Connectivity for Surface Water Fluxes? A Generalized Expression for Flow Through Heterogeneous Landscapes. Geophysical Research Letters 44:10,349-310,358.

Leavitt, P. R., C. S. Brock, C. Ebel, and A. Patoine. 2006. Landscape-scale effects of urban nitrogen on a chain of freshwater lakes in central North America. Limnology and Oceanography 51:2262-2277.

Lottig, N. R., I. Buffam, and E. H. Stanley. 2013. Comparisons of wetland and drainage lake influences on stream dissolved carbon concentrations and yields in a north temperate lake-rich region. Aquatic Sciences 75:619-630.

Lottig, N. R., E. H. Stanley, P. C. Hanson, and T. K. Kratz. 2011. Comparison of regional stream and lake chemistry: Differences, similarities, and potential drivers. Limnology and Oceanography 56:1551-1562.

Mack, M. C., M. S. Bret-Harte, T. N. Hollingsworth, R. R. Jandt, E. A. Schuur, G. R. Shaver, and D. L. Verbyla. 2011. Carbon loss from an unprecedented Arctic tundra wildfire. Nature 475:489.

Mack, M. C., E. A. G. Schuur, M. S. Bret-Harte, G. R. Shaver, and F. S. Chapin Iii. 2004. Ecosystem carbon storage in arctic tundra reduced by long-term nutrient fertilization. Nature 431:440.

McDonald, C. P., and R. C. Lathrop. 2017. Seasonal shifts in the relative importance of local versus upstream sources of phosphorus to individual lakes in a chain. Aquatic Sciences 79:385-394.

McLaren, J. R., A. Darrouzet-Nardi, M. N. Weintraub, and L. Gough. 2017. Seasonal patterns of soil nitrogen availability in moist acidic tundra. Arctic Science 4:98-109.

McNamara, J. P., D. L. Kane, J. E. Hobbie, and G. W. Kling. 2008. Hydrologic and biogeochemical controls on the spatial and temporal patterns of nitrogen and phosphorus in the Kuparuk River, arctic Alaska. Hydrological Processes 22:3294-3309.

Mulholland, P. J., A. M. Helton, G. C. Poole, R. O. Hall, S. K. Hamilton, B. J. Peterson, J. L. Tank, L. R. Ashkenas, L. W. Cooper, C. N. Dahm, W. K. Dodds, S. E. G. Findlay, S. V. Gregory, N. B. Grimm, S. L. Johnson, W. H. McDowell, J. L. Meyer, H. M. Valett, J. R. Webster, C. P. Arango, J. J. Beaulieu, M. J. Bernot, A. J. Burgin, C. L. Crenshaw, L. T. Johnson, B. R. Niederlehner, J. M. O'Brien, J. D. Potter, R. W. Sheibley, D. J. Sobota, and S. M. Thomas. 2008. Stream denitrification across biomes and its response to anthropogenic nitrate loading. Nature 452:202-U246.

Muller, S., D. Walker, F. Nelson, J. Bockheim, S. Guyer, and D. Sherba. 1998. Accuracy assessment of a land-cover map of the Kuparuk river basin, Alaska: considerations for remote regions. Photogrammetric Engineering and Remote Sensing 64:619-628.

Myers-Smith, I. H., S. C. Elmendorf, P. S. A. Beck, M. Wilmking, M. Hallinger, D. Blok, K. D. Tape, S. A. Rayback, M. Macias-Fauria, B. C. Forbes, J. D. M. Speed, N. Boulanger-Lapointe, C. Rixen, E. Lévesque, N. M. Schmidt, C. Baittinger, A. J. Trant, L. Hermanutz, L. S. Collier, M. A. Dawes, T. C. Lantz, S. Weijers, R. H. Jørgensen, A. Buchwal, A. Buras, A. T. Naito, V. Ravolainen, G. Schaepman-Strub, J. A. Wheeler, S. Wipf, K. C. Guay, D. S. Hik, and M. Vellend. 2015. Climate sensitivity of shrub growth across the tundra biome. Nature Climate Change 5:887.

Olefeldt, D., S. Goswami, G. Grosse, D. Hayes, G. Hugelius, P. Kuhry, A. D. McGuire, V. E. Romanovsky, A. B. K. Sannel, E. A. G. Schuur, and M. R. Turetsky. 2016. Circumpolar distribution and carbon storage of thermokarst landscapes. Nature Communications 7:13043.

Oswood, M. W., L. K. Miller, and J. G. Irons III. 1995. River and stream ecosystems of Alaska.in C. E. Cushing, K. W. Cumming, and G. W. Minshall, editors. Ecosystems of the World 22: River and Stream Ecosystems. Elsevier, Amsterdam.

Paltan, H., J. Dash, and M. Edwards. 2015. A refined mapping of Arctic lakes using Landsat imagery. International Journal of Remote Sensing 36:5970-5982.

Parker, S. P., W. B. Bowden, M. B. Flinn, C. D. Giles, K. A. Arndt, J. P. Beneš, and D. G. Jent. 2018. Effect of particle size and heterogeneity on sediment biofilm metabolism and nutrient uptake scaled using two approaches. Ecosphere 9:e02137.

Parsons, T. R., Y. Maita, and C. M. Lalli. 1984. 1.6 - Determination of Phosphate. Pages 22-25 in T. R. P. M. M. Lalli, editor. A Manual of Chemical & Biological Methods for Seawater Analysis. Pergamon, Amsterdam.

Pastick, N. J., M. T. Jorgenson, S. J. Goetz, B. M. Jones, B. K. Wylie, B. J. Minsley, H. Genet, J. F. Knight, D. K. Swanson, and J. C. Jorgenson. 2018. Spatiotemporal remote sensing of ecosystem change and causation across Alaska. Global Change Biology 0.

Peterson, B. J., L. Deegan, J. Helfrich, J. E. Hobbie, M. Hullar, B. Moller, T. E. Ford, A. Hershey, A. Hiltner, G. Kipphut, M. A. Lock, D. M. Fiebig, V. McKinley, M. C. Miller, J. R. Vestal, R. Ventullo, and G. Volk. 1993. Biological responses of a tundra river to fertilization. Ecology 74:653-672.

Peterson, B. J., J. E. Hobbie, A. E. Hershey, M. A. Lock, T. E. Ford, J. R. Vestal, V. L. McKinley, M. A. J. Hullar, M. C. Miller, R. M. Ventullo, and G. S. Volk. 1985. Transformation of a tundra river from heterotrophy to autotrophy by addition of phosphorus. Science 229:1383-1386.

Peterson, B. J., R. M. Holmes, J. W. McClelland, C. J. Vörösmarty, R. B. Lammers, A. I. Shiklomanov, I. A. Shiklomanov, and S. Rahmstorf. 2002. Increasing River Discharge to the Arctic Ocean. Science 298:2171-2173.

Peterson, B. J., W. M. Wollheim, P. J. Mulholland, J. R. Webster, J. L. Meyer, J. L. Tank, E. Martí, W. B. Bowden, H. M. Valett, A. E. Hershey, W. H. McDowell, W. K. Dodds, S. K. Hamilton, S. Gregory, and D. D. Morrall. 2001. Control of Nitrogen Export from Watersheds by Headwater Streams. Science 292:86-90.

Pettorelli, N., M. Wegmann, A. Skidmore, S. Mücher, T. P. Dawson, M. Fernandez, R. Lucas, M. E. Schaepman, T. Wang, B. O'Connor, R. H. G. Jongman, P. Kempeneers, R. Sonnenschein, A. K. Leidner, M. Böhm, K. S. He, H. Nagendra, G. Dubois, T. Fatoyinbo, M. C. Hansen, M. Paganini, H. M. Klerk, G. P. Asner, J. T. Kerr, A. B. Estes, D. S. Schmeller, U. Heiden, D. Rocchini, H. M. Pereira, E.

Turak, N. Fernandez, A. Lausch, M. A. Cho, D. Alcaraz-Segura, M. A. McGeoch, W. Turner, A. Mueller, V. St-Louis, J. Penner, P. Vihervaara, A. Belward, B. Reyers, and G. N. Geller. 2016. Framing the concept of satellite remote sensing essential biodiversity variables: challenges and future directions. Remote Sensing in Ecology and Conservation 2:122-131.

Phoenix, G. K., and J. W. Bjerke. 2016. Arctic browning: extreme events and trends reversing arctic greening. Global Change Biology 22:2960-2962.

Piñeiro, G., S. Perelman, J. P. Guerschman, and J. M. Paruelo. 2008. How to evaluate models: Observed vs. predicted or predicted vs. observed? Ecological modelling 216:316-322.

Poole, G. C. 2002. Fluvial landscape ecology: addressing uniqueness within the river discontinuum. Freshwater Biology 47:641-660.

Powers, S. M., D. M. Robertson, and E. H. Stanley. 2014. Effects of lakes and reservoirs on annual river nitrogen, phosphorus, and sediment export in agricultural and forested landscapes. Hydrological Processes 28:5919-5937.

Raymond, P. A., J. E. Saiers, and W. V. Sobczak. 2016. Hydrological and biogeochemical controls on watershed dissolved organic matter transport: pulse-shunt concept. Ecology 97:5-16.

Röman, E., P. Ekholm, S. Tattari, J. Koskiaho, and N. Kotamäki. 2018. Catchment characteristics predicting nitrogen and phosphorus losses in Finland. River Research and Applications 34:397-405.

Sadro, S., C. E. Nelson, and J. M. Melack. 2012. The influence of landscape position and catchment characteristics on aquatic biogeochemistry in high-elevation lake-chains. Ecosystems 15:363-386.

Schuur, E. A. G., A. D. McGuire, C. Schädel, G. Grosse, J. W. Harden, D. J. Hayes, G. Hugelius, C. D. Koven, P. Kuhry, D. M. Lawrence, S. M. Natali, D. Olefeldt, V. E.

Romanovsky, K. Schaefer, M. R. Turetsky, C. C. Treat, and J. E. Vonk. 2015. Climate change and the permafrost carbon feedback. Nature 520:171.

Shaver, G. R., and F. S. Chapin. 1995. Long–term responses to factorial, NPK fertilizer treatment by Alaskan wet and moist tundra sedge species. Ecography 18:259-275.

Sliva, L., and D. Dudley Williams. 2001. Buffer Zone versus Whole Catchment Approaches to Studying Land Use Impact on River Water Quality. Water Research 35:3462-3472.

Snyder, L., and W. B. Bowden. 2014. Nutrient dynamics in an oligotrophic arctic stream monitored in situ by wet chemistry methods. Water Resources Research 50:2039-2049.

Soranno, P. A., K. S. Cheruvelil, T. Wagner, K. E. Webster, and M. T. Bremigan. 2015. Effects of Land Use on Lake Nutrients: The Importance of Scale, Hydrologic Connectivity, and Region. Plos One 10:e0135454.

Strahler, A. N. 1954. Quantitative geomorphology of erosional landscapes. Pages 341-354 in International Geologic Congress.

Tranvik, L. J., J. J. Cole, and Y. T. Prairie. 2018. The study of carbon in inland waters—from isolated ecosystems to players in the global carbon cycle. Limnology and Oceanography Letters 3:41-48.

Tranvik, L. J., J. A. Downing, J. B. Cotner, S. A. Loiselle, R. G. Striegl, T. J. Ballatore, P. Dillon, K. Finlay, K. Fortino, L. B. Knoll, P. L. Kortelainen, T. Kutser, S. Larsen, I. Laurion, D. M. Leech, S. L. McCallister, D. M. McKnight, J. M. Melack, E. Overholt, J. A. Porter, Y. Prairie, W. H. Renwick, F. Roland, B. S. Sherman, D. W. Schindler, S. Sobek, A. Tremblay, M. J. Vanni, A. M. Verschoor, E. von Wachenfeldt, and G. A.

Weyhenmeyer. 2009. Lakes and reservoirs as regulators of carbon cycling and climate. Limnology and Oceanography 54:2298-2314.

Turak, E., I. Harrison, D. Dudgeon, R. Abell, A. Bush, W. Darwall, C. M. Finlayson, S. Ferrier, J. Freyhof, V. Hermoso, D. Juffe-Bignoli, S. Linke, J. Nel, H. C. Patricio, J. Pittock, R. Raghavan, C. Revenga, J. P. Simaika, and A. De Wever. 2017. Essential Biodiversity Variables for measuring change in global freshwater biodiversity. Biological Conservation 213:272-279.

Vannote, R. L., G. W. Minshall, K. W. Cummins, J. R. Sedell, and C. E. Cushing. 1980. River continuum concept. Canadian Journal of Fisheries and Aquatic Sciences 37:130-137.

Walker, D. A., F. J. Daniëls, N. V. Matveyeva, J. Šibík, M. D. Walker, A. L. Breen, L. A. Druckenmiller, M. K. Raynolds, H. Bültmann, and S. Hennekens. 2017. Circumpolar Arctic Vegetation Classification. Phytocoenologia.

Walker, D. A., M. K. Raynolds, F. J. Daniëls, E. Einarsson, A. Elvebakk, W. A. Gould, A. E. Katenin, S. S. Kholod, C. J. Markon, and E. S. Melnikov. 2005. The circumpolar Arctic vegetation map. Journal of Vegetation Science 16:267-282.

Walker, M. D., D. A. Walker, and N. A. Auerbach. 1994. Plant communities of a tussock tundra landscape in the Brooks Range Foothills, Alaska. Journal of Vegetation Science 5:843-866.

Ward, J. V., and J. A. Stanford. 1983. The serial discontinuity concept of lotic ecosystems. Pages 29-42 in T. D. Fontaine and S. M. Bartell, editors. Dynamics of Lotic Systems. Ann Arbor Science, Ann Arbor.

Whittinghill, K. A., and S. E. Hobbie. 2011. Effects of Landscape Age on Soil Organic Matter Processing in Northern Alaska. Soil Science Society of America Journal 75:907-917.

Xenopoulos, M. A., J. A. Downing, M. D. Kumar, S. Menden-Deuer, and M. Voss. 2017. Headwaters to oceans: Ecological and biogeochemical contrasts across the aquatic continuum. Limnology and Oceanography 62:S3-S14.

Xu, Z., and Y. J. Xu. 2018. Dissolved carbon transport in a river-lake continuum: A case study in a subtropical watershed, USA. Science of the Total Environment 643:640-650.

Zuur, A. F., E. N. Ieno, and C. S. Elphick. 2010. A protocol for data exploration to avoid common statistical problems. Methods in Ecology and Evolution 1:3-14.

4.5 Acknowledgements

We would like to thank Frances Iannucci and the researchers and technicians of the Toolik Field Station, Arctic LTER program, and Rubenstein Ecosystem Science Laboratory. This material is based on work supported by the National Science Foundation under grant numbers EF-1065682, EF-1065267, and DEB/LTER-1026843. DEMs provided by the Polar Geospatial Center under NSF-OPP awards 1043681, 1559691, and 1542736. Any opinions, findings, and conclusions or recommendations expressed in this material are those of the authors and do not reflect the views of the National Science Foundation.

4.6 Tables

Table 4.1 Median event discharge, discharge recurrence interval, median event sum of 7-day precipitation, station count by lakes present status, and supplemental stations for each synoptic sampling event. Primary stations used for two-way ANOVA and model development, supplemental stations used for model validation.

Event Date	Med. Event Q (L s-1)	Discharge Recurrence (Percentile)	Med. Sum 7-Day Precip. (mm)	*n* Stations			Primary Stations	Supplemental Stations
				No Lakes	Lakes	Total		
2012/08/05	4,292	Q95th	89	10	9	19	S01-S19	None
2012/08/11	951	Q65th	22	13	10	23	S01-S19	S20, S21, S22, S23
2013/07/03-04	1,138	Q70th	23	13	12	25	S01-S19	S20, S21, S22, S23, S24, S25
2013/07/20	2,155	Q85th	38	8	3	11		S01, S02, S05, S06, S07, S09, S18, S19, S20, S21, S22
2013/07/22	1,663	Q80th	39	4	0	4		S11, S12, S13, S23
2013/07/23	1,162	Q70th	37	1	6	7		S08, S10, S15, S16, S17, S24, S25
2013/07/24	1,114	Q70th	27	0	3	3		S03, S04, S14
2013/08/03-07	622	Q50th	8	15	14	29	S01-S19	S20, S21, S22, S23, S24, S25, S26, S27, S28, S29
2014/07/08	1,018	Q65th	30	15	3	18		S09, S10, S16, S25, S26, S28, S29, S73, S74, S76, S75, S77, S78, S79, S80, S82, S85, S86
2014/07/16	1,972	Q80th	41	3	13	16		S05, S06, S07, S08, S08a, S08b, S17, S19, S24, S36, S38, S62, S65, S66, S68, S89
2014/07/18	1,206	Q70th	42	39	47	86	S01-S19	S08b, S20, S21, S22, S23, S24, S25, S26, S27, S28, S29, S30, S31, S32, S33, S34, S35, S36, S37, S38, S39, S40, S41, S42, S43, S44, S45, S46, S47, S48, S49, S50, S51, S52, S53, S54, S55, S56, S57, S58,

Event Date	Med. Event Q (L s-1)	Discharge Recurrence (Percentile)	Med. Sum 7-Day Precip. (mm)	*n* Stations			Primary Stations	Supplemental Stations
				No Lakes	Lakes	Total		
								S59, S60, S61, S62, S63, S64, S65, S66, S67, S68, S69, S70, S72, S73, S74, S76, S77, S78, S79, S80, S81, S82, S85, S86, S87, S88, S89
2015/08/09 (Drought-Sampling)	93	Q10th	4	16	18	34		S05, S06, S07, S08, S08b, S09, S10, S16, S17, S19, S25, S26, S28, S29, S33, S34, S35, S36, S37, S38, S62, S65, S66, S68, S73, S74, S75, S76, S79, S80, S81, S82, S85, S86

Table 4.2 Model input variables, description and units for model development.

Variable	Description (units)
Landscape and Hydrological Characteristics	
DAkm2	Cumulative upslope drainage area (km^2)
Order	Stream order
LakesPresNum	Lakes present upslope (1/0)
Dist2Lakem	Distance to upslope lake (m)
Sum7dayPmm	Sum of 7-day antecedant precipitation (mm)
slopePct	Stream slope (%)
Reach Scale Vegetation Cover	
rBarrPct	Reach barren land (%)
rDtunPct	Reach dry tundra (acidic/non-acidic) (%)
rMtunPct	Reach moist tundra (acidic/non-acidic) (%)
rShrubPct	Reach scrub/shrub land (%)
rFensPct	Reach fens (%)
rWaterPct	Reach open water (%)
Watershed Scale Vegetation Cover	
wBarrPct	Cumulative upslope barren land (%)
wDtunPct	Cumulative upslope dry tundra (acidic/non-acidic) (%)
wMtunPct	Cumulative upslope moist tundra (acidic/non-acidic) (%)
wShrubPct	Cumulative upslope scrub/shrub land (%)
wFensPct	Cumulative upslope fens (%)
wWaterPct	Cumulative upslope open water (%)

Table 4.3 Two-way ANOVA p-values for transformed nutrient concentrations by median event discharge type and lake presence. Bolded values denote significance at $\alpha = 0.05$.

Effect	*p*-Value by Log Transformed Nutrient Concentration								
	DOC	DON	TDN	NH_4-N	NO_x-N	DIN	TDP	SRP	DOP
MedQType	**0.002**	0.522	**<0.001**	0.233	0.222	0.074	0.318	**<0.001**	0.522
LakesPres	**<0.001**	0.061	**<0.001**	**0.029**	0.494	**0.016**	**<0.001**	**0.046**	**0.061**
MedQType* LakesPres	0.901	0.235	0.983	0.617	0.458	0.323	0.255	0.956	0.235

Table 4.4 Summary of BIC, fit statistics, and adjusted r2 for the most parsimonious model identified for each nutrient based on glmulti BIC optimization and independent variable inflation factor (VIF) < 3.

Nutr-ient	BIC	df	F	*p*	Adj. r^2	Max. VIF	Mean ± SD VIF	Model
DOC	-200.9	4 and 90	75.0	<0.001	0.759	1.64	1.31 ± 0.32	LogDOCugL = 3.895 + 0.0014*Sum7dayPmm + -0.0113*wWaterPct + 0.0113*wBarrPct + -0.0196*wDtunPct
DON	-117.8	4 and 90	42.0	<0.001	0.636	1.64	1.31 ± 0.32	LogDONugL = 2.3235 + 0.0027*Sum7dayPmm + -0.0108*wWaterPct + 0.0203*wBarrPct + -0.0224*wDtunPct
TDN	-124.6	6 and 88	20.3	<0.001	0.552	2.86	1.75 ± 0.81	LogTDNugL = 2.3644 + -0.0558*Order + 0.0021*Sum7dayPmm + 0.0053*rBarrPct + -0.0069*rFensPct + -0.0067*wDtunPct + 0.0078*wFensPct
NH_4-N	-42.0	4 and 90	30.3	<0.001	0.555	2.59	1.79 ± 0.90	LogNH4NugL = 0.7777 + -0.002*Sum7dayPmm + 0.0213*rBarrPct + -0.015*rFensPct + 0.0162*wFensPct
NO_3-N	212.1	5 and 89	32.0	<0.001	0.622	2.39	1.63 ± 0.52	LogNO3NugL = 2.1619 + 0.0251*DAkm2 + 0.0001*Dist2Lakem + -0.0375*rFensPct + -0.0553*rWaterPct + -0.0594*wMtunPct
DIN	98.0	2 and 92	23.9	<0.001	0.328	1.20	1.20 ± 0.00	LogDINugL = 1.9397 + 0*Dist2Lakem + -0.0253*wMtunPct
TDP	-29.5	2 and 92	13.0	<0.001	0.203	1.15	1.15 ± 0.00	LogTDPugL = 0.4685 + -0.0147*wWaterPct + 0.0053*wFensPct
SRP	-34.8	5 and 88	14.0	<0.001	0.411	2.81	1.73 ± 0.94	LogSRPugL = 0.0935 + 0.0053*DAkm2 + -0.1158*Order + 0.004*Sum7dayPmm + 0.0063*rDtunPct + 0.0042*wFensPct
DOP	--	--	395	--	--	--	--	LogDOPugL = -0.59853

Table 4.5 Linear model statistics and parameter estimates for observed vs. predicted model validation for primary stations (model development), supplemental stations (model validation), and drought sampling. DOC, DON, NOx-N, and TDN retained for further investigation. Root mean squared deviation (RMSD) represents sum of squares deviation of predicted values with respect to observed.

Nutrient	Statistics					Slope			Intercept		
Source	n	RMSD	r^2	F	*p*-value	Est.	SE	*p*-value	Est.	SE	*p*-value
Dissolved Organic Carbon (DOC)											
Primary	95	0.07	0.769	310.0	0.000	1.00	0.06	0.000	0.00	0.21	1.000
Supp.	146	0.12	0.459	122.4	0.000	0.68	0.06	0.000	1.16	0.23	0.000
Drought	34	0.31	0.273	12.0	0.002	1.69	0.49	0.002	-2.69	1.78	0.140
Dissolved Organic Nitrogen (DON)											
Primary	95	0.11	0.651	173.6	0.000	1.00	0.08	0.000	0.00	0.17	1.000
Supp.	146	0.16	0.291	59.0	0.000	0.43	0.06	0.000	1.20	0.12	0.000
Drought	32	0.17	0.655	56.9	0.000	1.46	0.19	0.000	-1.03	0.41	0.018
Ammonium-Nitrogen (NH_4-N)											
Primary	95	0.17	0.574	125.1	0.000	1.00	0.09	0.000	0.00	0.08	1.000
Supp.	146	0.27	0.082	12.8	0.000	0.22	0.06	0.000	0.53	0.05	0.000
Drought	34	0.51	0.004	0.1	0.708	-0.10	0.26	0.708	1.12	0.22	0.000
Nitrate/Nitrite-Nitrogen (NO_x-N)											
Primary	95	0.63	0.642	167.0	0.000	1.00	0.08	0.000	0.00	0.07	1.000
Supp.	146	1.15	0.207	37.5	0.000	0.32	0.05	0.000	0.42	0.06	0.000
Drought	34	1.46	0.475	28.9	0.000	0.64	0.12	0.000	1.32	0.13	0.000
Dissolved Inorganic Nitrogen (DIN)											
Primary	95	0.37	0.342	48.4	0.000	1.00	0.14	0.000	0.00	0.17	1.000
Supp.	146	0.51	0.049	7.5	0.007	0.19	0.07	0.007	0.85	0.09	0.000
Drought	34	0.77	0.352	17.4	0.000	1.00	0.24	0.000	0.63	0.30	0.047
Soluble Reactive Phosphorus (SRP)											
Primary	94	0.17	0.443	73.0	0.000	1.00	0.12	0.000	0.00	0.03	1.000
Supp.	146	0.24	0.007	0.9	0.333	0.16	0.16	0.333	0.22	0.03	0.000
Drought	34	0.46	0.000	0.0	0.923	-0.06	0.60	0.923	0.35	0.04	0.000

Nutrient	Statistics					Slope			Intercept		
Source	n	RMSD	r^2	F	*p*-value	Est.	SE	*p*-value	Est.	SE	*p*-value
Total Dissolved Nitrogen (TDN)											
Primary	95	0.10	0.581	128.7	0.000	1.00	0.09	0.000	0.00	0.20	1.000
Supp.	146	0.14	0.188	33.3	0.000	0.44	0.08	0.000	1.20	0.17	0.000
Drought	32	0.25	0.010	0.3	0.584	0.12	0.21	0.584	2.12	0.46	0.000
Total Dissolved Phosphorus (TDP)											
Primary	95	0.19	0.220	26.2	0.000	1.00	0.20	0.000	0.00	0.09	1.000
Supp.	144	0.22	0.033	4.8	0.030	0.46	0.21	0.030	0.23	0.09	0.012
Drought	34	0.29	0.002	0.1	0.784	-0.14	0.52	0.784	0.66	0.22	0.004

4.7 Figures

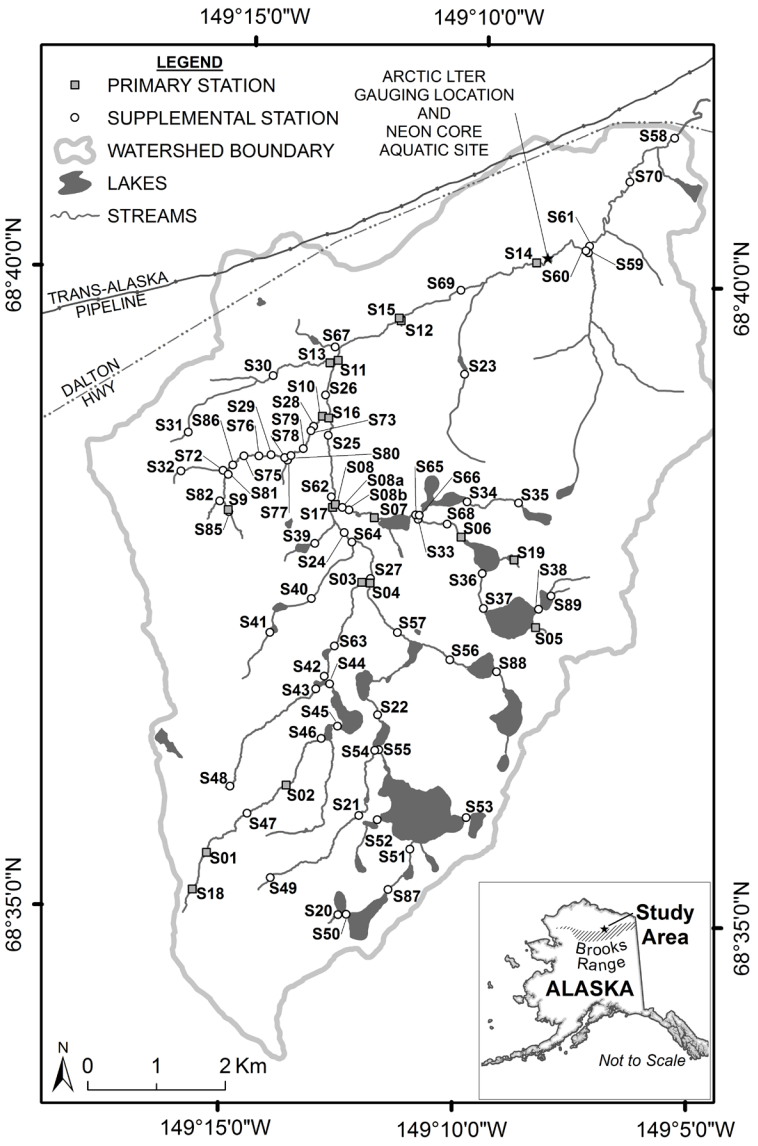

Figure 4.1 Oksrukuyik Creek watershed with sampling station locations by primary and supplemental event type.

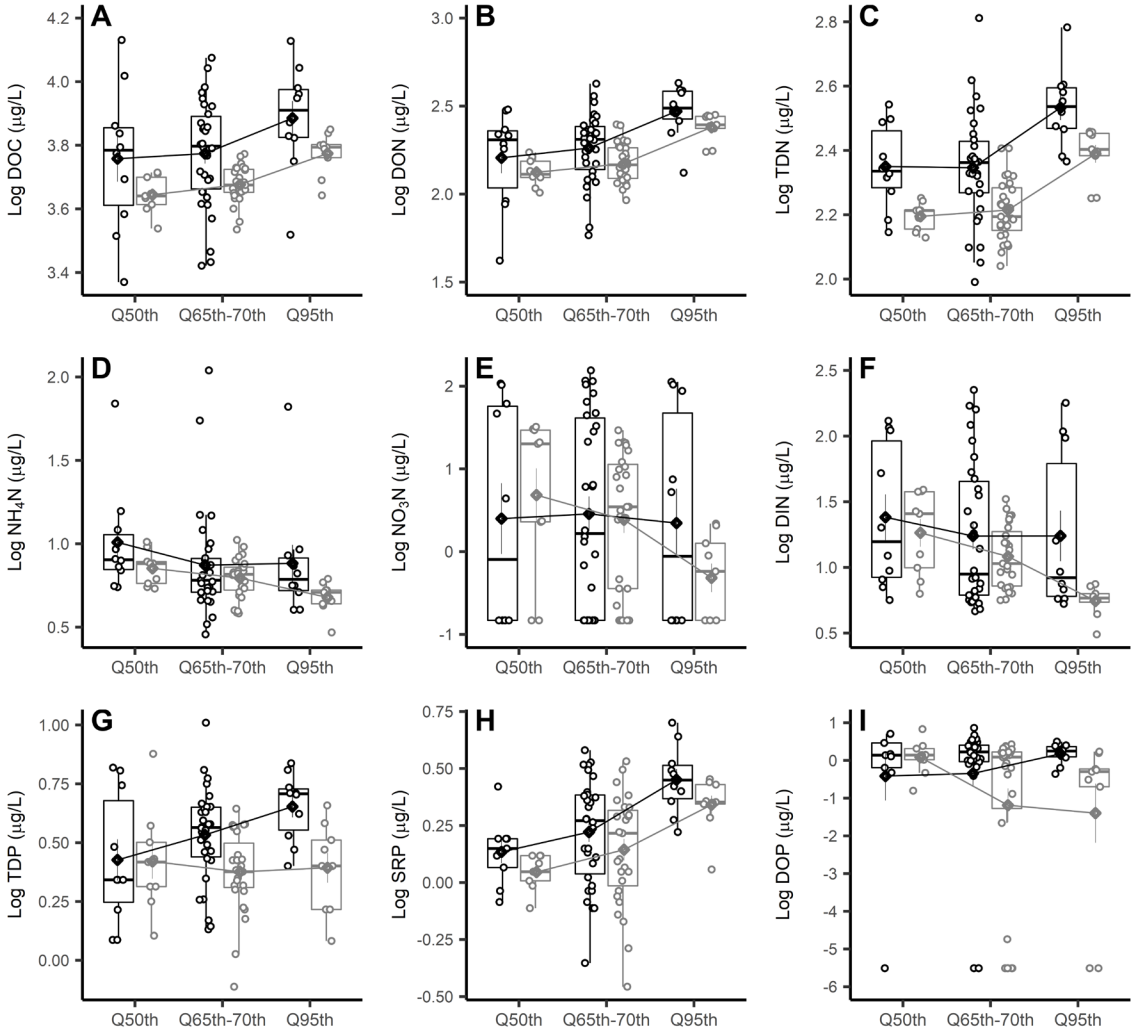

Figure 4.2 Box and whiskers and point scatterplots illustrating Log_{10} transformed (A) DOC, (B) DON, (C) TDN, (D) NH4-N, (E) NO_x-N, (F) DIN, (G) TDP, (H) SRP, and (I) DOP concentrations for primary stations by discharge event type. Gray indicates stream synoptic with lakes present and black indicates stream stations without lakes present. Circles denote station concentrations, thick horizontal box and whisker line represents median concentration and diamond with thick vertical line is mean concentration ± standard error. Significant interactions of two-way ANOVA summarized in Table 3..

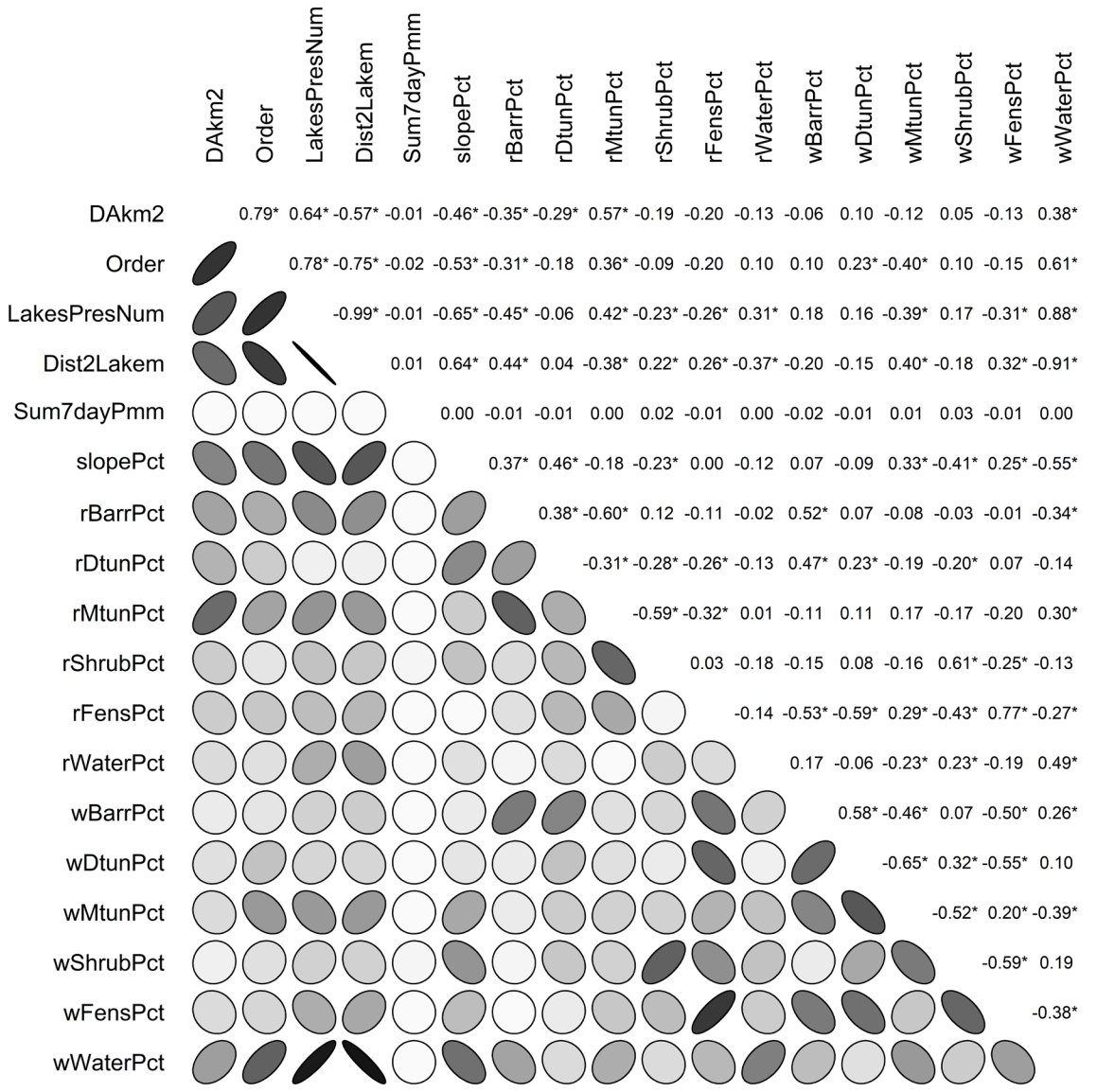

Figure 4.3 Correlation matrix of explanatory variables used in model development. Ellipses denote relationship pattern with darker shading indicative of more negative or positive Pearson correlation coefficient. Numbers denote Pearson Correlation coefficient with asterisk indicating significant relationships at $\alpha < 0.05$.

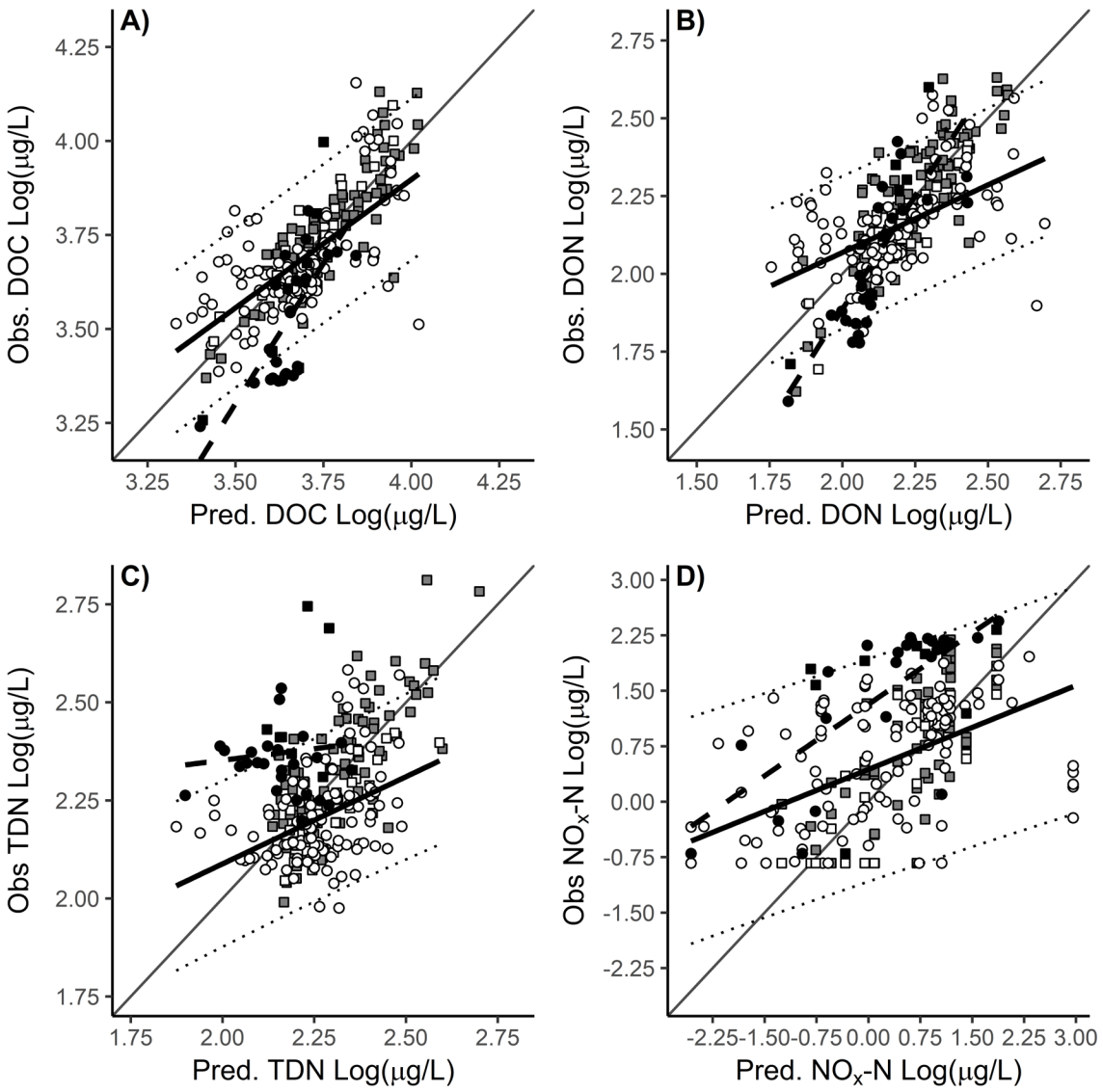

Figure 4.4 Observed vs. predicted Log10 transformed (A) DOC, (B) DON, (C) TDN, and (D) NO_x-N concentrations. Gray points indicate stations used for model development, white points indicate stations used for model validation and black points indicate stations from the 2015 drought-sampling event. Squares indicate primary sampling stations S01-S19 and circles indicate supplemental sampling stations. Thick black line denotes linear model fit of predicted on observed concentrations for the validation data set with 95th percentile prediction intervals indicated by thin dotted line. Thick dashed line denotes linear model fit of predicted on observed concentrations for the drought-sampling event. Thin black line is 1:1 for reference.

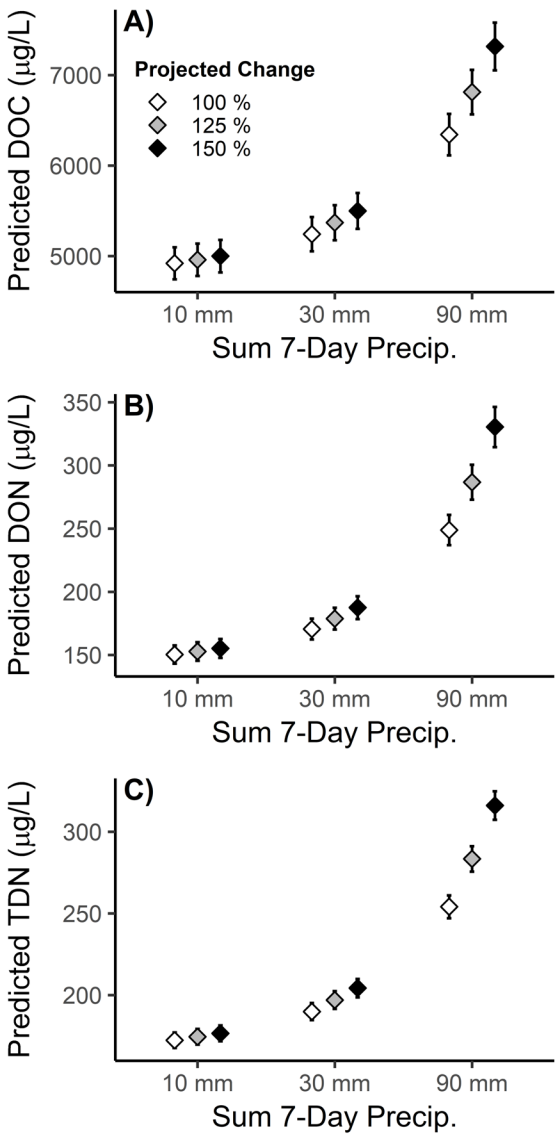

Figure 4.5 Sensitivity assessment of predicted mean ± standard error (A) DOC, (B) DON, and (C) TDN concentrations across antecedent sum of 7-day precipitation conditions consistent with Q50th (10 mm), Q70th (30 mm) and Q95th (90 mm) discharge recurrence intervals. White, grey, and black points indicate projected changes to precipitation regime based on (Bintanja and Selten 2014, Bintanja and Andry 2017). Significant differences across future precipitation regime type were noted in the greatest 7-day precipitation condition for all three nutrients (p<0.05).

4.8 Supplemental Tables

Supplemental Table 4.1 Landscape characteristics and reach/contributing watershed vegetation cover type distribution by station.

				Reach Vegetation Cover							Contributing Watershed Vegetation Cover						
Station	Order	Lakes Present	Slope (%)	Area (km^2)	Barren Land (%)	Dry Tundra (%)	Moist Tundra (%)	Shrub (%)	Fens (%)	Open Water (%)	Area (km^2)	Barren Land (%)	Dry Tundra (%)	Moist Tundra (%)	Shrub (%)	Fens (%)	Open Water (%)
S01	1	No	4.31	0.33	22.7	25.1	22.5	23.6	6.1	0.0	1.7	8.5	9.4	36.0	22.0	24.1	0.0
S02	1	No	7.72	0.27	0.0	28.0	53.2	18.8	0.0	0.0	2.7	6.3	17.2	39.3	21.0	16.3	0.0
S03	2	Yes	0.66	0.99	0.1	25.8	41.7	19.5	13.0	0.0	9.9	6.2	16.9	33.6	26.5	14.2	2.7
S04	2	Yes	0.54	0.55	3.0	3.4	46.4	37.8	9.5	0.0	13.5	9.0	16.1	31.5	26.8	4.0	12.6
S05	1	No	2.66	0.72	17.9	17.9	34.6	29.5	0.0	0.0	0.7	17.9	17.9	34.6	29.5	0.0	0.0
S06	2	Yes	2.08	0.67	4.6	4.6	59.2	10.4	0.0	21.2	4.2	9.3	11.5	31.3	33.5	2.7	11.7
S07	2	Yes	0.53	1.40	0.1	5.7	38.1	38.5	11.1	6.5	7.8	8.7	9.3	40.8	26.7	4.4	10.1
S08	2	Yes	2.00	0.03	0.0	22.9	56.6	20.5	0.0	0.0	8.1	8.3	9.6	41.5	26.4	4.6	9.7
S08a	2	Yes	2.00	0.06	0.0	30.4	49.5	20.1	0.0	0.0	8.1	8.4	9.5	41.4	26.4	4.6	9.7
S08b	2	Yes	1.55	0.25	0.0	12.7	57.5	17.3	10.6	1.9	8.0	8.4	9.4	41.3	26.4	4.6	9.8
S09	1	No	1.22	0.02	0.0	0.0	62.3	37.7	0.0	0.0	1.4	6.9	29.1	27.5	36.5	0.0	0.0
S10	2	No	2.34	0.05	9.8	0.0	18.3	61.8	10.0	0.0	5.8	2.6	12.6	42.5	38.2	3.9	0.2
S11	0	No	2.95	0.16	0.0	0.1	58.6	41.3	0.0	0.0	0.2	0.0	0.1	58.6	41.3	0.0	0.0
S12	0	No	2.07	0.46	0.0	0.0	64.1	11.7	24.2	0.0	0.5	0.0	0.0	64.1	11.7	24.2	0.0
S13	2	No	2.59	0.36	0.0	0.0	47.1	26.6	25.5	0.7	3.2	0.0	0.5	51.7	13.7	34.0	0.1
S14	3	Yes	0.84	1.51	0.0	1.5	73.9	14.8	9.8	0.0	57.8	4.9	10.8	44.7	25.5	9.2	5.0
S15	3	Yes	0.65	1.75	0.0	1.3	68.5	30.3	0.0	0.0	50.7	5.6	12.1	41.0	27.3	8.4	5.6
S16	3	Yes	1.76	0.16	0.0	3.8	87.4	8.8	0.0	0.0	36.0	7.3	14.8	38.2	24.7	7.1	7.8
S17	3	Yes	0.90	0.14	0.0	4.9	78.5	16.6	0.0	0.0	26.8	7.3	16.9	35.5	24.5	8.2	7.5
S18	1	No	5.48	1.36	5.1	5.6	39.2	21.7	28.5	0.0	1.4	5.1	5.6	39.2	21.7	28.5	0.0

				Reach Vegetation Cover							Contributing Watershed Vegetation Cover						
Station	Order	Lakes Present	Slope (%)	Area (km^2)	Barren Land (%)	Dry Tundra (%)	Moist Tundra (%)	Shrub (%)	Fens (%)	Open Water (%)	Area (km^2)	Barren Land (%)	Dry Tundra (%)	Moist Tundra (%)	Shrub (%)	Fens (%)	Open Water (%)
S19	1	No	7.04	0.48	10.9	14.9	63.9	10.3	0.0	0.0	0.5	10.9	14.9	63.9	10.3	0.0	0.0
S20	1	No	4.66	1.13	2.7	24.5	5.7	62.2	4.9	0.0	1.1	2.7	24.5	5.7	62.2	4.9	0.0
S21	1	No	1.89	1.84	0.4	19.8	55.4	19.1	5.3	0.0	2.0	0.3	20.0	56.4	18.0	5.3	0.0
S22	2	Yes	1.35	0.29	18.5	0.8	42.6	16.9	2.9	18.3	8.2	9.2	17.1	32.7	23.4	2.6	14.9
S23	1	No	6.00	1.52	0.0	3.0	75.2	8.4	13.4	0.0	1.5	0.0	3.0	75.2	8.4	13.4	0.0
S24	3	Yes	0.45	0.05	0.0	23.7	72.2	1.1	3.0	0.0	25.9	7.3	17.2	34.5	24.9	8.4	7.7
S25	3	Yes	0.69	0.12	0.0	6.2	71.4	22.4	0.0	0.0	35.8	7.3	14.9	38.0	24.8	7.2	7.8
S26	3	Yes	1.67	0.11	18.6	0.0	47.1	34.4	0.0	0.0	41.9	6.7	14.5	38.9	26.6	6.7	6.7
S27	3	Yes	0.54	0.03	0.0	0.0	0.7	55.8	43.5	0.0	23.4	7.8	16.4	32.4	26.7	8.3	8.4
S28	2	No	1.54	0.02	0.0	0.0	8.3	62.9	28.8	0.0	5.8	2.6	12.7	42.6	38.0	3.8	0.2
S29	2	No	1.94	0.06	0.0	0.0	82.7	0.0	17.3	0.0	4.6	2.4	14.4	38.7	41.8	2.8	0.0
S30	2	No	1.21	1.72	0.0	0.0	44.0	8.2	47.8	0.0	2.9	0.0	0.5	52.3	12.0	35.1	0.1
S31	1	No	1.24	1.13	0.0	1.4	65.1	17.9	15.6	0.2	1.1	0.0	1.4	65.1	17.9	15.6	0.2
S32	1	No	1.30	0.38	0.0	5.6	56.3	38.1	0.0	0.0	0.4	0.0	5.6	56.3	38.1	0.0	0.0
S33	2	Yes	0.77	0.14	25.5	0.0	45.4	0.0	29.1	0.0	4.4	9.8	10.9	32.2	32.6	3.5	11.1
S34	1	Yes	2.20	0.42	9.5	4.2	75.7	10.4	0.1	0.0	1.1	20.1	11.4	55.0	8.0	0.0	5.4
S35	1	Yes	1.59	0.64	27.1	16.1	41.5	6.4	0.0	8.9	0.6	27.1	16.1	41.5	6.4	0.0	8.9
S36	2	Yes	3.84	0.45	0.0	5.0	8.8	63.1	23.1	0.0	3.1	10.1	12.5	20.1	42.2	3.7	11.4
S37	2	Yes	2.44	0.78	7.7	9.5	19.9	22.2	1.5	39.3	2.6	11.9	13.7	22.0	38.6	0.4	13.4
S38	2	Yes	0.00	1.00	10.0	14.3	16.8	54.8	0.0	4.1	1.1	10.9	14.0	15.3	56.2	0.0	3.7
S39	1	Yes	1.46	0.56	12.4	7.5	69.0	1.0	5.5	4.6	0.6	12.4	7.5	69.0	1.0	5.5	4.6
S40	1	Yes	1.34	0.75	5.1	23.6	63.6	0.0	3.3	4.4	1.7	4.2	29.1	60.9	0.0	3.6	2.2
S41	1	No	2.01	0.91	3.6	33.6	58.6	0.0	4.0	0.3	0.9	3.6	33.6	58.6	0.0	4.0	0.3
S42	2	Yes	0.54	0.09	0.0	0.0	20.2	39.8	22.5	17.5	8.1	7.6	15.3	33.1	27.1	13.8	3.1

				Reach Vegetation Cover							Contributing Watershed Vegetation Cover						
Station	Order	Lakes Present	Slope (%)	Area (km^2)	Barren Land (%)	Dry Tundra (%)	Moist Tundra (%)	Shrub (%)	Fens (%)	Open Water (%)	Area (km^2)	Barren Land (%)	Dry Tundra (%)	Moist Tundra (%)	Shrub (%)	Fens (%)	Open Water (%)
S43	1	No	1.15	2.03	9.1	19.0	14.3	38.2	16.6	2.9	2.6	11.6	16.6	11.2	38.8	19.6	2.2
S44	2	Yes	0.83	0.76	8.2	3.5	34.4	27.7	7.7	18.5	5.4	5.8	14.9	43.9	21.3	10.9	3.2
S45	2	Yes	2.65	0.09	9.7	8.3	42.6	7.0	2.4	30.1	4.6	5.4	16.8	45.5	20.2	11.4	0.7
S46	1	No	7.41	0.88	2.5	16.0	46.7	33.1	1.7	0.0	3.6	5.3	16.9	41.1	23.9	12.7	0.0
S47	1	No	3.57	0.78	3.5	30.5	41.7	19.5	4.8	0.0	2.5	6.9	16.0	37.8	21.2	18.0	0.0
S48	1	No	7.28	0.57	20.3	8.2	0.0	41.0	30.5	0.0	0.6	20.3	8.2	0.0	41.0	30.5	0.0
S49	1	No	11.05	0.13	0.0	22.2	71.2	1.4	5.2	0.0	0.1	0.0	22.2	71.2	1.4	5.2	0.0
S50	1	Yes	2.47	0.30	0.5	38.3	26.9	18.7	0.0	15.6	1.4	2.2	27.4	10.2	53.1	3.8	3.3
S51	1	Yes	6.63	0.33	22.7	16.3	45.8	7.9	0.0	7.4	2.5	8.1	25.6	19.8	34.5	2.2	9.7
S52	1	Yes	4.68	0.46	25.8	12.4	45.5	6.6	0.0	9.7	0.5	25.8	12.4	45.5	6.6	0.0	9.7
S53	1	Yes	13.26	0.46	33.7	12.8	26.0	14.4	0.0	13.2	0.5	33.7	12.8	26.0	14.4	0.0	13.2
S54	2	Yes	1.72	2.08	6.8	9.7	20.1	23.8	0.8	38.7	5.5	11.3	17.4	22.6	26.4	1.3	21.0
S55	1	No	1.58	0.41	17.3	10.8	48.0	14.0	7.2	2.7	2.4	3.2	18.4	55.0	17.3	5.6	0.5
S56	1	Yes	0.77	0.68	0.1	20.8	20.5	36.9	6.7	15.0	2.4	16.0	22.3	23.5	18.8	5.7	13.8
S57	2	Yes	0.95	0.48	2.6	12.4	31.4	39.5	1.5	12.6	12.9	9.2	16.6	30.9	26.4	3.7	13.1
S58	3	Yes	0.39	1.60	0.7	8.6	69.4	7.6	10.1	3.5	71.5	4.8	9.6	50.1	22.9	8.5	4.1
S59	3	Yes	0.39	0.01	0.0	1.3	71.6	27.1	0.0	0.0	68.2	4.9	9.8	48.9	23.6	8.6	4.2
S60	2	No	2.13	1.58	4.8	8.5	80.4	6.3	0.0	0.0	7.2	6.9	6.0	73.6	11.1	1.9	0.5
S61	3	Yes	0.39	1.88	0.7	0.0	69.6	20.2	9.4	0.0	61.0	4.6	10.3	45.9	25.0	9.4	4.7
S62	3	Yes	0.96	0.03	0.0	6.1	63.7	30.2	0.0	0.0	34.9	7.5	15.2	36.9	24.9	7.4	8.0
S63	2	Yes	0.85	0.80	0.0	21.5	28.4	29.0	19.3	1.9	8.9	6.9	15.9	32.7	27.3	14.3	3.0
S64	1	Yes	0.84	0.50	0.0	26.7	43.7	8.0	21.7	0.0	2.2	3.3	28.5	56.9	1.9	7.8	1.7

				Reach Vegetation Cover							Contributing Watershed Vegetation Cover						
Station	Order	Lakes Present	Slope (%)	Area (km^2)	Barren Land (%)	Dry Tundra (%)	Moist Tundra (%)	Shrub (%)	Fens (%)	Open Water (%)	Area (km^2)	Barren Land (%)	Dry Tundra (%)	Moist Tundra (%)	Shrub (%)	Fens (%)	Open Water (%)
S65	2	Yes	0.77	0.00	0.0	0.0	54.1	0.0	45.9	0.0	6.4	10.6	10.0	41.4	24.1	2.9	10.9
S66	1	Yes	1.17	0.85	3.0	4.2	72.3	0.3	3.6	16.6	1.9	12.5	8.2	62.8	4.5	1.7	10.4
S67	1	Yes	2.70	2.67	0.0	0.0	46.8	42.9	9.4	0.9	2.7	0.0	0.0	46.8	42.9	9.4	0.9
S68	2	Yes	1.01	0.04	22.3	0.0	73.6	4.1	0.0	0.0	4.3	9.3	11.2	31.8	33.6	2.7	11.4
S69	3	Yes	0.84	1.07	0.0	0.0	67.4	28.4	4.2	0.0	52.2	5.4	11.8	41.8	27.2	8.4	5.4
S70	3	Yes	0.19	1.76	3.9	4.1	80.7	11.3	0.0	0.0	69.9	4.9	9.7	49.7	23.3	8.4	4.1
S72	1	No	1.14	0.25	0.0	0.5	43.9	49.0	6.6	0.0	0.6	0.0	3.6	51.4	42.3	2.6	0.0
S73	2	No	0.91	0.55	3.5	6.3	53.3	24.5	10.3	2.1	5.7	2.6	12.8	42.8	37.9	3.7	0.2
S74	2	No	1.25	0.33	0.0	0.6	34.4	54.1	10.9	0.0	4.3	2.5	15.6	34.7	45.2	1.9	0.0
S75	2	No	1.25	0.16	0.0	0.0	85.7	0.0	14.3	0.0	4.4	2.5	15.1	36.5	43.6	2.3	0.0
S76	2	No	2.48	0.14	0.0	0.0	89.8	0.0	10.2	0.0	4.6	2.4	14.6	38.2	42.3	2.6	0.0
S77	1	No	2.71	0.25	8.1	3.3	62.4	15.3	10.9	0.0	0.3	8.1	3.3	62.4	15.3	10.9	0.0
S78	2	No	1.48	0.22	0.0	6.2	77.3	15.6	0.9	0.0	4.9	2.2	14.1	40.5	40.6	2.7	0.0
S79	2	No	1.17	0.08	0.0	11.0	50.3	38.6	0.0	0.0	5.2	2.5	13.5	41.7	39.3	3.0	0.0
S80	2	No	1.48	0.00	0.0	0.0	0.0	100.0	0.0	0.0	5.1	2.5	13.5	41.5	39.3	3.1	0.0
S81	2	No	0.63	0.61	1.3	2.8	69.3	24.2	2.5	0.0	3.3	3.3	19.6	31.3	45.3	0.5	0.0
S82	1	No	1.72	0.24	0.0	15.0	51.5	33.5	0.0	0.0	0.2	0.0	15.0	51.5	33.5	0.0	0.0
S85	1	No	1.22	1.36	7.0	29.5	27.0	36.5	0.0	0.0	1.4	7.0	29.5	27.0	36.5	0.0	0.0
S86	2	No	0.93	0.01	0.0	0.0	72.1	4.4	23.5	0.0	3.9	2.8	16.9	34.7	44.5	1.1	0.0
S87	1	Yes	1.07	0.74	12.9	26.3	26.8	10.7	0.0	23.1	2.2	5.9	27.0	15.9	38.6	2.5	10.1
S88	1	Yes	0.68	1.68	22.5	22.9	24.7	11.4	5.2	13.3	1.7	22.5	22.9	24.7	11.4	5.2	13.3
S89	0	No	16.43	0.10	19.3	10.7	0.0	70.0	0.0	0.0	0.1	19.3	10.7	0.0	70.0	0.0	0.0

Supplemental Table 4.2 Summary of BIC, fit statistics, and adjusted r^2 for the candidate models model identified for each nutrient based on glmulti BIC optimization and independent variable inflation factor (VIF) < 3. Bolded rows indicate selected model.

Nutrient	*n* Var.	k	BIC	df	F	p	Adj. r^2	Max. VIF	Mean ± SD VIF	*n* VIF >3	Model
DOC	1	3	-155.5	1 and 93	123.5	< 2.2E-16	0.566	--	--	--	LogDOCugL = 3.9394 + -0.0165*wDtunPct
DOC	2	4	-169.0	2 and 92	83.46	< 2.2E-16	0.637	1.01	1.01 ± 0.00	0	LogDOCugL = 3.9662 + -0.0092*wWaterPct + -0.0158*wDtunPct
DOC	3	5	-184.2	3 and 91	74.8	< 2.2E-16	0.702	1.01	1.01 ± 0.01	0	LogDOCugL = 3.9162 + 0.0014*Sum7dayPmm + -0.0092*wWaterPct + -0.0158*wDtunPct
DOC	4	6	-200.9	4 and 90	75	< 2.2E-16	0.759	1.64	1.31 ± 0.32	0	LogDOCugL = 3.895 + 0.0014*Sum7dayPmm + -0.0113*wWaterPct + 0.0113*wBarrPct + -0.0196*wDtunPct
DOC	5	7	-203.8	5 and 89	65.69	< 2.2E-16	0.775	3.64	2.18 ± 0.98	1	LogDOCugL = 3.904 + 0.0014*Sum7dayPmm + -0.0049*rBarrPct + -0.015*wWaterPct + 0.0181*wBarrPct + -0.0213*wDtunPct
DOC	6-8	8	-206.1	6 and 88	59.2	< 2.2E-16	0.788	3.91	2.26 ± 0.99	1	LogDOCugL = 3.9408 + 0.0014*Sum7dayPmm + 0.0112*slopePct + -0.005*rBarrPct

Nutrient	*n* Var.	k	BIC	df	F	p	Adj. r^2	Max. VIF	Mean ± SD VIF	*n* VIF >3	Model
											+ -0.0184*wWaterPct + 0.0205*wBarrPct + -0.0222*wDtunPct
TDN	1	3	-86.3	1 and 93	23.54	4.90E-06	0.193	--	--	--	LogTDNugL = 2.4502 + -0.0781*Order
TDN	2	4	-99.9	2 and 92	23.74	4.85E-09	0.326	1.00	1.00 ± 0.00	0	LogTDNugL = 2.3738 + -0.0782*Order + 0.0021*Sum7dayPmm
TDN	3	5	-111.5	3 and 91	24.23	1.30E-11	0.426	1.02	1.01 ± 0.01	0	LogTDNugL = 2.3091 + -0.0708*Order + 0.0021*Sum7dayPmm + 0.0051*wFensPct
TDN	4	6	-122.8	4 and 90	25.29	4.71E-14	0.508	1.09	1.05 ± 0.04	0	LogTDNugL = 2.235 + 0*Dist2Lakem + 0.0021*Sum7dayPmm + 0.0053*rDtunPct + -0.0094*wDtunPct
TDN	5	6	-122.8	4 and 90	25.29	4.71E-14	0.508	1.09	1.05 ± 0.04	0	LogTDNugL = 2.235 + 0*Dist2Lakem + 0.0021*Sum7dayPmm + 0.0053*rDtunPct + -0.0094*wDtunPct
TDN	6-8	8	-124.6	6 and 88	20.3	9.04E-15	0.552	2.86	1.75 ± 0.81	0	LogTDNugL = 2.3644 + -0.0558*Order + 0.0021*Sum7dayPmm + 0.0053*rBarrPct + -0.0069*rFensPct

Nutrient	*n* Var.	k	BIC	df	F	p	Adj. r^2	Max. VIF	Mean ± SD VIF	*n* VIF >3	Model
											+ -0.0067*wDtunPct + 0.0078*wFensPct
NH4N	1	3	-17.4	1 and 93	52.85	1.10E-10	0.356	--	--	--	LogNH4NugL = 0.753 + 0.0236*rBarrPct
NH4N	2	4	-23.7	2 and 92	34.87	5.35E-12	0.419	1.17	1.17 ± 0.00	0	LogNH4NugL = 0.705 + 0.0194*rBarrPct + 0.0074*rDtunPct
NH4N	3	5	-36.5	3 and 91	33.67	9.88E-15	0.510	2.59	2.06 ± 0.89	0	LogNH4NugL = 0.7052 + 0.0213*rBarrPct + -0.015*rFensPct + 0.0162*wFensPct
NH4N	4	6	-42.0	4 and 90	30.26	5.91E-16	0.555	2.59	1.79 ± 0.90	0	LogNH4NugL = 0.7777 + -0.002*Sum7dayPmm + 0.0213*rBarrPct + -0.015*rFensPct + 0.0162*wFensPct
NH4N	5	7	-45.8	5 and 89	27.79	< 2.2E-16	0.588	3.28	2.25 ± 0.96	2	LogNH4NugL = 0.9443 + -0.0838*Order + -0.0453*slopePct + 0.0223*rBarrPct + -0.0215*rFensPct + 0.0222*wFensPct
NH4N	6	8	-53.7	6 and 88	28.15	< 2.2E-16	0.634	3.28	2.04 ± 1.00	2	LogNH4NugL = 1.0176 + -0.084*Order + -0.002*Sum7dayPmm + -0.0455*slopePct + 0.0222*rBarrPct + -0.0215*rFensPct + 0.0222*wFensPct

Nutrient	*n* Var.	k	BIC	df	F	p	Adj. r^2	Max. VIF	Mean ± SD VIF	*n* VIF >3	Model
NH4N	7-8	9	-59.0	7 and 87	27.85	< 2.2E-16	0.667	4.18	2.64 ± 1.32	4	LogNH4NugL = 0.6951 + -0.1544*Order + 0.3332*LakesPresNum + -0.002*Sum7dayPmm + 0.0242*rBarrPct + 0.005*rShrubPct + -0.0208*rFensPct + 0.0251*wFensPct
NO3N	1	3	259.4	1 and 93	37.53	2.14E-08	0.280	--	--	--	LogNO3NugL = -0.5902 + 0.0806*wDtunPct
NO3N	2	4	247.3	2 and 92	30.92	5.35E-11	0.389	1.06	1.06 ± 0.00	0	LogNO3NugL = 2.869 + -0.0999*rWaterPct + -0.0562*wMtunPct
NO3N	3	5	233.8	3 and 91	31	6.75E-14	0.489	1.78	1.51 ± 0.28	0	LogNO3NugL = 1.7725 + 0.035*DAkm2 + 0.0002*Dist2Lakem + -0.0656*wMtunPct
NO3N	4	6	218.9	4 and 90	33.33	< 2.2E-16	0.579	1.80	1.43 ± 0.30	0	LogNO3NugL = 1.7192 + 0.0331*DAkm2 + 0.0002*Dist2Lakem + -0.0357*rFensPct + -0.0587*wMtunPct
NO3N	5	7	212.1	5 and 89	31.96	< 2.2E-16	0.622	2.39	1.63 ± 0.52	0	LogNO3NugL = 2.1619 + 0.0251*DAkm2 + 0.0001*Dist2Lakem + -0.0375*rFensPct + -

Nutrient	*n* Var.	k	BIC	df	F	p	Adj. r^2	Max. VIF	Mean ± SD VIF	*n* VIF >3	Model
											0.0553*rWaterPct + -0.0594*wMtunPct
NO3N	6	8	198.3	6 and 88	35.1	< 2.2E-16	0.685	3.19	2.52 ± 0.82	2	LogNO3NugL = -1.622 + 0.0372*DAkm2 + -0.5125*Order + 0.0351*rShrubPct + -0.0845*rFensPct + 0.0948*wDtunPct + 0.0978*wFensPct
NO3N	7	9	187.2	7 and 87	37.31	< 2.2E-16	0.730	21.78	6.98 ± 7.38	5	LogNO3NugL = 0.1254 + 0.0761*DAkm2 + -5.423*LakesPresNum + -0.2995*slopePct + 0.104*rDtunPct + 0.3572*wWaterPct + -0.1209*wBarrPct + 0.0976*wDtunPct
NO3N	8	10	184.6	8 and 86	35.61	< 2.2E-16	0.747	22.71	6.91 ± 7.29	5	LogNO3NugL = 1.2166 + 0.0747*DAkm2 + -5.1528*LakesPresNum + -0.2532*slopePct + 0.0954*rDtunPct + 0.3247*wWaterPct + -0.1166*wBarrPct + 0.0782*wDtunPct + -0.0219*wMtunPct
DIN	1	3	114.4	1 and 93	20.4	1.84E-05	0.171	--	--	--	LogDINugL = 0.8362 + 0.0277*wDtunPct

Nutrient	*n* Var.	k	BIC	df	F	p	Adj. r^2	Max. VIF	Mean ± SD VIF	*n* VIF >3	Model
DIN	2	4	98.0	2 and 92	23.93	4.29E-09	0.328	1.20	1.20 ± 0.00	0	LogDINugL = 1.9397 + 0*Dist2Lakem + -0.0253*wMtunPct
DIN	3	5	83.8	3 and 91	25.87	3.43E-12	0.443	3.11	2.42 ± 1.02	1	LogDINugL = 0.7507 + 0.0143*rShrubPct + -0.0548*rFensPct + 0.0441*wFensPct
DIN	4	6	64.9	4 and 90	30.84	3.65E-16	0.559	3.17	2.27 ± 1.04	2	LogDINugL = 0.3294 + 0.0141*rShrubPct + -0.0465*rFensPct + 0.0275*wDtunPct + 0.0479*wFensPct
DIN	5	7	59.8	5 and 89	28.91	< 2.2E-16	0.598	3.17	2.05 ± 1.03	2	LogDINugL = 0.4915 + -0.104*Order + 0.0132*rShrubPct + -0.0468*rFensPct + 0.0309*wDtunPct + 0.0478*wFensPct
DIN	6	8	42.9	6 and 88	33.57	< 2.2E-16	0.675	3.19	2.52 ± 0.82	2	LogDINugL = 0.5069 + 0.0125*DAkm2 + -0.2881*Order + 0.0152*rShrubPct + -0.0449*rFensPct + 0.0361*wDtunPct + 0.0493*wFensPct
DIN	7	9	34.7	7 and 87	34.33	< 2.2E-16	0.713	3.19	2.30 ± 0.94	2	LogDINugL = 0.6193 + 0.0124*DAkm2 + -0.2865*Order + -0.0031*Sum7dayPmm + 0.0152*rShrubPct + -

Nutrient	*n* Var.	k	BIC	df	F	p	Adj. r^2	Max. VIF	Mean ± SD VIF	*n* VIF >3	Model
											0.0449*rFensPct + 0.0361*wDtunPct + 0.0493*wFensPct
DIN	8	10	30.4	8 and 86	33.65	< 2.2E-16	0.735	5.29	2.91 ± 1.45	4	LogDINugL = 0.5059 + 0.0153*DAkm2 + -0.4038*Order + -0.0031*Sum7dayPmm + 0.0176*rShrubPct + -0.0471*rFensPct + 0.025*wWaterPct + 0.0412*wDtunPct + 0.0567*wFensPct
DON	1	3	-70.8	1 and 93	47.82	5.81E-10	0.333	--	--	--	LogDONugL = 2.4404 + -0.016*wDtunPct
DON	2	4	-93.7	2 and 92	46.93	8.95E-15	0.494	1.00	1.00 ± 0.00	0	LogDONugL = 2.3412 + 0.0027*Sum7dayPmm + -0.0161*wDtunPct
DON	3	5	-107.1	3 and 91	43.72	< 2.2E-16	0.577	1.53	1.36 ± 0.31	0	LogDONugL = 2.3008 + 0.0027*Sum7dayPmm + 0.0167*wBarrPct + -0.0219*wDtunPct
DON	4-8	6	-117.8	4 and 90	41.99	< 2.2E-16	0.636	1.64	1.31 ± 0.32	0	LogDONugL = 2.3235 + 0.0027*Sum7dayPmm + 0.0108*wWaterPct + 0.0203*wBarrPct + -0.0224*wDtunPct

Nutrient	*n* Var.	k	BIC	df	F	p	Adj. r^2	Max. VIF	Mean ± SD VIF	*n* VIF >3	Model
TDP	1	3	-27.6	1 and 93	18.27	4.63E-05	0.155	--	--	--	LogTDPugL = 0.5389 + -0.019*wWaterPct
TDP	2-8	4	-29.5	2 and 92	12.95	1.11E-05	0.203	1.15	1.15 ± 0.00	0	LogTDPugL = 0.4685 + -0.0147*wWaterPct + 0.0053*wFensPct
SRP	1	3	-25.6	1 and 92	31.37	2.20E-07	0.246	--	--	--	LogSRPugL = 0.0615 + 0.004*Sum7dayPmm
SRP	2	4	-30.7	2 and 91	22.05	1.55E-08	0.312	1.00	1.00 ± 0.00	0	LogSRPugL = 0.1141 + 0.004*Sum7dayPmm + -0.0135*wWaterPct
SRP	3	5	-32.9	3 and 90	17.89	3.44E-09	0.353	1.02	1.01 ± 0.01	0	LogSRPugL = 0.0632 + 0.004*Sum7dayPmm + 0.0051*rDtunPct + -0.0119*wWaterPct
SRP	4	6	-33.9	4 and 89	15.4	1.32E-09	0.382	1.07	1.04 ± 0.03	0	LogSRPugL = 0.104 + 0.004*Sum7dayPmm + 0.0062*rDtunPct + -0.0111*rWaterPct + -0.0067*wDtunPct
SRP	5-8	7	-34.8	5 and 88	13.97	4.79E-10	0.411	2.81	1.73 ± 0.94	0	LogSRPugL = 0.0935 + 0.0053*DAkm2 + -0.1158*Order + 0.004*Sum7dayPmm + 0.0063*rDtunPct + 0.0042*wFensPct

Nutrient	*n* Var.	k	BIC	df	F	p	Adj. r^2	Max. VIF	Mean ± SD VIF	*n* VIF >3	Model
DOP	1-8				395.70						LogDOPugL = -0.59853

4.9 Supplemental Figures

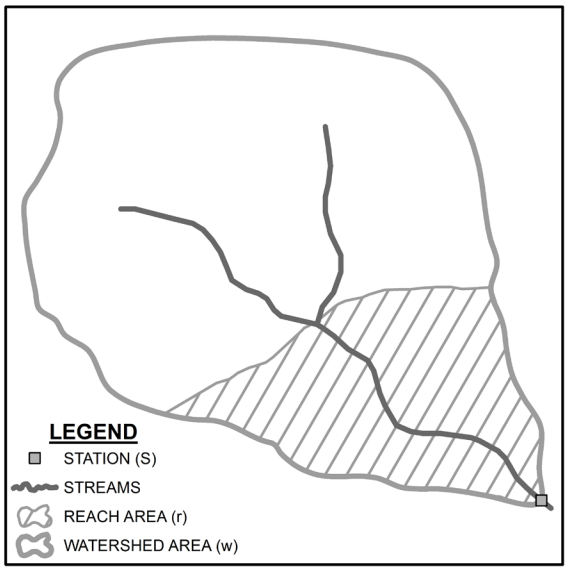

Supplemental Figure 4.1 Conceptual diagram showing reach area (r) and watershed area (w) for a given station (S).

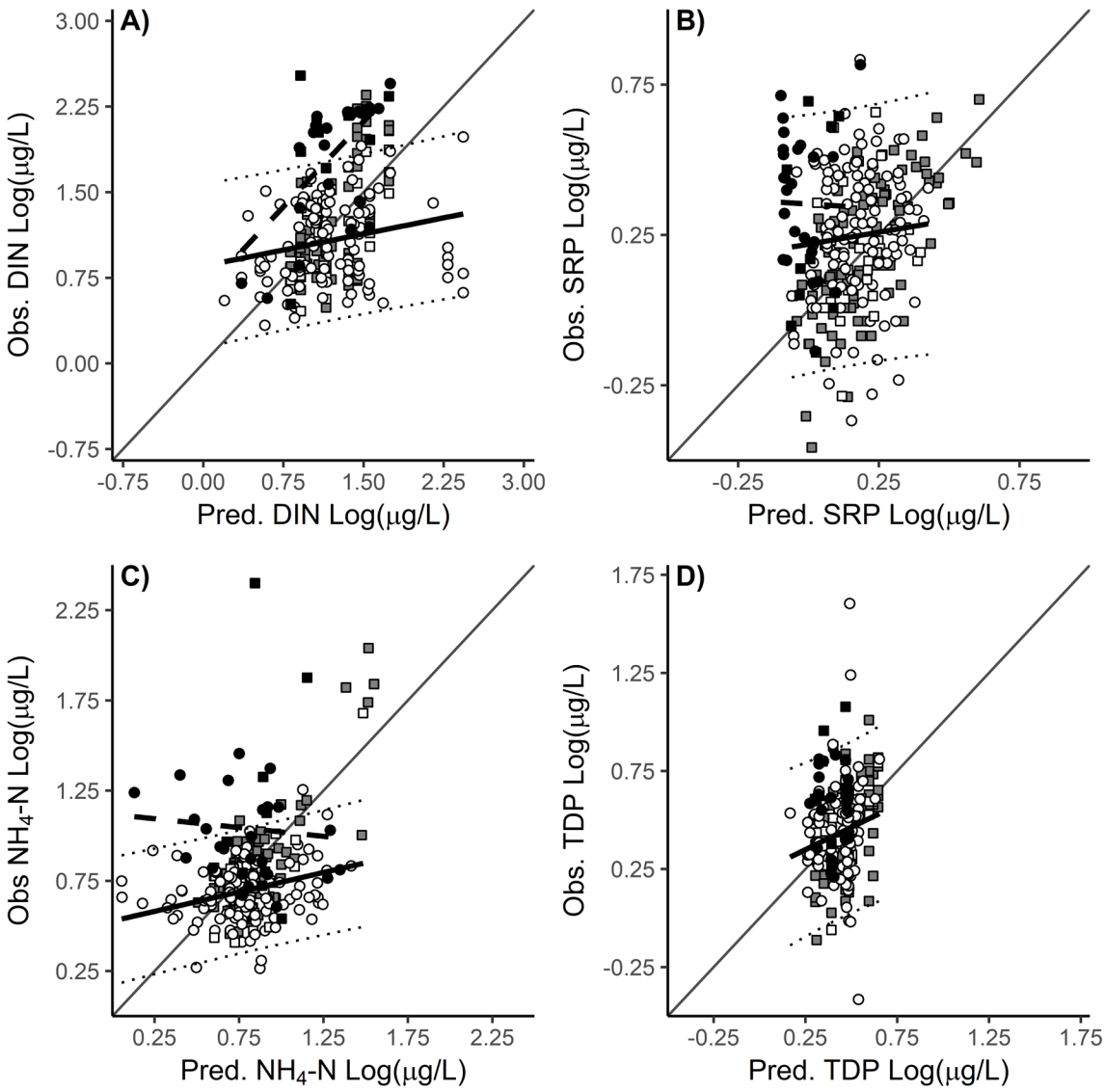

Supplemental Figure 4.2 Observed vs. predicted $\log_{10}$ transformed (A) DIN, (B) SRP, (C) NH_4-N, and (D) TDP concentrations. Gray points indicate stations used for model development, white points indicate stations used for model validation and black points indicate stations from the 2015 drought-sampling event. Squares indicate primary sampling stations S01-S19 and circles indicate supplemental sampling stations. Thick black line denotes linear model fit of predicted on observed concentrations for the validation data set with 95th percentile prediction intervals indicated by thin dotted line. Thick dashed line denotes linear model fit of predicted on observed concentrations for the drought-sampling event. Thin black line is 1:1 for reference.

CHAPTER 5: COMPREHENSIVE BIBLIOGRAPHY

Ackerman, D., D. Griffin, S. E. Hobbie, and J. C. Finlay. 2017. Arctic shrub growth trajectories differ across soil moisture levels. Global Change Biology **23**:4294-4302.

Aho, K., D. Derryberry, and T. Peterson. 2014. Model selection for ecologists: the worldviews of AIC and BIC. Ecology **95**:631-636.

Allen, G. H., and T. M. Pavelsky. 2018. Global extent of rivers and streams. Science **361**:585-588.

Allen, T. F. H., and T. W. Hoekstra. 1990. The Confusion between Scale-Defined Levels and Conventional Levels of Organization in Ecology. Journal of Vegetation Science **1**:5-12.

APHA. 2012. Method 10200 H Chlorophyll.*in* E. W. Rice, L. Bridgewater, and A. P. H. Association, editors. Standard methods for the examination of water and wastewater. American Public Health Association Washington, DC.

ARCTIC-LTER. 2016. Arctic Long-Term Ecological Research Streams and Rivers Database. Accessed December 2016. http://arc-lter.ecosystems.mbl.edu/arctic-lter-streams-and-rivers.

Argerich, A., R. Haggerty, E. Marti, F. Sabater, and J. Zarnetske. 2011. Quantification of metabolically active transient storage (MATS) in two reaches with contrasting transient storage and ecosystem respiration. J. Geophys. Res. **116**:G03034.

Arscott, D. B., W. B. Bowden, and J. C. Finlay. 1998. Comparison of Epilithic Algal and Bryophyte Metabolism in an Arctic Tundra Stream, Alaska. Journal of the North American Benthological Society **17**:210-227.

Arvola, L. 1981. Spectrophotometric determination of chlorophyll a and phaeopigments in ethanol extractions. Annales Botanici Fennici **18**:221-227.

Aubeneau, A. F., B. Hanrahan, D. Bolster, and J. Tank. 2016. Biofilm growth in gravel bed streams controls solute residence time distributions. Journal of Geophysical Research: Biogeosciences **121**:1840-1850.

Barnes, J. B., I. P. Vaughan, and S. J. Ormerod. 2013. Reappraising the effects of habitat structure on river macroinvertebrates. Freshwater Biology **58**:2154-2167.

Battin, T. J., K. Besemer, M. M. Bengtsson, A. M. Romani, and A. I. Packmann. 2016. The ecology and biogeochemistry of stream biofilms. Nat Rev Micro **14**:251-263.

Benda, L., N. L. Poff, D. Miller, T. Dunne, G. Reeves, G. Pess, and M. Pollock. 2004. The Network Dynamics Hypothesis: How Channel Networks Structure Riverine Habitats. Bioscience **54**:413-427.

Bertuzzo, E., A. M. Helton, R. O. Hall, and T. J. Battin. 2017. Scaling of dissolved organic carbon removal in river networks. Advances in Water Resources **110**:136-146.

Besemer, K. 2015. Biodiversity, community structure and function of biofilms in stream ecosystems. Research in Microbiology **166**:774-781.

Besemer, K., G. Singer, I. Hödl, and T. J. Battin. 2009. Bacterial community composition of stream biofilms in spatially variable-flow environments. Applied and environmental microbiology **75**:7189-7195.

Bilton, D. T., J. R. Freeland, and B. Okamura. 2001. DISPERSAL IN FRESHWATER INVERTEBRATES. Annual Review of Ecology and Systematics **32**:159-181.

Bintanja, R., and O. Andry. 2017. Towards a rain-dominated Arctic. Nature Climate Change **7**:263.

Bintanja, R., and F. M. Selten. 2014. Future increases in Arctic precipitation linked to local evaporation and sea-ice retreat. Nature **509**:479.

Bormann, F. H. 1953. The Statistical Efficiency of Sample Plot Size and Shape in Forest Ecology. Ecology **34**:474-487.

Bott, T. L., J. T. Brock, C. E. Cushing, S. V. Gregory, D. King, and R. C. Petersen. 1978. Comparison of methods for measuring primary productivity and community respiration in streams. Hydrobiologia **60**:3-12.

Boulton, A. J., T. Datry, T. Kasahara, M. Mutz, and J. A. Stanford. 2010. Ecology and management of the hyporheic zone: stream-groundwater interactions of running waters and their floodplains. Journal of the North American Benthological Society **29**:26-40.

Boulton, A. J., S. Findlay, P. Marmonier, E. H. Stanley, and H. M. Valett. 1998. The functional significance of the hyporheic zone in streams and rivers. Annual Review of Ecology and Systematics **29**:59-81.

Bowden, W. B., B. J. Peterson, J. C. Finlay, and J. Tucker. 1992. Epilithic chlorophyll-a, photosynthesis, and respiration in control and fertilized reaches of a tundra stream. Hydrobiologia **240**:121-131.

Bowles, N. D., H. W. Paerl, and J. Tucker. 1985. Effective solvents and extraction periods employed in phytoplankton carotenoid and chlorophyll determinations. Canadian Journal of Fisheries and Aquatic Sciences **42**:1127-1131.

Boyce, D. G., M. Lewis, and B. Worm. 2012. Integrating global chlorophyll data from 1890 to 2010. Limnology and Oceanography: Methods **10**:840-852.

Briggs, M. A., F. D. Day-Lewis, J. P. Zarnetske, and J. W. Harvey. 2015. A physical explanation for the development of redox microzones in hyporheic flow. Geophysical Research Letters **42**:4402-4410.

Brown, J. H., J. F. Gillooly, A. P. Allen, V. M. Savage, and G. B. West. 2004. Toward a Metabolic Theory of Ecology. Ecology **85**:1771-1789.

Brunke, M., and T. Gonser. 1997. The ecological significance of exchange processes between rivers and groundwater. Freshwater Biology **37**:1-33.

Calcagno, V., and C. de Mazancourt. 2010. glmulti: An R Package for Easy Automated Model Selection with (Generalized) Linear Models. 2010 **34**:29.

Calder, W. A. 1983. Ecological Scaling: Mammals and Birds. Annual Review of Ecology and Systematics **14**:213-230.

Campbell Grant, E. H., W. H. Lowe, and W. F. Fagan. 2007. Living in the branches: population dynamics and ecological processes in dendritic networks. Ecology Letters **10**:165-175.

Cardinale, B. J., K. Gross, K. Fritschie, P. Flombaum, J. W. Fox, C. Rixen, J. van Ruijven, P. B. Reich, M. Scherer-Lorenzen, and B. J. Wilsey. 2013. Biodiversity simultaneously enhances the production and stability of community biomass, but the effects are independent. Ecology **94**:1697-1707.

Cardinale, B. J., M. A. Palmer, C. M. Swan, S. Brooks, and N. L. Poff. 2002. The influence of substrate heterogeneity on biofilm metabolism in a stream ecosystem. Ecology **83**:412-422.

Carpenter, S. R. 1996. Microcosm experiments have limited relevance for community and ecosystem ecology. Ecology **77**:677-680.

Chase, J. M., and T. M. Knight. 2013. Scale-dependent effect sizes of ecological drivers on biodiversity: why standardised sampling is not enough. Ecology Letters **16**:17-26.

Claret, C., and D. Fontvieille. 1997. Characteristics of biofilm assemblages in two contrasted hydrodynamic and tophic contexts. Microbial Ecology **34**:49-57.

Clifford, N. J., P. J. Soar, O. P. Harmar, A. M. Gurnell, G. E. Petts, and J. C. Emery. 2005. Assessment of hydrodynamic simulation results for eco-hydraulic and eco-hydrological applications: a spatial semivariance approach. Hydrological Processes **19**:3631-3648.

Clow, D. W., S. M. Stackpoole, K. L. Verdin, D. E. Butman, Z. Zhu, D. P. Krabbenhoft, and R. G. Striegl. 2015. Organic Carbon Burial in Lakes and Reservoirs of the Conterminous United States. Environmental Science & Technology **49**:7614-7622.

Cole, J. J., Y. T. Prairie, N. F. Caraco, W. H. McDowell, L. J. Tranvik, R. G. Striegl, C. M. Duarte, P. Kortelainen, J. A. Downing, J. J. Middelburg, and J. Melack. 2007. Plumbing the global carbon cycle: Integrating inland waters into the terrestrial carbon budget. Ecosystems **10**:171-184.

Cooper, C. M., and S. Testa. 2001. A quick method of determining rock surface area for quantification of the invertebrate community. Hydrobiologia **452**:203-208.

Cooper, S. D., L. Barmuta, O. Sarnelle, K. Kratz, and S. Diehl. 1997. Quantifying spatial heterogeneity in streams. Journal of the North American Benthological Society **16**:174-188.

Cooper, S. D., S. Diehl, K. Kratz, and O. Sarnelle. 1998. Implications of scale for patterns and processes in stream ecology. Australian Journal of Ecology **23**:27-40.

Cory, R. M., C. P. Ward, B. C. Crump, and G. W. Kling. 2014. Sunlight controls water column processing of carbon in arctic fresh waters. Science **345**:925-928.

Covino, T. 2017. Hydrologic connectivity as a framework for understanding biogeochemical flux through watersheds and along fluvial networks. Geomorphology **277**:133-144.

Crump, B. C., L. A. Amaral-Zettler, and G. W. Kling. 2012. Microbial diversity in arctic freshwaters is structured by inoculation of microbes from soils. ISME J **6**:1629-1639.

Cui, L., W. Li, C. Gao, M. Zhang, X. Zhao, Z. Yang, Y. Lei, D. Huang, and W. Ma. 2018. Identifying the influence factors at multiple scales on river water chemistry in the Tiaoxi Basin, China. Ecological Indicators **92**:228-238.

Davis, C. A., A. S. Ward, A. J. Burgin, T. D. Loecke, D. A. Riveros-Iregui, D. J. Schnoebelen, C. L. Just, S. A. Thomas, L. J. Weber, and M. A. St. Clair. 2014. Antecedent Moisture Controls on Stream Nitrate Flux in an Agricultural Watershed. Journal of Environmental Quality **43**:1494-1503.

Dodds, W. K., V. H. Smith, and K. Lohman. 2002. Nitrogen and phosphorus relationships to benthic algal biomass in temperate streams. Canadian Journal of Fisheries and Aquatic Sciences **59**:865-874.

Dong, X., A. Ruhí, and N. B. Grimm. 2017. Evidence for self-organization in determining spatial patterns of stream nutrients, despite primacy of the geomorphic template. Proceedings of the National Academy of Sciences **114**:E4744-E4752.

Downes, B. J., P. S. Lake, E. S. G. Schreiber, and A. Glaister. 1998. Habitat structure and regulation of local species diversity in a stony, upland stream. Ecological Monographs **68**:237-257.

Elmendorf, S. C., G. H. R. Henry, R. D. Hollister, R. G. Björk, N. Boulanger-Lapointe, E. J. Cooper, J. H. C. Cornelissen, T. A. Day, E. Dorrepaal, T. G. Elumeeva, M. Gill, W. A. Gould, J. Harte, D. S. Hik, A. Hofgaard, D. R. Johnson, J. F. Johnstone, I. S. Jónsdóttir, J. C. Jorgenson, K. Klanderud, J. A. Klein, S. Koh, G. Kudo, M. Lara, E. Lévesque, B. Magnússon, J. L. May, J. A. Mercado-Dı´az, A. Michelsen, U. Molau, I. H. Myers-Smith, S. F. Oberbauer, V. G. Onipchenko, C. Rixen, N. Martin Schmidt, G. R. Shaver, M. J. Spasojevic, Þ. E. Þórhallsdóttir, A. Tolvanen, T. Troxler, C. E. Tweedie, S. Villareal, C.-H. Wahren, X. Walker, P. J. Webber, J. M. Welker, and S. Wipf. 2012. Plot-scale evidence of tundra vegetation change and links to recent summer warming. Nature Climate Change **2**:453.

Elrifi, I. R., and D. H. Turpin. 1986. Nitrate and ammonium induced photosynthetic suppression in N-limited Selenastrum minutum. Plant Physiology **81**:273-279.

Elrifi, I. R., and D. H. Turpin. 1987. Short-term physiological indicators of N deficiency in phytoplankton - a unifying model. Marine Biology **96**:425-432.

Fellows, C. S., H. M. Valett, and C. N. Dahm. 2001. Whole-Stream Metabolism in Two Montane Streams: Contribution of the Hyporheic Zone. Limnol. Oceanogr. **46**:523-531.

Fellows, C. S., H. M. Valett, C. N. Dahm, P. J. Mulholland, and S. A. Thomas. 2006. Coupling nutrient uptake and energy flow in headwater streams. Ecosystems **9**:788-804.

Finlay, J. C., and W. B. Bowden. 1994. Controls on production of bryophytes in an arctic tundra stream. Freshwater Biology **32**:455-465.

Forman, R. T. T., and M. Godron. 1981. Patches and Structural Components for a Landscape Ecology. Bioscience **31**:733-740.

Frey, K. E., J. W. McClelland, R. M. Holmes, and L. C. Smith. 2007. Impacts of climate warming and permafrost thaw on the riverine transport of nitrogen and phosphorus to the Kara Sea. Journal of Geophysical Research: Biogeosciences **112**.

Frissell, C. A., W. J. Liss, C. E. Warren, and M. D. Hurley. 1986. A hierarchical framework for stream habitat classification - Viewing streams in a watershed context. Environmental management **10**:199-214.

Frost, T. M., D. L. DeAngelis, S. M. Bartell, D. J. Hall, and S. H. Hurlbert. 1988. Scale in the design and interpretation of aquatic community research. Pages 229-258 *in* S. Carpenter, editor. Complex Interactions in Lake Communities. Springer New York.

Gayraud, S., and M. Philippe. 2003. Influence of Bed-Sediment Features on the Interstitial Habitat Available for Macroinvertebrates in 15 French Streams. International Review of Hydrobiology **88**:77-93.

Gomi, T., R. C. Sidle, and J. S. Richardson. 2002. Understanding processes and downstream linkages of headwater systems. Bioscience **52**:905-916.

Goodman, K. J., M. A. Baker, and W. A. Wurtsbaugh. 2011. Lakes as buffers of stream dissolved organic matter (DOM) variability: Temporal patterns of DOM characteristics in mountain stream-lake systems. Journal of Geophysical Research: Biogeosciences **116**.

Goovaerts, P. 1998. Geostatistical tools for characterizing the spatial variability of microbiological and physico-chemical soil properties. Biology and Fertility of Soils **27**:315-334.

Graba, M., S. Sauvage, N. Majdi, B. Mialet, F. Y. Moulin, G. Urrea, E. Buffan-Dubau, M. Tackx, S. Sabater, and J.-M. Sanchez-Pérez. 2014. Modelling epilithic biofilms combining hydrodynamics, invertebrate grazing and algal traits. Freshwater Biology **59**:1213-1228.

Graff, J. R., and T. A. Rynearson. 2011. Extraction method influences the recovery of phytoplankton pigments from natural assemblages. Limnology and Oceanography: Methods **9**:129-139.

Graham, M. H. 2003. CONFRONTING MULTICOLLINEARITY IN ECOLOGICAL MULTIPLE REGRESSION. Ecology **84**:2809-2815.

Grant, S. B., M. Azizian, P. Cook, F. Boano, and M. A. Rippy. 2018. Factoring stream turbulence into global assessments of nitrogen pollution. Science **359**:1266-1269.

Griffin, C., J. McClelland, K. Frey, G. Fiske, and R. Holmes. 2018. Quantifying CDOM and DOC in major Arctic rivers during ice-free conditions using Landsat TM and ETM+ data.

Grimm, N., and S. Fisher. 1984. Exchange between interstitial and surface water: Implications for stream metabolism and nutrient cycling. Hydrobiologia **111**:219 - 228.

Guo, Y., C. Song, W. Tan, X. Wang, and Y. Lu. 2018. Hydrological processes and permafrost regulate magnitude, source and chemical characteristics of dissolved organic carbon export in a peatland catchment of northeastern China. Hydrol. Earth Syst. Sci. **22**:1081-1093.

Hagerthey, S. E., J. William Louda, and P. Mongkronsri. 2006. Evaluation of pigment extraction methods and a recommended protocol for periphyton chlorophyll-a

determination and chemotaxonomic assessment. Journal of Phycology **42**:1125-1136.

Haggerty, R., M. Ribot, G. A. Singer, E. Martí, A. Argerich, G. Agell, and T. J. Battin. 2014. Ecosystem respiration increases with biofilm growth and bed forms: Flume measurements with resazurin. Journal of Geophysical Research: Biogeosciences **119**:2220-2230.

Hall, R. O., J. L. Tank, M. A. Baker, E. J. Rosi-Marshall, and E. R. Hotchkiss. 2016. Metabolism, gas exchange, and carbon spiraling in rivers. Ecosystems **19**:73-86.

Hansson, L.-A. 1988. Chlorophyll a determination of periphyton on sediments: identification of problems and recommendation of method. Freshwater Biology **20**:347-352.

Harvey, C. J., B. J. Peterson, W. B. Bowden, A. E. Hershey, M. C. Miller, L. A. Deegan, and J. C. Finlay. 1998. Biological responses to fertilization of Oksrukuyik Creek, a tundra stream. Journal of the North American Benthological Society **17**:190-209.

Henderson, I. M. 2015. Ratios, proportions, and mixtures of chlorophylls: Corrections to spectrophotometric methods and an approach to diagnosis. Limnology and Oceanography: Methods **13**:617-629.

Hewitt, J. E., S. F. Thrush, P. K. Dayton, and E. Bonsdorff. 2007. The Effect of Spatial and Temporal Heterogeneity on the Design and Analysis of Empirical Studies of Scale-Dependent Systems. The American Naturalist **169**:398-408.

Hoellein, T. J., J. L. Tank, S. A. Entrekin, E. J. Rosi-Marshall, M. L. Stephen, and G. A. Lamberti. 2012. Effects of benthic habitat restoration on nutrient uptake and ecosystem metabolism in three headwater streams. River Research and Applications **28**:1451-1461.

Hoellein, T. J., J. L. Tank, E. J. Rosi-Marshall, and S. A. Entrekin. 2009. Temporal variation in substratum-specific rates of N uptake and metabolism and their contribution at the stream-reach scale. Journal of the North American Benthological Society **28**:305-318.

Holm-Hansen, O., and B. Riemann. 1978. Chlorophyll a determination: Improvements in methodology. Oikos **30**:438-447.

Hope, A., W. McDowell, and W. Wollheim. 2014. Ecosystem metabolism and nutrient uptake in an urban, piped headwater stream. Biogeochemistry **121**:167-187.

Horne, J. K., and D. C. Schneider. 1995. Spatial variance in ecology. Oikos **74**:18-26.

Hynes, H. 1970. The ecology of running waters. University of Toronto Press, Toronto, Ontario.

Isaaks, E., and R. Srivastava. 1989. Applied Geostatistics. London: Oxford University.

Jeff, S., K. Hunter, D. Vandergucht, and J. Hudson. 2012. Photochemical mineralization of dissolved organic nitrogen to ammonia in prairie lakes. Hydrobiologia **693**:71-80.

Jeffrey, S. W., R. F. C. Mantoura, S. W. Wright, I. C. o. S. U. S. C. o. O. Research, and Unesco. 1997. Phytoplankton Pigments in Oceanography: Guidelines to Modern Methods. UNESCO Publishing.

Jespersen, A. M., and K. Christoffersen. 1987. Measurements of chlorophyll-a from phytoplankton using ethanol as extraction solvent. Archiv Fur Hydrobiologie **109**:445-454.

Jones, J. B., S. G. Fisher, and N. B. Grimm. 1995. Vertical hydrologic exchange and ecosystem metabolism in a Sonoran desert stream. Ecology **76**:942-952.

Jones, J. B., and R. M. Holmes. 1996. Surface-subsurface interactions in stream ecosystems. Trends in Ecology & Evolution **11**:239-242.

Jones, N. E. 2010a. Incorporating lakes within the river discontinuum: longitudinal changes in ecological characteristics in stream-lake networks. Canadian Journal of Fisheries and Aquatic Sciences **67**:1350-1362.

Jones, N. E. 2010b. Incorporating lakes within the river discontinuum: longitudinal changes in ecological characteristics in stream–lake networks. Canadian Journal of Fisheries and Aquatic Sciences **67**:1350-1362.

Joslyn, M. A., and G. Mackinney. 1938. The Rate of Conversion of Chlorophyll to Pheophytin. Journal of the American Chemical Society **60**:1132-1136.

Kalinin, A., T. Covino, and B. McGlynn. 2016. The influence of an in-network lake on the timing, form, and magnitude of downstream dissolved organic carbon and nutrient flux. Water Resources Research **52**:8668-8684.

Kattsov, V. M., J. E. Walsh, W. L. Chapman, V. A. Govorkova, T. V. Pavlova, and X. Zhang. 2007. Simulation and Projection of Arctic Freshwater Budget Components by the IPCC AR4 Global Climate Models. Journal of Hydrometeorology **8**:571-589.

Kemp, M. J., and W. K. Dodds. 2002. The influence of ammonium, nitrate, and dissolved oxygen concentrations on uptake, nitrification, and denitrification rates associated with prairie stream substrata. Limnology and Oceanography **47**:1380-1393.

Kendrick, M. R., and A. D. Huryn. 2015. Discharge, legacy effects and nutrient availability as determinants of temporal patterns in biofilm metabolism and accrual in an arctic river. Freshwater Biology **60**:2323-2336.

Khosh, M. S., J. W. McClelland, A. D. Jacobson, T. A. Douglas, A. J. Barker, and G. O. Lehn. 2017. Seasonality of dissolved nitrogen from spring melt to fall freezeup in Alaskan Arctic tundra and mountain streams. Journal of Geophysical Research: Biogeosciences **122**:1718-1737.

Kling, G. W., G. W. Kipphut, M. M. Miller, and W. J. O'Brien. 2000. Integration of lakes and streams in a landscape perspective: the importance of material processing on spatial patterns and temporal coherence. Freshwater Biology **43**:477-497.

Kovalenko, K. E., S. M. Thomaz, and D. M. Warfe. 2012. Habitat complexity: approaches and future directions. Hydrobiologia **685**:1-17.

Lake, P. S. 2000. Disturbance, patchiness, and diversity in streams. Journal of the North American Benthological Society **19**:573-592.

Lara, M. J., I. Nitze, G. Grosse, P. Martin, and A. D. McGuire. 2018. Reduced arctic tundra productivity linked with landform and climate change interactions. Scientific Reports **8**:2345.

Larouche, J. R., B. W. Abbott, W. B. Bowden, and J. B. Jones. 2015. The role of watershed characteristics, permafrost thaw, and wildfire on dissolved organic carbon biodegradability and water chemistry in Arctic headwater streams. Biogeosciences **12**:4221-4233.

Larsen, L. G., J. Ma, and D. Kaplan. 2017. How Important Is Connectivity for Surface Water Fluxes? A Generalized Expression for Flow Through Heterogeneous Landscapes. Geophysical Research Letters **44**:10,349-310,358.

Laub, B. G., D. W. Baker, B. P. Bledsoe, and M. A. Palmer. 2012. Range of variability of channel complexity in urban, restored and forested reference streams. Freshwater Biology **57**:1076-1095.

Lawrence, J. R., B. Scharf, G. Packroff, and T. R. Neu. 2002. Microscale Evaluation of the Effects of Grazing by Invertebrates with Contrasting Feeding Modes on River Biofilm Architecture and Composition. Microbial Ecology **44**:199-207.

Leavitt, P. R., C. S. Brock, C. Ebel, and A. Patoine. 2006. Landscape-scale effects of urban nitrogen on a chain of freshwater lakes in central North America. Limnology and Oceanography **51**:2262-2277.

Lefcheck, J. S., J. E. K. Byrnes, F. Isbell, L. Gamfeldt, J. N. Griffin, N. Eisenhauer, M. J. S. Hensel, A. Hector, B. J. Cardinale, and J. E. Duffy. 2015. Biodiversity enhances ecosystem multifunctionality across trophic levels and habitats. Nat Commun **6**.

Legleiter, C. J. 2014. A geostatistical framework for quantifying the reach-scale spatial structure of river morphology: 1. Variogram models, related metrics, and relation to channel form. Geomorphology **205**:65-84.

Lehman, P. W. 1981. Comparison of chlorophyll-*a* and carotenoid-pigments as predictors of phytoplankton biomass. Marine Biology **65**:237-244.

Leopold, L. B., and W. B. Langbein. 1962. The Concept of Entropy in Landscape Evolution. Page 20 *in* U. S. G. Survey, editor. United States Government Printing Office, Washington D. C. .

Leopold, L. B., and T. Maddock, Jr. 1953. The Hydraulic Geometry of Stream Channels and Some Physiographic Implications. Page 56 *in* U. S. G. Survey, editor. United States Government Printing Office, Washington D. C. .

Levin, S. A. 1992. The problem of pattern and scale in ecology. Ecology **73**:1943-1967.

Levin, S. A., and R. T. Paine. 1974. Disturbance, Patch Formation, and Community Structure. Proceedings of the National Academy of Sciences **71**:2744-2747.

Levine, S., and D. Schindler. 1992. Modification of the N: P ratio in lakes by in situ processes. OCEANOGRAPHY **37**.

Levine, S. N., A. d. Shambaugh, S. E. Pomeroy, and M. Braner. 1997. Phosphorus, Nitrogen, and Silica as Controls on Phytoplankton Biomass and Species Composition in Lake Champlain (USA-Canada). Journal of Great Lakes Research **23**:131-148.

Lock, M. A., R. R. Wallace, J. W. Costerton, R. M. Ventullo, and S. E. Charlton. 1984. River Epilithon: Toward a Structural-Functional Model. Oikos **42**:10-22.

Lorenzen, C. J. 1967. Determination of chlorophyll and pheo-pigments: Spectrophotometric equations. Limnology and Oceanography **12**:343-346.

Lottig, N. R., I. Buffam, and E. H. Stanley. 2013. Comparisons of wetland and drainage lake influences on stream dissolved carbon concentrations and yields in a north temperate lake-rich region. Aquatic Sciences **75**:619-630.

Lottig, N. R., and E. H. Stanley. 2007. Benthic sediment influence on dissolved phosphorus concentrations in a headwater stream. Biogeochemistry **84**:297-309.

Lottig, N. R., E. H. Stanley, P. C. Hanson, and T. K. Kratz. 2011. Comparison of regional stream and lake chemistry: Differences, similarities, and potential drivers. Limnology and Oceanography **56**:1551-1562.

Lowe, W. H., G. E. Likens, and M. E. Power. 2006. Linking scales in stream ecology. Bioscience **56**:591-597.

Mack, M. C., E. A. G. Schuur, M. S. Bret-Harte, G. R. Shaver, and F. S. Chapin Iii. 2004. Ecosystem carbon storage in arctic tundra reduced by long-term nutrient fertilization. Nature **431**:440.

Majdi, N., B. Mialet, S. Boyer, M. Tackx, J. Leflaive, S. Boulêtreau, L. Ten-Hage, F. Julien, R. Fernandez, and E. Buffan-Dubau. 2012. The relationship between epilithic biofilm stability and its associated meiofauna under two patterns of flood disturbance. Freshwater Science **31**:38-50.

Majdi, N., I. Threis, and W. Traunspurger. 2017. It's the little things that count: Meiofaunal density and production in the sediment of two headwater streams. Limnology and Oceanography **62**:151-163.

Marker, A. F. H. 1972. The use of acetone and methanol in the estimation of chlorophyll in the presence of phaeophytin. Freshwater Biology **2**:361-385.

McDonald, C. P., and R. C. Lathrop. 2017. Seasonal shifts in the relative importance of local versus upstream sources of phosphorus to individual lakes in a chain. Aquatic Sciences **79**:385-394.

McLaren, J. R., A. Darrouzet-Nardi, M. N. Weintraub, and L. Gough. 2017. Seasonal patterns of soil nitrogen availability in moist acidic tundra. Arctic Science **4**:98-109.

McNamara, J. P., D. L. Kane, J. E. Hobbie, and G. W. Kling. 2008. Hydrologic and biogeochemical controls on the spatial and temporal patterns of nitrogen and phosphorus in the Kuparuk River, arctic Alaska. Hydrological Processes **22**:3294-3309.

Miller, M. C., P. Deoliveira, and G. G. Gibeau. 1992. Epilithic diatom community response to years of PO4 fertilization - Kuparuk River, Alaska (68 N Lat.). Hydrobiologia **240**:103-119.

Minshall, G. W. 1988. Stream ecosystem theory: A global perspective. Journal of the North American Benthological Society **7**:263-288.

Moed, J. R., and G. M. Hallegraeff. 1978. Some problems in the estimation of chlorophyll-a and phaeopigments from pre- and post-acidification spectrophotometric

measurements. Internationale Revue der gesamten Hydrobiologie und Hydrographie **63**:787-800.

Montgomery, D. R. 1999. Process Domains and the River Continuum. JAWRA Journal of the American Water Resources Association **35**:397-410.

Morin, A., W. Lamoureux, and J. Busnarda. 1999. Empirical Models Predicting Primary Productivity from Chlorophyll a and Water Temperature for Stream Periphyton and Lake and Ocean Phytoplankton. Journal of the North American Benthological Society **18**:299-307.

Mulholland, P. J., C. S. Fellows, J. L. Tank, N. B. Grimm, J. R. Webster, S. K. Hamilton, E. Marti, L. Ashkenas, W. B. Bowden, W. K. Dodds, W. H. McDowell, M. J. Paul, and B. J. Peterson. 2001. Inter-biome comparison of factors controlling stream metabolism. Freshwater Biology **46**:1503-1517.

Mulholland, P. J., A. M. Helton, G. C. Poole, R. O. Hall, S. K. Hamilton, B. J. Peterson, J. L. Tank, L. R. Ashkenas, L. W. Cooper, C. N. Dahm, W. K. Dodds, S. E. G. Findlay, S. V. Gregory, N. B. Grimm, S. L. Johnson, W. H. McDowell, J. L. Meyer, H. M. Valett, J. R. Webster, C. P. Arango, J. J. Beaulieu, M. J. Bernot, A. J. Burgin, C. L. Crenshaw, L. T. Johnson, B. R. Niederlehner, J. M. O'Brien, J. D. Potter, R. W. Sheibley, D. J. Sobota, and S. M. Thomas. 2008. Stream denitrification across biomes and its response to anthropogenic nitrate loading. Nature **452**:202-U246.

Muller, S., D. Walker, F. Nelson, J. Bockheim, S. Guyer, and D. Sherba. 1998. Accuracy assessment of a land-cover map of the Kuparuk river basin, Alaska: considerations for remote regions. Photogrammetric Engineering and Remote Sensing **64**:619-628.

Myers-Smith, I. H., S. C. Elmendorf, P. S. A. Beck, M. Wilmking, M. Hallinger, D. Blok, K. D. Tape, S. A. Rayback, M. Macias-Fauria, B. C. Forbes, J. D. M. Speed, N. Boulanger-Lapointe, C. Rixen, E. Lévesque, N. M. Schmidt, C. Baittinger, A. J. Trant, L. Hermanutz, L. S. Collier, M. A. Dawes, T. C. Lantz, S. Weijers, R. H. Jørgensen, A. Buchwal, A. Buras, A. T. Naito, V. Ravolainen, G. Schaepman-Strub, J. A. Wheeler, S. Wipf, K. C. Guay, D. S. Hik, and M. Vellend. 2015. Climate sensitivity of shrub growth across the tundra biome. Nature Climate Change **5**:887.

Naegeli, M. W., and U. Uehlinger. 1997. Contribution of the hyporheic zone to ecosystem metabolism in a prealpine gravel-bed river. J. North Am. Benthol Soc. **16**:794-804.

Newbold, J. D., R. V. Oneill, J. W. Elwood, and W. Vanwinkle. 1982. Nutrient spiralling in streams: implications for nutrient limitation and invertebrate activity. American Naturalist **120**:628-652.

Nusch, E. 1980. Comparison of different methods for chlorophyll and phaeopigment determination. Arch. Hydrobiol. Beih **14**:14-36.

O'Neill, R. V., A. R. Johnson, and A. W. King. 1989. A hierarchical framework for the analysis of scale. Landscape Ecology **3**:193-205.

Odum, E. P. 1971. Fundamentals of Ecology: 3d Ed. Saunders, Philadelphia, Pennsylvania.

Odum, H. T. 1956. Primary Production in Flowing Waters. Limnology and Oceanography **1**:102-117.

Ohmori, M., K. Ohmori, and H. Strotmann. 1977. Inhibition of nitrate uptake by ammonia in a blue-green alga, Anabaena cylindrica. Archives of Microbiology **114**:225-229.

Olefeldt, D., S. Goswami, G. Grosse, D. Hayes, G. Hugelius, P. Kuhry, A. D. McGuire, V. E. Romanovsky, A. B. K. Sannel, E. A. G. Schuur, and M. R. Turetsky. 2016. Circumpolar distribution and carbon storage of thermokarst landscapes. Nature Communications **7**:13043.

Oswood, M. W., L. K. Miller, and J. G. Irons III. 1995. River and stream ecosystems of Alaska.*in* C. E. Cushing, K. W. Cumming, and G. W. Minshall, editors. Ecosystems of the World 22: River and Stream Ecosystems. Elsevier, Amsterdam.

Paine, R. T., and S. A. Levin. 1981. Inter-tidal lanscapes: Distrubance and the dynamics of pattern. Ecological Monographs **51**:145-178.

Palmer, M. A., J. D. Allan, and C. A. Butman. 1996. Dispersal as a regional process affecting the local dynamics of marine and stream benthic invertebrates. Trends in Ecology & Evolution **11**:322-326.

Palmer, M. A., H. L. Menninger, and E. Bernhardt. 2010. River restoration, habitat heterogeneity and biodiversity: a failure of theory or practice? Freshwater Biology **55**:205-222.

Palmer, M. A., and N. L. Poff. 1997. The influence of environmental heterogeneity on patterns and processes in streams. Journal of the North American Benthological Society **16**:169-173.

Palmer, M. A., C. M. Swan, K. Nelson, P. Silver, and R. Alvestad. 2000. Streambed landscapes: evidence that stream invertebrates respond to the type and spatial arrangement of patches. Landscape Ecology **15**:563-576.

Paltan, H., J. Dash, and M. Edwards. 2015. A refined mapping of Arctic lakes using Landsat imagery. International Journal of Remote Sensing **36**:5970-5982.

Parker, S. M., and A. D. Huryn. 2011. Effects of natural disturbance on stream communities: a habitat template analysis of arctic headwater streams. Freshwater Biology **56**:1342-1357.

Parker, S. P., W. B. Bowden, and M. B. Flinn. 2016. The effect of acid strength and postacidification reaction time on the determination of chlorophyll a in ethanol extracts of aquatic periphyton. Limnology and Oceanography: Methods **14**:839-852.

Parker, S. P., W. B. Bowden, M. B. Flinn, C. D. Giles, K. A. Arndt, J. P. Beneš, and D. G. Jent. 2018. Effect of particle size and heterogeneity on sediment biofilm metabolism and nutrient uptake scaled using two approaches. Ecosphere **9**:e02137.

Parsons, T. R., Y. Maita, and C. M. Lalli. 1984. 1.6 - Determination of Phosphate. Pages 22-25 *in* T. R. P. M. M. Lalli, editor. A Manual of Chemical & Biological Methods for Seawater Analysis. Pergamon, Amsterdam.

Passarelli, C., F. Olivier, D. M. Paterson, T. Meziane, and C. Hubas. 2014. Organisms as cooperative ecosystem engineers in intertidal flats. Journal of Sea Research **92**:92-101.

Pastick, N. J., M. T. Jorgenson, S. J. Goetz, B. M. Jones, B. K. Wylie, B. J. Minsley, H. Genet, J. F. Knight, D. K. Swanson, and J. C. Jorgenson. 2018. Spatiotemporal remote sensing of ecosystem change and causation across Alaska. Global Change Biology **0**.

Peterson, B. J., L. Deegan, J. Helfrich, J. E. Hobbie, M. Hullar, B. Moller, T. E. Ford, A. Hershey, A. Hiltner, G. Kipphut, M. A. Lock, D. M. Fiebig, V. McKinley, M. C. Miller, J. R. Vestal, R. Ventullo, and G. Volk. 1993. Biological responses of a tundra river to fertilization. Ecology **74**:653-672.

Peterson, B. J., J. E. Hobbie, A. E. Hershey, M. A. Lock, T. E. Ford, J. R. Vestal, V. L. McKinley, M. A. J. Hullar, M. C. Miller, R. M. Ventullo, and G. S. Volk. 1985. Transformation of a tundra river from heterotrophy to autotrophy by addition of phosphorus. Science **229**:1383-1386.

Peterson, B. J., W. M. Wollheim, P. J. Mulholland, J. R. Webster, J. L. Meyer, J. L. Tank, E. Martí, W. B. Bowden, H. M. Valett, A. E. Hershey, W. H. McDowell, W. K. Dodds, S. K. Hamilton, S. Gregory, and D. D. Morrall. 2001. Control of Nitrogen Export from Watersheds by Headwater Streams. Science **292**:86-90.

Peterson, D. L., and V. T. Parker. 1998. Ecological scale: theory and applications. Columbia University Press.

Peterson, E. E., J. M. Ver Hoef, D. J. Isaak, J. A. Falke, M.-J. Fortin, C. E. Jordan, K. McNyset, P. Monestiez, A. S. Ruesch, A. Sengupta, N. Som, E. A. Steel, D. M.

Theobald, C. E. Torgersen, and S. J. Wenger. 2013. Modelling dendritic ecological networks in space: an integrated network perspective. Ecology Letters **16**:707-719.

Pettorelli, N., M. Wegmann, A. Skidmore, S. Mücher, T. P. Dawson, M. Fernandez, R. Lucas, M. E. Schaepman, T. Wang, B. O'Connor, R. H. G. Jongman, P. Kempeneers, R. Sonnenschein, A. K. Leidner, M. Böhm, K. S. He, H. Nagendra, G. Dubois, T. Fatoyinbo, M. C. Hansen, M. Paganini, H. M. Klerk, G. P. Asner, J. T. Kerr, A. B. Estes, D. S. Schmeller, U. Heiden, D. Rocchini, H. M. Pereira, E. Turak, N. Fernandez, A. Lausch, M. A. Cho, D. Alcaraz-Segura, M. A. McGeoch, W. Turner, A. Mueller, V. St-Louis, J. Penner, P. Vihervaara, A. Belward, B. Reyers, and G. N. Geller. 2016. Framing the concept of satellite remote sensing essential biodiversity variables: challenges and future directions. Remote Sensing in Ecology and Conservation **2**:122-131.

Phoenix, G. K., and J. W. Bjerke. 2016. Arctic browning: extreme events and trends reversing arctic greening. Global Change Biology **22**:2960-2962.

Piñeiro, G., S. Perelman, J. P. Guerschman, and J. M. Paruelo. 2008. How to evaluate models: Observed vs. predicted or predicted vs. observed? Ecological modelling **216**:316-322.

Poff, N. L. 1997. Landscape Filters and Species Traits: Towards Mechanistic Understanding and Prediction in Stream Ecology. Journal of the North American Benthological Society **16**:391-409.

Poole, G. C. 2002. Fluvial landscape ecology: addressing uniqueness within the river discontinuum. Freshwater Biology **47**:641-660.

Porra, R. J. 1990. A simple method for extracting chlorophylls from the recalcitrang alga, Nannochloris-atomus, without formation of spectroscopically-different magnesium-rhodochlorin derivatives. Biochimica Et Biophysica Acta **1019**:137-141.

Porra, R. J., and L. H. Grimme. 1974. A new procedure for the determination of chlorophylls a and b and its application to normal and regreening Chlorella. Analytical Biochemistry **57**:255-267.

Powers, S. M., D. M. Robertson, and E. H. Stanley. 2014. Effects of lakes and reservoirs on annual river nitrogen, phosphorus, and sediment export in agricultural and forested landscapes. Hydrological Processes **28**:5919-5937.

Pringle, C. M. 1990. Nutrient spatial heterogeneity: Effects on community structure, physiognomy, and diversity of stream algae. Ecology **71**:905-920.

Pringle, C. M., R. J. Naiman, G. Bretschko, J. R. Karr, M. W. Oswood, R. W. Jackson, R. L. Welcomme, and M. J. Winterbourn. 1988. Patch dynamics in lotic systems: The

stream as a mosaic. Journal of the North American Benthological Society **7**:503-524.

Qin, H., S. Li, and D. Li. 2013. An improved method for determining phytoplankton chlorophyll a concentration without filtration. Hydrobiologia **707**:81-95.

Raymond, P. A., J. E. Saiers, and W. V. Sobczak. 2016. Hydrological and biogeochemical controls on watershed dissolved organic matter transport: pulse-shunt concept. Ecology **97**:5-16.

Reuss, N., and D. J. Conley. 2005. Effects of sediment storage conditions on pigment analyses. Limnology and Oceanography: Methods **3**:477-487.

Riemann, B. 1978. Carotenoid interference in spectrophotometric determination of chlorophyll degradation products from natural populations of phytoplankton. Limnology and Oceanography **23**:1059-1066.

Ritchie, R. J. 2006. Consistent sets of spectrophotometric chlorophyll equations for acetone, methanol and ethanol solvents. Photosynthesis Research **89**:27-41.

Ritchie, R. J. 2008. Universal chlorophyll equations for estimating chlorophylls a, b, c, and d and total chlorophylls in natural assemblages of photosynthetic organisms using acetone, methanol, or ethanol solvents. Photosynthetica **46**:115-126.

Roberts, B. J., P. J. Mulholland, and W. R. Hill. 2007. Multiple scales of temporal variability in ecosystem metabolism rates: Results from 2 years of continuous monitoring in a forested headwater stream. Ecosystems **10**:588-606.

Röman, E., P. Ekholm, S. Tattari, J. Koskiaho, and N. Kotamäki. 2018. Catchment characteristics predicting nitrogen and phosphorus losses in Finland. River Research and Applications **34**:397-405.

Rossi, R. E., D. J. Mulla, A. G. Journel, and H. F. Eldon. 1992. Geostatistical tools for modeling and interpreting ecological spatial dependence. Ecological Monographs **62**:277-314.

Rüegg, J., J. D. Brant, D. M. Larson, M. T. Trentman, and W. K. Dodds. 2015a. A portable, modular, self-contained recirculating chamber to measure benthic processes under controlled water velocity. Freshwater Science **34**:831-844.

Rüegg, J., W. K. Dodds, M. D. Daniels, K. R. Sheehan, C. L. Baker, W. B. Bowden, K. J. Farrell, M. B. Flinn, T. K. Harms, J. B. Jones, L. E. Koenig, J. S. Kominoski, W. H. McDowell, S. P. Parker, A. D. Rosemond, M. T. Trentman, M. Whiles, and W. M. Wollheim. 2015b. Baseflow physical characteristics differ at multiple spatial scales in stream networks across diverse biomes. Landscape Ecology **31**:119-136.

Runkel, R. L., and K. E. Bencala. 1995. Transport of reacting solutes in rivers and streams. Pages 137-164 Environmental hydrology. Springer.

Sadro, S., C. E. Nelson, and J. M. Melack. 2012. The influence of landscape position and catchment characteristics on aquatic biogeochemistry in high-elevation lake-chains. Ecosystems **15**:363-386.

Sandel, B., and A. B. Smith. 2009. Scale as a lurking factor: incorporating scale-dependence in experimental ecology. Oikos **118**:1284-1291.

Sartory, D., and J. Grobbelaar. 1984. Extraction of chlorophyll a from freshwater phytoplankton for spectrophotometric analysis. Hydrobiologia **114**:177-187.

Sartory, D. P. 1982. Spectrophotometric analysis of chlorophyll a in freshwater phytoplankton. Technical Report TR 115 January 1982. 163 p, 14 fig, 26 tab, 100 ref.

Schiemer, F., H. Keckeis, W. Reckendorfer, and G. Winkler. 2001. The" inshore retention concept" and its significance for large rivers. Arch. Hydrobiol.(Suppl.)(Large Rivers) **135**:509-516.

Schindler, D. W. 1998. Whole-Ecosystem Experiments: Replication Versus Realism: The Need for Ecosystem-Scale Experiments. Ecosystems **1**:323-334.

Schneider, D. C. 2001. The Rise of the Concept of Scale in Ecology: The concept of scale is evolving from verbal expression to quantitative expression. Bioscience **51**:545-553.

Schuur, E. A. G., A. D. McGuire, C. Schädel, G. Grosse, J. W. Harden, D. J. Hayes, G. Hugelius, C. D. Koven, P. Kuhry, D. M. Lawrence, S. M. Natali, D. Olefeldt, V. E. Romanovsky, K. Schaefer, M. R. Turetsky, C. C. Treat, and J. E. Vonk. 2015. Climate change and the permafrost carbon feedback. Nature **520**:171.

Seiferling, I., R. Proulx, and C. Wirth. 2014. Disentangling the environmental-heterogeneity species-diversity relationship along a gradient of human footprint. Ecology **95**:2084-2095.

Shaver, G. R., and F. S. Chapin. 1995. Long–term responses to factorial, NPK fertilizer treatment by Alaskan wet and moist tundra sedge species. Ecography **18**:259-275.

Sliva, L., and D. Dudley Williams. 2001. Buffer Zone versus Whole Catchment Approaches to Studying Land Use Impact on River Water Quality. Water Research **35**:3462-3472.

Snyder, L., and W. B. Bowden. 2014. Nutrient dynamics in an oligotrophic arctic stream monitored in situ by wet chemistry methods. Water Resources Research **50**:2039-2049.

Soranno, P. A., K. S. Cheruvelil, T. Wagner, K. E. Webster, and M. T. Bremigan. 2015. Effects of Land Use on Lake Nutrients: The Importance of Scale, Hydrologic Connectivity, and Region. Plos One **10**:e0135454.

Staehr, P. A., J. M. Testa, W. M. Kemp, J. J. Cole, K. Sand-Jensen, and S. V. Smith. 2012. The metabolism of aquatic ecosystems: history, applications, and future challenges. Aquatic Sciences **74**:15-29.

Statzner, B., and B. Higler. 1985. Questions and comments on the river continuum concept. Canadian Journal of Fisheries and Aquatic Sciences **42**:1038-1044.

Stegen, J. C., J. K. Fredrickson, M. J. Wilkins, A. E. Konopka, W. C. Nelson, E. V. Arntzen, W. B. Chrisler, R. K. Chu, R. E. Danczak, S. J. Fansler, D. W. Kennedy, C. T. Resch, and M. Tfaily. 2016. Groundwater-surface water mixing shifts ecological assembly processes and stimulates organic carbon turnover. Nat Commun **7**.

Strahler, A. N. 1954. Quantitative geomorphology of erosional landscapes. Pages 341-354 *in* International Geologic Congress.

Strahler, A. N. 1957. Quantitative analysis of watershed geomorphology. Transactions of the American Geophysical Union **38**:913-920.

Tait, C. K., J. L. Li, G. A. Lamberti, T. N. Pearsons, and H. W. Li. 1994. Relationships between Riparian Cover and the Community Structure of High Desert Streams. Journal of the North American Benthological Society **13**:45-56.

Tews, J., U. Brose, V. Grimm, K. Tielbörger, M. C. Wichmann, M. Schwager, and F. Jeltsch. 2004. Animal species diversity driven by habitat heterogeneity/diversity: the importance of keystone structures. Journal of Biogeography **31**:79-92.

Thompson, R. C., M. L. Tobin, S. J. Hawkins, and T. A. Norton. 1999. Problems in extraction and spectrophotometric determination of chlorophyll from epilithic microbial biofilms: towards a standard method. Journal of the Marine Biological Association of the United Kingdom **79**:551-558.

Thoms, M. C., and M. Parsons. 2002. Eco-geomorphology: an interdisciplinary approach to river science. International Association of Hydrological Sciences, Publication:113-119.

Thomson, J. R., M. P. Taylor, K. A. Fryirs, and G. J. Brierley. 2001. A geomorphological framework for river characterization and habitat assessment. Aquatic Conservation-Marine and Freshwater Ecosystems **11**:373-389.

Thorp, J. H., M. C. Thoms, and M. D. Delong. 2006. The riverine ecosystem synthesis: biocomplexity in river networks across space and time. River Research and Applications **22**:123-147.

Thrush, S. F., D. C. Schneider, P. Legendre, R. B. Whitlatch, P. K. Dayton, J. E. Hewitt, A. H. Hines, V. J. Cummings, S. M. Lawrie, J. Grant, R. D. Pridmore, S. J. Turner, and B. H. McArdle. 1997. Scaling-up from experiments to complex ecological systems: Where to next? Journal of Experimental Marine Biology and Ecology **216**:243-254.

Townsend, C., S. DolÉDec, and M. Scarsbrook. 1997a. Species traits in relation to temporal and spatial heterogeneity in streams: a test of habitat templet theory. Freshwater Biology **37**:367-387.

Townsend, C. R. 1989. The patch dynamics concept of stream community ecology. Journal of the North American Benthological Society **8**:36-50.

Townsend, C. R., and A. G. Hildrew. 1994. Species traits in relation to a habitat templet for river systems. Freshwater Biology **31**:265-275.

Townsend, C. R., M. R. Scarsbrook, and S. Doledec. 1997b. The intermediate disturbance hypothesis, refugia, and biodiversity in streams. Limnology and Oceanography **42**:938-949.

Tranvik, L. J., J. J. Cole, and Y. T. Prairie. 2018. The study of carbon in inland waters—from isolated ecosystems to players in the global carbon cycle. Limnology and Oceanography Letters **3**:41-48.

Tranvik, L. J., J. A. Downing, J. B. Cotner, S. A. Loiselle, R. G. Striegl, T. J. Ballatore, P. Dillon, K. Finlay, K. Fortino, L. B. Knoll, P. L. Kortelainen, T. Kutser, S. Larsen, I. Laurion, D. M. Leech, S. L. McCallister, D. M. McKnight, J. M. Melack, E. Overholt, J. A. Porter, Y. Prairie, W. H. Renwick, F. Roland, B. S. Sherman, D. W. Schindler, S. Sobek, A. Tremblay, M. J. Vanni, A. M. Verschoor, E. von Wachenfeldt, and G. A. Weyhenmeyer. 2009. Lakes and reservoirs as regulators of carbon cycling and climate. Limnology and Oceanography **54**:2298-2314.

Turak, E., I. Harrison, D. Dudgeon, R. Abell, A. Bush, W. Darwall, C. M. Finlayson, S. Ferrier, J. Freyhof, V. Hermoso, D. Juffe-Bignoli, S. Linke, J. Nel, H. C. Patricio, J. Pittock, R. Raghavan, C. Revenga, J. P. Simaika, and A. De Wever. 2017. Essential Biodiversity Variables for measuring change in global freshwater biodiversity. Biological Conservation **213**:272-279.

Turner, M. G., R. V. O'Neill, R. t. Gardner, and B. T. Milne. 1989. Effects of changing spatial scale on the analysis of landscape pattern. Landscape Ecology **3**:153-162.

Vannote, R. L., G. W. Minshall, K. W. Cummins, J. R. Sedell, and C. E. Cushing. 1980. River continuum concept. Canadian Journal of Fisheries and Aquatic Sciences **37**:130-137.

Ver Hoef, J. M., and E. E. Peterson. 2010. A moving average approach for spatial statistical models of stream networks. Journal of the American Statistical Association **105**.

Verdouw, H., C. J. A. Van Echteld, and E. M. J. Dekkers. 1978. Ammonia determination based on indophenol formation with sodium salicylate. Water Research **12**:399-402.

Wadeson, R. A. 1994. A geomorphological approach to the identification and classification of instream flow environments. Southern African Journal of Aquatic Sciences **20**:38-61.

Wadeson, R. A., and K. M. Rowntree. 1998. Application of the hydraulic biotope concept to the classification of instream habitats. Aquatic Ecosystem Health and Management **1**:143-157.

Walker, D. A., F. J. Daniëls, N. V. Matveyeva, J. Šibík, M. D. Walker, A. L. Breen, L. A. Druckenmiller, M. K. Raynolds, H. Bültmann, and S. Hennekens. 2017. Circumpolar Arctic Vegetation Classification. Phytocoenologia.

Walker, D. A., M. K. Raynolds, F. J. Daniëls, E. Einarsson, A. Elvebakk, W. A. Gould, A. E. Katenin, S. S. Kholod, C. J. Markon, and E. S. Melnikov. 2005. The circumpolar Arctic vegetation map. Journal of Vegetation Science **16**:267-282.

Walker, M. D., D. A. Walker, and N. A. Auerbach. 1994. Plant communities of a tussock tundra landscape in the Brooks Range Foothills, Alaska. Journal of Vegetation Science **5**:843-866.

Ward, J. V. 1989. The four-dimensional nature of lotic ecosystems. Journal of the North American Benthological Society **8**:2-8.

Ward, J. V., and J. A. Stanford. 1983. The serial discontinuity concept of lotic ecosystems. Pages 29-42 *in* T. D. Fontaine and S. M. Bartell, editors. Dynamics of Lotic Systems. Ann Arbor Science, Ann Arbor.

Warfe, D. M., L. A. Barmuta, and S. Wotherspoon. 2008. Quantifying habitat structure: surface convolution and living space for species in complex environments. Oikos **117**:1764-1773.

Wasmund, N. 1984. Problems of the spectrophotometric determination of chlorophyll. Acta Hydrochimica Et Hydrobiologica **12**:255-272.

Wasmund, N., I. Topp, and D. Schories. 2006. Optimising the storage and extraction of chlorophyll samples. Oceanologia **48**:125-144.

Webster, J. R., P. J. Mulholland, J. L. Tank, H. M. Valett, W. K. Dodds, B. J. Peterson, W. B. Bowden, C. N. Dahm, S. Findlay, S. V. Gregory, N. B. Grimm, S. K. Hamilton, S. L. Johnson, E. Marti, W. H. McDowell, J. L. Meyer, D. D. Morrall, S. A. Thomas, and W. M. Wollheim. 2003. Factors affecting ammonium uptake in streams - an inter-biome perspective. Freshwater Biology **48**:1329-1352.

Webster, J. R., and B. C. Patten. 1979. Effects of watershed perturbation on stream potassium and calcium dynamics. Ecological Monographs **49**:51-72.

Whittinghill, K. A., J. C. Finlay, and S. E. Hobbie. 2014. Bioavailability of dissolved organic carbon across a hillslope chronosequence in the Kuparuk River region, Alaska. Soil Biology and Biochemistry **79**:25-33.

Whittinghill, K. A., and S. E. Hobbie. 2011. Effects of Landscape Age on Soil Organic Matter Processing in Northern Alaska. Soil Science Society of America Journal **75**:907-917.

Wiens, J. A. 1989. Spatial scaling in ecology. Functional Ecology **3**:385-397.

Wiens, J. A. 2002. Riverine landscapes: taking landscape ecology into the water. Freshwater Biology **47**:501-515.

Winemiller, K. O., A. S. Flecker, and D. J. Hoeinghaus. 2010. Patch dynamics and environmental heterogeneity in lotic ecosystems. Journal of the North American Benthological Society **29**:84-99.

Wintermans, J. F. G. M., and A. De Mots. 1965. Spectrophotometric characteristics of chlorophylls a and b and their phenophytins in ethanol. Biochimica et Biophysica Acta (BBA) - Biophysics including Photosynthesis **109**:448-453.

Wise, D. H., and M. C. Molles. 1979. Colonization of artifical substrates by stream insects: Influence of susbtrate size and diversity. Hydrobiologia **65**:69-74.

Wu, J., and O. L. Loucks. 1995. From balance-of-nature to hierarchical path dynamics: a paradigm shift in ecology. Quarterly review of biology.

Xenopoulos, M. A., J. A. Downing, M. D. Kumar, S. Menden-Deuer, and M. Voss. 2017. Headwaters to oceans: Ecological and biogeochemical contrasts across the aquatic continuum. Limnology and Oceanography **62**:S3-S14.

Xu, Z., and Y. J. Xu. 2018. Dissolved carbon transport in a river-lake continuum: A case study in a subtropical watershed, USA. Science of the Total Environment **643**:640-650.

Zarnetske, J. P., M. N. Gooseff, T. R. Brosten, J. H. Bradford, J. P. McNamara, and W. B. Bowden. 2007. Transient storage as a function of geomorphology, discharge, and permafrost active layer conditions in Arctic tundra streams. Water Resour. Res. **43**:W07410.

Zuur, A. F., E. N. Ieno, and C. S. Elphick. 2010. A protocol for data exploration to avoid common statistical problems. Methods in Ecology and Evolution **1**:3-14.